8-8-2024

Imaging Genetic Prediction of Cognition and Symptoms in Both Small and Big Cohorts

Pranav Nadigapu Suresh
Georgia State University

Imaging Genetic Prediction of Cognition and Symptoms in Both Small and Big Cohorts

by

Pranav Nadigapu Suresh

Under the Direction of Jingyu Liu, PhD

A Dissertation Submitted in Partial Fulfillment of the Requirements for the Degree of

Doctor of Philosophy

in the College of Arts and Sciences

Georgia State University

2024

ABSTRACT

With recent technological advances in acquiring multimodal brain imaging data and high-throughput genomics data, brain imaging genomics is emerging as a rapidly growing research field. This field performs integrative studies that analyze genetic variations such as single nucleotide polymorphisms (SNPs), and brain imaging quantitative traits (QTs), coupled with other biomarkers, clinical, and environmental data. The goal is to gain new insights into the phenotypic characteristics and the genetic mechanisms of the brain, as well as their impact on normal and disordered brain function and behavior. Our research proposes a series of algorithms to analyze imaging genomics. Initially, we investigated the ability to predict the trajectory of symptoms in both inattention and hyperactivity domains using features from sMRI images and genomics of an ADHD cohort of 77 subjects. We performed stepwise linear regression coupled with stability selection and permutation tests to identify the top predictive features. In the inattention domain, age, genes OSBPL1A, CTNNB1, PRPSAP2, ACADM, and one GM component in the insula region were associated with symptom change, while in the hyperactivity domain, no features were associated with symptom change. In our second study, we proposed a strategy for training convolutional neural networks (CNN) with limited samples using a self-transfer-training (STT) method, which refines and reuses layers to optimize model performance. Thirdly, we examined the potential of CNN models trained on structural MRI images to classify working memory capacity and understand the brain regions contributing to memory tasks. A CNN model trained on brain age prediction of 39,755 subjects was transferred to a working memory classification task with fewer subjects, leveraging the features learned on brain age prediction. Lastly, our fourth study integrates neuroimaging and genetics via contrastive learning for working memory prediction. We utilized data from the UK Biobank, combining structural MRI and SNP data with

advanced machine learning techniques, including contrastive learning and sparse canonical correlation analysis (sCCA), to uncover significant relationships between genetic variants and brain regions. This integrated approach achieved superior classification accuracy, providing new insights into the genetic and neural mechanisms underlying working memory, and demonstrating the potential of multi-modal data integration in cognitive research.

INDEX WORDS: Imaging genomics, Feature selection, Deep learning, Contrastive learning, Working memory, Genetic variants, Neuroimaging, Contrastive learning, Sparse canonical correlation analysis

Imaging Genetic Prediction on Cognition and Symptoms in Both Small and Big Cohorts

by

Pranav Nadigapu Suresh

Committee Chair: Jingyu Liu

Committee: Sergey Plis

Jessica Turner

Dong Hye Ye

Electronic Version Approved:

Office of Graduate Services

College of Arts and Sciences

Georgia State University

August 2024

DEDICATION

This dissertation is dedicated to my family, whose unwavering support and love have been my greatest strength throughout this journey. To my late Ammamma and Peddananna, whose memories continue to inspire me. To my wife, thank you for your incredible patience, understanding, and support over the past year. I extend my deepest gratitude to Prem mama for inspiration and to Srinu mama for instilling in me the value of financial discipline and for many memories since childhood. To Middu peddamma, Indu peddamma, and Amma, thank you for your constant prayers and everything you have done for me since childhood. Your guidance and nurturing have been invaluable. To anna and vadina, your support and counsel have been instrumental in my growth. Lastly, to my dad, whose belief in me has been a constant source of motivation.

ACKNOWLEDGEMENTS

I would like to express my deepest gratitude to my advisor, Dr. Jingyu Liu, for her unwavering trust and belief in my potential, despite my lack of prior research experience. Her guidance, support, and encouragement have been invaluable in helping me navigate the complexities of this Ph.D. journey and accomplish my research goals. Dr. Liu's expertise and dedication have inspired me to strive for excellence and have significantly shaped my academic growth.

I would also like to extend my heartfelt thanks to my colleagues at the TReNDS center. Their collaboration, insights, and camaraderie have made this journey a fulfilling and enriching experience. The supportive and intellectually stimulating environment at TReNDS has been instrumental in my development as a researcher, and I am grateful for the friendships and professional relationships I have built during my time here.

Thank you all for your contributions and support, which have made this dissertation possible.

TABLE OF CONTENTS

LIST OF TABLES

LIST OF FIGURES

LIST OF ABBREVIATIONS

ADHD: Attention-Deficit/Hyperactivity Disorder

BOLD: Blood-Oxygen-Level-Dependent

CNN: Convolutional Neural Network

DMN: Default Mode Network

DTI: Diffusion Tensor Imaging

EEG: Electroencephalography

fMRI: Functional Magnetic Resonance Imaging

GWAS: Genome-Wide Association Studies

ICA: Independent Component Analysis

MDD: Major Depressive Disorder

MEG: Magnetoencephalography

MRI: Magnetic Resonance Imaging

PET: Positron Emission Tomography

PLS: Partial Least Squares

pICA: Parallel Independent Component Analysis

ROI: Region of Interest

SNP: Single Nucleotide Polymorphism

sMRI: Structural Magnetic Resonance Imaging

sCCA: Sparse Canonical Correlation Analysis

STT: Self-Transfer-Training

1 INTRODUCTION

Imaging genomics, also known as imaging genetics, is a burgeoning interdisciplinary field that combines neuroimaging and genetic data to investigate the genetic basis of brain structure and function (Bodalal et al., 2019). The field leverages advanced imaging technologies, such as magnetic resonance imaging (MRI) and positron emission tomography (PET), alongside high-throughput genomic techniques, including genome-wide association studies (GWAS) and single nucleotide polymorphism (SNP) analysis. This integrative approach aims to understand how genetic variations influence brain morphology, connectivity, and activity, thereby impacting cognitive functions and behaviors (Liu et al., 2021).

Cognition encompasses a range of mental processes that are essential for acquiring knowledge and understanding through thought, experience, and the senses. The primary components of cognition include attention, memory, language, perception, and executive functions. Attention is the cognitive process that allows individuals to focus on specific stimuli while ignoring others, and it is crucial for effectively processing information in our environment (Posner & Petersen, 1990). Memory, another key component, involves encoding, storing, and retrieving information, and it is divided into various types such as short-term memory, long-term memory, and working memory (Baddeley, 2000). Language is the ability to understand and produce spoken and written communication, playing a critical role in cognitive development and social interaction (Pinker, 1994).

The human brain's complexity, encompassing billions of neurons and intricate networks, is influenced by a combination of genetic and environmental factors. Understanding the genetic basis of brain structure and function has been a longstanding goal in neuroscience. Traditional genetic studies have identified numerous genes associated with neurological and psychiatric

disorders, but these studies often lack the spatial resolution to pinpoint how genetic variations manifest in brain structures and functions. Conversely, neuroimaging studies provide detailed insights into brain morphology and activity but often overlook genetic contributions. Imaging genomics bridges this gap by integrating genetic data with brain imaging, offering a comprehensive view of how genes influence the brain.

1.1 Background and Motivation

The primary goal of imaging genomics is to uncover the complex interactions between genetic factors and brain imaging phenotypes, which can provide insights into the underlying mechanisms of various neuropsychiatric and neurodevelopmental disorders. By mapping genetic variations to specific brain structures and functions, researchers can identify potential biomarkers for early diagnosis and targets for therapeutic interventions (Glahn et al., 2007).

Technological advancements have significantly propelled the field of imaging genomics. High-resolution neuroimaging techniques allow for detailed visualization of brain anatomy and function, while next-generation sequencing technologies enable comprehensive analysis of the genome (Shen & Thompson, 2020). The integration of these modalities has led to discoveries linking genetic polymorphisms to brain phenotypes associated with conditions such as Alzheimer's disease, schizophrenia, and attention-deficit/hyperactivity disorder (ADHD).

Medical imaging plays a vital role in patient healthcare. It aids in disease prevention, early detection, diagnosis, and treatment. However, efforts to employ machine learning algorithms to support in clinical settings are often hampered by the high costs of required expert annotations (Grünberg et al., 2017). At the same time, large-scale biobank studies have recently started to aggregate unprecedented scales of multimodal data on human health. For example, the UK

Biobank (UKB) contains data on 500,000 individuals, including a wide range of imaging modalities such as cardiac, abdominal, and brain MRI (Alfaro-Almagro et al., 2018).

On the other hand, genetic data is increasingly abundant. While chip-based genotyping technology has enabled the study of common genetic variation at scale (Verlouw et al., 2021), the exponentially decreasing costs of genomic sequencing is driving progress for rare genetic variation (Park & Kim, 2016). Due to these advances, the UKB and other biobanks often contain a rich array of genetic and genomic measurements. Genetic data is generally less susceptible to biased factors, and many diseases have at least a partially genetic cause, with some genetic disorders being almost exclusively attributed to genetic mutations. Similarly, most other traits – not directly related to diseases, e.g., height and human personality, are also strongly influenced by genetics (Lippert et al., 2017; Zwir et al., 2020).

The field has also benefited from the development of sophisticated computational methods. Machine learning and statistical modeling techniques are employed to analyze large-scale, high-dimensional data, facilitating the identification of significant genetic-imaging associations (Duan et al., 2023; Jiang et al., 2020; Liu et al., 2020). These methods include univariate approaches such as Genome-Wide Association Studies (GWAS) to multivariate approaches such as sparse canonical correlation analysis (sCCA), which can handle the complexity and high dimensionality of imaging genomics data.

Despite significant progress, several challenges remain in the field of imaging genomics. One of the primary challenges is the integration of multimodal data from diverse sources, such as structural MRI, functional MRI, and genomic data, which requires sophisticated computational methods. Additionally, the high dimensionality and complexity of these datasets necessitate advanced machine learning techniques to extract meaningful patterns and associations. Our

research aims to address these challenges by developing and applying novel algorithms to analyze imaging genomics data. This dissertation focuses on two main areas: understanding the genetic basis of cognitive functions, specifically working memory, and predicting symptom trajectories in neuropsychiatric disorders like ADHD.

1.2 Research Objectives

The overarching aim of this dissertation is to deepen our understanding of the genetic and neural mechanisms underlying cognitive functions and their disorders, particularly focusing on working memory and ADHD. This research is motivated by the need to address existing challenges in the integration and analysis of multimodal data, including neuroimaging and genomics. Our specific research objectives are as follows:

Aim 1: To investigate the ability to predict the trajectory of symptoms in both inattention and hyperactivity domains using features derived from structural MRI (sMRI) images and genomic data from an ADHD cohort. ADHD is a common neurodevelopmental disorder characterized by persistent patterns of inattention, hyperactivity, and impulsivity. Understanding the genetic and neural bases of these symptoms can aid in early diagnosis and personalized treatment. This objective focuses on identifying key predictive features from sMRI and SNP data to predict changes in ADHD symptoms over time.

Aim 2: To develop a strategy for training convolutional neural networks (CNN) models effectively with limited sample sizes using a self-transfer-training (STT) method. One of the significant challenges in neuroimaging and genomics research is the limited availability of large datasets, which can hinder the training and generalization of machine learning models. The STT method aims to optimize the training process of CNNs by reusing and refining layers from pre-trained models.

Aim 3: To examine the potential of CNN models trained on structural MRI images to classify working memory capacity and identify relevant brain regions. Working memory is a critical cognitive function, and its capacity varies across individuals. Understanding the neural correlates of working memory can provide insights into cognitive processes and their genetic bases. This objective focuses on using CNNs to learn from structural MRI data to classify individuals' working memory capacity.

Aim 4: To integrate neuroimaging and genetic data using contrastive learning for the prediction of working memory, utilizing data from the UK Biobank. The integration of multimodal data is crucial for a comprehensive understanding of cognitive functions and their genetic underpinnings. Contrastive learning allows for the alignment of imaging and genetic modalities, improving the identification of significant associations.

1.3 Significance of the Study

The significance of this research lies in its potential to advance the field of cognitive neuroscience and improve clinical outcomes. By elucidating the genetic and neural underpinnings of cognitive functions, this study could lead to the development of more precise diagnostic tools and personalized therapeutic strategies for cognitive impairments and neuropsychiatric disorders. Furthermore, the methodologies developed in this dissertation could be applied to other complex traits and conditions, broadening the impact of this work.

1.4 Overview of Research Methodology

Our research methodology involves the integration of multimodal data, including sMRI and SNP data, with advanced machine learning techniques. We employ stepwise linear regression coupled with stability selection and permutation tests, convolutional neural networks (CNN) with self-transfer-training (STT), and contrastive learning with sparse canonical correlation analysis

(sCCA). These methods are designed to address the complexity and high dimensionality of imaging genomics data, facilitating the identification of significant genetic-imaging associations.

1.5 Structure of the Dissertation

This dissertation is structured to provide a comprehensive examination of the genetic and neural mechanisms underlying cognitive functions, particularly focusing on working memory and ADHD. The research is presented in a series of interconnected chapters, each dedicated to specific aspects of the study. Below is an overview of each chapter and its contribution to the overall research objectives.

Chapter 1 introduces the field of imaging genomics, outlining the significance of integrating neuroimaging and genetic data to understand brain structure and function. It includes the background and motivation for the study, defines the research objectives, highlights the significance of the study, and gives an overview of the research methodology and the structure of the dissertation.

Chapter 2: Literature Review reviews the current state of research in imaging genomics, covering theoretical frameworks, key concepts, and previous studies relevant to the dissertation. It identifies research gaps and provides a foundation for the subsequent chapters.

Chapter 3: Predicting Symptom Trajectories in ADHD Using Imaging Genomics investigates the ability to predict the trajectory of symptoms in ADHD, focusing on inattention and hyperactivity domains using features from sMRI images and genomic data. The methods include stepwise linear regression, stability selection, and permutation tests. The results identify key predictive features, and the discussion interprets these findings in the context of existing literature.

Chapter 4: Training CNN Models with Limited Samples Using Self-Transfer-Training (STT) addresses the challenge of limited sample sizes in neuroimaging and genomics research by developing a self-transfer-training (STT) method for training convolutional neural networks (CNN) models. It describes the initial training and hyperparameter tuning, followed by retraining with frozen and refined layers. The results demonstrate the effectiveness of the STT approach, with a discussion on its benefits and limitations.

Chapter 5: Classifying Working Memory Capacity Using CNN Models examines the potential of CNN models trained on structural MRI images to classify working memory capacity and identify relevant brain regions. It details the training process, the application of transfer learning techniques, and the results, which highlight the classification accuracy and the brain regions involved in working memory. The discussion provides an interpretation of these findings.

Chapter 6: Integrating Neuroimaging and Genetics via Contrastive Learning for Working Memory Prediction focuses on the integration of neuroimaging and genetic data using contrastive learning techniques to predict working memory capacity. It combines structural MRI and SNP data from the UK Biobank, employing contrastive learning and sparse canonical correlation analysis (sCCA) to uncover significant genetic-imaging associations. The results and discussion explore the implications for understanding the genetic basis of working memory.

Chapter 7: Conclusions and Future Directions summarizes the research aims, methods, and key findings of the dissertation. It highlights the main contributions to the field, discusses potential limitations, and provides recommendations for future research directions. The chapter emphasizes the significance of the study and its potential applications in cognitive neuroscience and clinical practice.

2 LITERATURE REVIEW

The field of imaging genomics, also known as imaging genetics, is a rapidly evolving interdisciplinary area that combines neuroimaging and genetic data to investigate the genetic basis of brain structure and function. This literature review aims to provide a comprehensive overview of the current state of research in imaging genomics, focusing on advancements in neuroimaging techniques, the role of genetic variations in cognitive functions, and the integration of these modalities through advanced computational techniques. By reviewing key studies and methodologies, this chapter aims to identify research gaps and establish a theoretical and empirical foundation for the current dissertation.

The purpose of this literature review is to critically evaluate existing research on the intersection of neuroimaging and genomics, with a particular emphasis on understanding cognitive functions such as working memory and disorders like ADHD. The scope of the review includes advancements in neuroimaging technologies, genetic analyses, and the computational methods employed to integrate and analyze multimodal data. This review also aims to highlight the challenges and limitations in the current research landscape and suggest potential areas for future investigation.

2.1 Structure of the Literature Review

This literature review is organized into several key sections:

1. **Theoretical Framework**: An overview of the key theories and concepts that underpin the field of imaging genomics. This section will discuss the theoretical foundations that guide the integration of neuroimaging and genetic data.
2. **Advancements in Neuroimaging Techniques**: A detailed examination of the various neuroimaging technologies, including structural MRI (sMRI), functional MRI (fMRI), and

other imaging modalities such as PET and EEG. This section will highlight significant studies and findings that have advanced our understanding of brain structure and function.

3. **Genomics and Genetic Variations**: An exploration of genomic technologies and the genetic variations that are most relevant to cognitive functions. This section will review key genetic factors identified through genome-wide association studies (GWAS) and other genomic analyses.
4. **Imaging Genomics: Integrating Neuroimaging and Genetic Data**: An analysis of the methods used to combine neuroimaging and genetic data, including both univariate and multivariate approaches. This section will discuss significant findings from imaging genomics studies that have provided insights into the genetic basis of brain phenotypes.
5. **Machine Learning and Computational Techniques in Imaging Genomics**: A review of the computational methods, particularly machine learning techniques, used to analyze imaging genomics data. This section will cover convolutional neural networks (CNN), contrastive learning, and sparse canonical correlation analysis (sCCA), among others.
6. **Specific Focus Areas in Imaging Genomics**: Focused reviews on specific applications of imaging genomics, particularly in ADHD and working memory research. This section will summarize the key studies that have linked neuroimaging and genetic data to these cognitive functions and disorders.
7. **Challenges and Research Gaps in Imaging Genomics**: An identification of the main challenges and limitations in current imaging genomics research, such as data integration issues and the high dimensionality of datasets. This section will also highlight the gaps in literature and propose areas for future research.

8. **Summary**: A recap of the main points covered in the literature review, emphasizing the relevance of the reviewed literature to the current dissertation's research objectives.
9. **Conclusion**: A summary of the theoretical and empirical background, leading into the methodology chapter.

By systematically reviewing the existing literature, this chapter aims to provide a comprehensive background for understanding the complex interactions between genetic variations and brain phenotypes. This foundation is critical for advancing our knowledge of cognitive functions and their disorders, ultimately guiding the research presented in this dissertation.

2.2 Theoretical Framework

Imaging genomics, also known as imaging genetics, is a multidisciplinary field that bridges neuroimaging and genetics to elucidate how genetic variations affect brain structure and function. This section outlines the fundamental theories and concepts underpinning imaging genomics, including neurogenetics, neuroimaging principles, multimodal data integration, and the application of machine learning techniques.

2.2.1 Genetics

Genetics is the study of heredity and the variation of inherited characteristics. In the context of imaging genomics, it focuses on identifying genetic variations that influence brain structure and function. The following are key genetic modalities used in this field:

2.2.1.1 Single Nucleotide Polymorphisms (SNPs)

Single nucleotide polymorphisms, commonly known as SNPs (pronounced "snips"), represent the most frequent type of genetic variation among humans. Each SNP involves a variation at a single position in the DNA sequence, where one nucleotide is substituted for another. For example, a SNP may change the DNA sequence from AAGGCT to ATGGCT, where the

nucleotide adenine (A) is replaced by thymine (T). SNPs occur approximately once in every 300 nucleotides, which means there are roughly 10 million SNPs in the human genome. This high frequency makes SNPs valuable markers for studying human genetic diversity and disease susceptibility (Health, 2019).

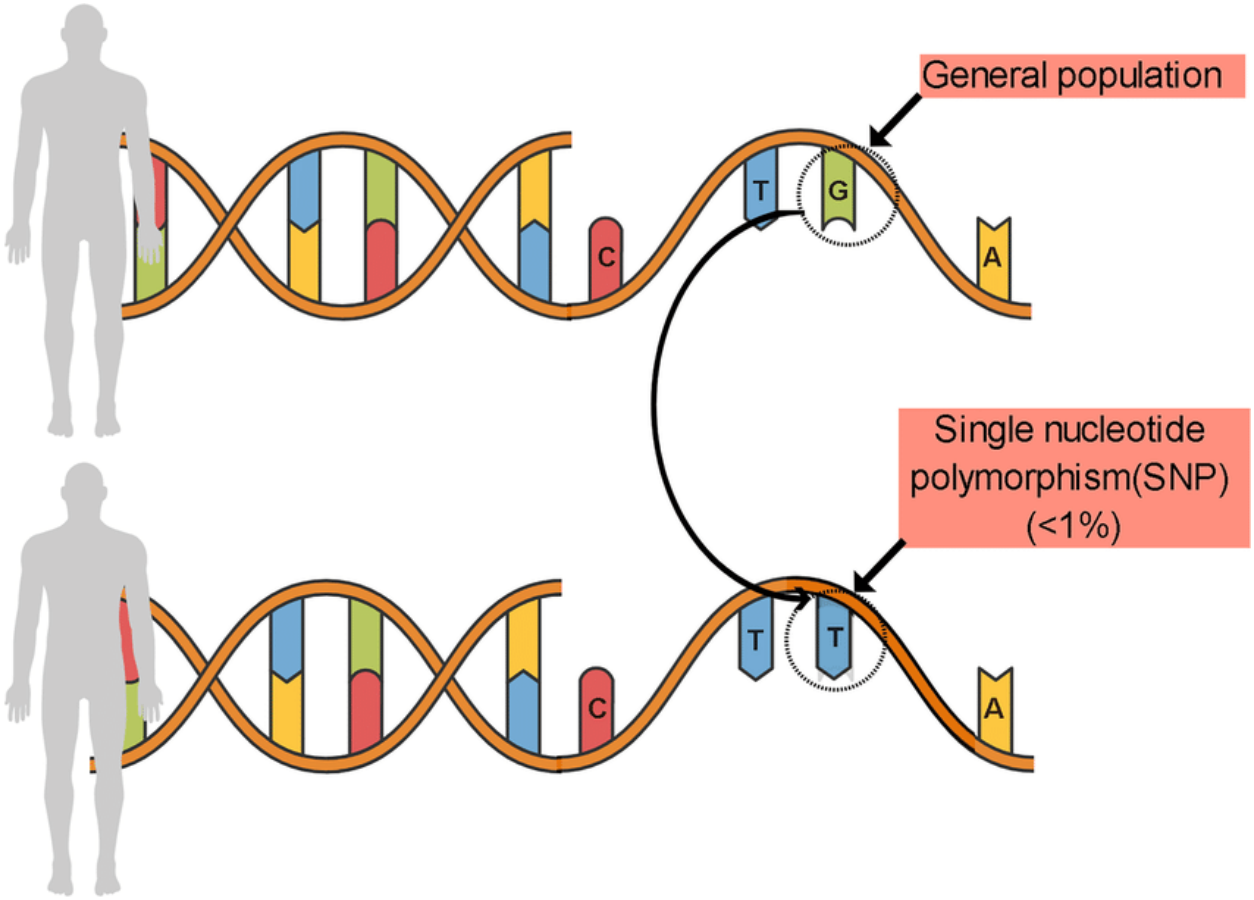

Figure 2.1: Single-nucleotide polymorphism (SNP)

SNPs are widely used in genetic research because they can serve as biological markers, helping scientists locate genes associated with disease. By comparing SNP patterns between individuals with and without a particular disease, researchers can identify genetic differences that may contribute to the disease's development. Genome-wide association studies (GWAS) leverage this approach to scan the entire genome of many individuals, searching for SNPs that occur more

frequently in people with a specific condition than in those without it (Visscher et al., 2012). These studies have successfully identified numerous SNPs linked to complex diseases such as diabetes, cancer, and neuropsychiatric disorders, including schizophrenia and Alzheimer's disease (Visscher et al., 2012).

In the context of imaging genomics, SNPs play a crucial role in understanding the genetic basis of brain structure and function. Researchers analyze the association between SNPs and various neuroimaging phenotypes, such as brain volume, cortical thickness, and connectivity patterns. For example, studies have identified SNPs in the gene BDNF (Brain-Derived Neurotrophic Factor) that are associated with differences in hippocampal volume, a brain region critical for memory and learning (Stein et al., 2012). These findings suggest that genetic variations can influence brain morphology, potentially affecting cognitive abilities and risk for neurological disorders.

The functional impact of SNPs can vary widely. Some SNPs may have no effect on gene function or protein production, while others can influence how a gene is expressed or alter the function of a protein. Non-coding SNPs, which are located in regions of the DNA that do not encode proteins, can affect gene regulation by altering transcription factor binding sites or RNA stability. Coding SNPs, which occur within gene exons, can lead to amino acid substitutions in proteins, potentially affecting their structure and function. Understanding the functional consequences of specific SNPs is essential for elucidating the molecular mechanisms underlying their associations with complex traits and diseases.

Furthermore, SNPs are valuable in personalized medicine, an emerging approach that tailor’s medical treatment to an individual’s genetic makeup. By identifying SNPs that influence drug metabolism, efficacy, and risk of adverse reactions, healthcare providers can optimize drug

selection and dosing for each patient. For instance, certain SNPs in the CYP2C19 gene affect the metabolism of the antiplatelet drug clopidogrel, influencing treatment outcomes in patients with cardiovascular disease. Genotyping these SNPs allows for more precise and effective medical interventions (Mega et al., 2009) (Pezawas et al., 2005).

Overall, SNPs are a fundamental tool in genetic research, providing insights into human diversity, disease mechanisms, and personalized medicine. Their application in imaging genomics enhances our understanding of how genetic variations shape brain structure and function, contributing to the broader field of cognitive neuroscience and mental health research.

2.2.1.2 Genome-Wide Association Studies (GWAS)

Genome-wide association studies (GWAS) are a powerful and widely used method for identifying genetic variations associated with complex traits and diseases. Unlike traditional genetic studies that focus on a small number of candidate genes, GWAS scan the entire genome to uncover associations between single nucleotide polymorphisms (SNPs) and specific traits (Tam et al., 2019). This comprehensive approach has revolutionized the field of genetics, leading to significant discoveries across a broad range of medical and biological research areas.

The fundamental principle behind GWAS is the use of high-throughput genotyping technologies to assess millions of SNPs across the genomes of large cohorts. These studies require a substantial sample size to detect genetic variants with modest effects, which are typical for complex traits influenced by multiple genes and environmental factors. The statistical power of GWAS lies in its ability to detect associations between SNPs and traits without prior hypotheses about candidate genes, making it an unbiased and comprehensive approach to genetic discovery (Visscher et al., 2012).

One of the landmark successes of GWAS is the identification of numerous genetic loci associated with common diseases such as diabetes, cardiovascular disease, and various forms of cancer. For instance, GWAS have uncovered several risk alleles in the FTO gene linked to obesity and type 2 diabetes, providing insights into the biological pathways involved in these conditions (Loos & Yeo, 2014). Similarly, multiple loci associated with coronary artery disease have been identified, shedding light on the genetic architecture of cardiovascular risk and highlighting potential targets for therapeutic intervention (Tcheandjieu et al., 2022).

In the context of neuropsychiatric disorders, GWAS have significantly advanced our understanding of the genetic basis of conditions like schizophrenia (Ripke et al., 2014), bipolar disorder (Mullins et al., 2021), and major depressive disorder (Meng et al., 2024). For example, a large-scale GWAS conducted by the Psychiatric Genomics Consortium identified over 100 loci associated with schizophrenia, implicating genes involved in synaptic function, neurotransmitter pathways, and immune system processes (Ripke et al., 2014). These findings have provided a deeper understanding of the molecular mechanisms underlying schizophrenia and have opened new avenues for research into its pathophysiology and treatment.

GWAS have also been instrumental in elucidating the genetic influences on brain structure and function. Studies integrating GWAS with neuroimaging data have identified SNPs associated with variations in brain morphology, such as cortical thickness and hippocampal volume (Horgusluoglu-Moloch et al., 2019). For instance, research has linked variants in the gene KIBRA to hippocampal volume and memory performance, suggesting a genetic basis for individual differences in cognitive abilities (Kirchner et al., 2023). These integrative approaches, often referred to as imaging genomics, bridge the gap between genetics and neuroscience, offering insights into how genetic variations influence brain phenotypes and cognitive functions.

Despite their successes, GWAS face several challenges and limitations. One significant challenge is the need for large sample sizes to achieve sufficient statistical power, particularly for detecting variants with small effect sizes. Additionally, GWAS typically identify associations rather than causal relationships, requiring further functional studies to elucidate the biological mechanisms underlying the identified loci. Another limitation is that GWAS findings can sometimes be difficult to replicate across different populations, highlighting the importance of considering population stratification and genetic diversity in study designs.

Moreover, while GWAS have been successful in identifying common variants associated with complex traits, they often leave a substantial portion of the heritability unexplained, a phenomenon known as "missing heritability." This suggests that other types of genetic variation, such as rare variants, structural variants, and gene-gene interactions, may also play crucial roles. Advances in sequencing technologies and analytical methods are helping to address these gaps, providing a more comprehensive understanding of the genetic architecture of complex traits (Manolio et al., 2009).

2.2.1.3 Epigenetics

Epigenetics is the study of heritable changes in gene expression that do not involve alterations to the underlying DNA sequence. These changes are mediated by various mechanisms, including DNA methylation, histone modification, and non-coding RNAs, which collectively influence how genes are turned on or off. Unlike genetic mutations, which alter the DNA sequence, epigenetic modifications are reversible and can be influenced by environmental factors, making epigenetics a dynamic interface between the genome and the environment (Bird, 2007).

One of the primary mechanisms of epigenetic regulation is DNA methylation, which involves the addition of a methyl group to the cytosine nucleotide in the context of a CpG

dinucleotide. DNA methylation typically acts to repress gene expression when located in gene promoter regions. Aberrant DNA methylation patterns have been implicated in various diseases, including cancer, where hypermethylation of tumor suppressor genes and hypomethylation of oncogenes can contribute to tumorigenesis. In neuropsychiatric disorders, alterations in DNA methylation have been associated with conditions such as schizophrenia, autism spectrum disorder, and depression, suggesting that epigenetic changes can significantly impact brain function and behavior (Tammen et al., 2013).

The field of epigenetics has profound implications for understanding complex traits and diseases. One of the most exciting aspects of epigenetic research is the concept of epigenetic plasticity, which refers to the ability of the epigenome to change in response to environmental stimuli. This plasticity means that lifestyle factors, such as diet, exercise, stress, and exposure to toxins, can influence epigenetic marks and, consequently, gene expression patterns. For example, studies have shown that early-life stress can lead to long-lasting changes in DNA methylation and histone modifications, affecting stress-response genes and potentially contributing to the development of mental health disorders later in life (Kular & Kular, 2018).

In the context of neuropsychiatric disorders, epigenetic modifications have been shown to play a critical role in brain development and function. For instance, aberrant DNA methylation patterns in genes involved in synaptic plasticity, neurodevelopment, and neurotransmitter systems have been associated with schizophrenia and autism spectrum disorder. These findings suggest that epigenetic dysregulation can disrupt normal brain function and contribute to the pathophysiology of these disorders. Moreover, epigenetic research has opened new avenues for therapeutic interventions. Drugs targeting epigenetic modifications, such as DNA methyltransferase inhibitors and histone deacetylase inhibitors, are being explored for their

potential to reverse aberrant epigenetic marks and restore normal gene expression patterns (Griffiths & Gore, 2008).

2.2.2 Neurogenetics

Neurogenetics is the study of how genetic variations influence the development, structure, and function of the nervous system. The field explores the role of genes in brain development and the manifestation of neurological and psychiatric disorders. Key theories in neurogenetics include the concept of gene-environment interactions, where genetic predispositions interact with environmental factors to influence brain phenotypes and behaviors.

2.2.2.1 Gene-Environment Interactions

Gene-environment interactions (GxE) refer to the complex interplay between genetic predispositions and environmental factors in determining an individual's phenotype. This concept underscores that neither genetic factors nor environmental influences alone can fully explain the variability in traits or the development of complex diseases. Instead, it is the interaction between these elements that shapes outcomes, contributing to the diversity seen in human health and behavior (Virolainen et al., 2022-12-30).

One example of GxE interactions is the relationship between genetic susceptibility to mental health disorders and exposure to stressful life events. For instance, individuals carrying a specific variant of the serotonin transporter gene (5-HTTLPR) are more likely to develop depression following stressful life events compared to those without this genetic variant (Goldman et al., 2010). This interaction was highlighted in a landmark study by Caspi et al. (2003), which demonstrated that the presence of the short allele of the 5-HTTLPR gene moderated the effect of stressful life events on the risk of developing depression (Caspi et al., 2003). This finding

emphasizes that genetic predispositions can influence how individuals respond to environmental stressors, leading to different psychological outcomes.

Another well-documented case of GxE interactions is in the development of asthma. Genetic factors such as variations in the IL4R gene, which encodes a receptor involved in the immune response, have been linked to an increased risk of asthma. However, environmental factors such as exposure to allergens, air pollution, and tobacco smoke also play a crucial role. Studies have shown that children with certain genetic variants are more susceptible to developing asthma when exposed to high levels of air pollution, illustrating the significant impact of GxE interactions on respiratory health (Wenzel et al., 2007).

In the realm of neurodevelopmental disorders, GxE interactions are equally significant. Autism spectrum disorder (ASD) is influenced by both genetic and environmental factors (Tordjman et al., 2014). For example, prenatal exposure to environmental toxins such as pesticides or maternal infection during pregnancy has been associated with an increased risk of ASD, particularly in genetically susceptible individuals. Research indicates that certain genetic mutations related to synaptic function and neural development can increase vulnerability to these environmental insults, thereby contributing to the development of ASD (Tordjman et al., 2014).

The study of GxE interactions also extends to cognitive functions. Cognitive abilities, such as intelligence and memory, are influenced by both genetic factors and environmental conditions, including education, nutrition, and social interactions (von Stumm et al., 2023). Twin studies have been instrumental in disentangling the relative contributions of genes and environment (Dick, 2011). For instance, the heritability of intelligence has been estimated to be around 50%, but this estimate can vary significantly depending on the environmental context. Children raised in enriched environments, with access to better educational resources and stimulation, often show

higher cognitive performance regardless of genetic background, highlighting the profound impact of GxE interactions on cognitive development (Provençal & Binder, 2015).

2.2.2.2 Endophenotypes

Endophenotypes are measurable components along the pathway between a genetic predisposition and the clinical manifestation of a disorder. These intermediate phenotypes are more closely related to the underlying genetic mechanisms than the complex traits or diseases themselves, making them valuable in genetic and neuropsychiatric research. The concept of endophenotypes bridges the gap between observable symptoms and the genetic architecture, providing a more straightforward target for genetic analysis (Irving I. Gottesman & Todd D. Gould, 2003).

The utility of endophenotypes lies in their ability to decompose complex traits into simpler, more quantifiable elements. This decomposition is particularly useful in the study of neuropsychiatric disorders, where symptoms can be highly heterogeneous and influenced by a myriad of genetic and environmental factors. By identifying endophenotypes, researchers can focus on specific biological or cognitive processes that may be disrupted in these disorders, thereby improving the power to detect genetic associations and understanding the underlying pathophysiology. For instance, in schizophrenia research, cognitive deficits such as working memory impairment and abnormal eye-tracking movements have been identified as potential endophenotypes (Park & Gooding, 2014). These traits are more heritable and less influenced by external factors compared to the broader clinical diagnosis of schizophrenia, making them more reliable indicators of genetic risk (Turetsky et al., 2007).

One of the key criteria for an endophenotype is that it must be heritable and co-segregate with the disorder within families. Additionally, endophenotypes should be present in unaffected

family members of individuals with the disorder, albeit to a lesser extent. This characteristic indicates that endophenotypes are not merely symptoms but are fundamentally linked to the genetic basis of the disorder. For example, studies have shown that first-degree relatives of individuals with schizophrenia exhibit similar, albeit milder, deficits in cognitive functions such as attention and memory, supporting the role of these cognitive deficits as endophenotypes.

In the realm of affective disorders, neuroimaging has been instrumental in identifying potential endophenotypes. Structural and functional brain abnormalities, such as reduced hippocampal volume and altered activity in the prefrontal cortex and amygdala, have been observed in individuals with major depressive disorder (MDD) and their unaffected relatives. These findings suggest that such brain abnormalities could serve as endophenotypes for MDD, reflecting underlying genetic vulnerabilities that predispose individuals to the disorder. Similarly, in bipolar disorder, traits like increased sensitivity to reward and emotional dysregulation have been proposed as endophenotypes, given their heritability and presence in unaffected family members.

The identification of endophenotypes extends beyond neuropsychiatric disorders to other complex traits and diseases. In addiction research, endophenotypes such as impulsivity, stress reactivity, and reward sensitivity are used to explore the genetic basis of substance use disorders. These traits are heritable, stable over time, and observed in individuals at risk for addiction, making them valuable targets for genetic studies. By focusing on these intermediate traits, researchers can better understand the genetic and neurobiological mechanisms that contribute to the development and maintenance of addictive behaviors (Belin et al., 2016).

Moreover, endophenotypes can facilitate the development of more precise and personalized treatment strategies. By targeting specific endophenotypes, interventions can be

tailored to address the underlying cognitive or biological deficits rather than just the symptoms of the disorder. For instance, cognitive remediation therapies designed to improve working memory and executive function have shown promise in individuals with schizophrenia, potentially ameliorating some of the cognitive deficits associated with the disorder. Similarly, interventions aimed at reducing impulsivity and improving stress management may be effective in preventing substance abuse in at-risk populations (Barlati et al., 2013).

Overall, the concept of endophenotypes provides a robust framework for dissecting the complexity of genetic influences on behavior and disease. By identifying and studying these intermediate phenotypes, researchers can gain deeper insights into the biological pathways that link genes to clinical outcomes, ultimately advancing our understanding of the etiology and treatment of complex disorders.

2.3 Advancements in Neuroimaging Techniques

Neuroimaging encompasses a range of techniques that allow scientists to visualize the structure and function of the brain in unprecedented detail. These techniques provide critical insights into the organization and workings of the brain, facilitating the study of neurological and psychiatric disorders, as well as normal cognitive functions. The ability to non-invasively examine the brain's architecture and activity has revolutionized neuroscience, offering a window into the neural substrates underlying behavior and mental processes.

2.3.1 Structural Magnetic Resonance Imaging (sMRI)

Structural magnetic resonance imaging (sMRI) is a pivotal neuroimaging technique that provides detailed images of the brain's anatomy. Utilizing strong magnetic fields and radiofrequency pulses, sMRI produces high-resolution images that allow for precise measurement of brain structures, including cortical thickness, surface area, and volumetric properties of different

brain regions. This non-invasive method is instrumental in both clinical and research settings, offering invaluable insights into brain morphology and its alterations associated with various neurological and psychiatric conditions (Jack et al., 1998).

One of the primary advantages of sMRI is its ability to detect subtle changes in brain structure. This capability is particularly important in the study of neurodegenerative diseases such as Alzheimer's disease, where early diagnosis and monitoring of disease progression are critical. sMRI can reveal brain atrophy patterns, such as the reduction in hippocampal volume, which is a hallmark of Alzheimer's disease (Jack et al., 1998). Longitudinal sMRI studies have shown that hippocampal atrophy rates correlate with the progression of cognitive decline, making sMRI a crucial tool for tracking disease progression and evaluating the efficacy of therapeutic interventions (Xiao et al., 2023).

In addition to its application in neurodegenerative diseases, sMRI is widely used in psychiatric research. Studies employing sMRI have identified structural brain abnormalities associated with various psychiatric disorders, including schizophrenia (Honea et al., 2005), bipolar disorder (Macoveanu et al., 2021), and major depressive disorder (Wu et al., 2020). For instance, individuals with schizophrenia often exhibit reduced gray matter volume in the prefrontal cortex, temporal lobes, and other brain regions involved in cognitive and emotional processing (Wu et al., 2020). These findings have provided insights into the neuroanatomical underpinnings of schizophrenia, supporting the hypothesis that the disorder involves widespread brain network dysfunctions.

sMRI also plays a crucial role in understanding brain development and aging. In developmental neuroscience, sMRI has been used to study the maturation of brain structures during childhood and adolescence (Johnson et al., 2009). These studies have revealed that brain

development follows a non-linear trajectory, with different regions maturing at different rates. For example, the prefrontal cortex, which is essential for executive functions such as decision-making and impulse control, continues to develop well into young adulthood (Gogtay et al., 2004). Conversely, in aging research, sMRI has been utilized to investigate age-related changes in brain volume and cortical thickness, contributing to our understanding of cognitive decline in older adults (Johnson et al., 2009).

Moreover, sMRI's ability to measure white matter integrity has expanded its applications to studying brain connectivity. Techniques such as diffusion tensor imaging (DTI), which is often performed in conjunction with sMRI, allow researchers to examine the microstructural properties of white matter tracts. This combination provides a comprehensive view of both gray and white matter structures, enabling a better understanding of how brain regions are interconnected and how these connections may be disrupted in various conditions. For example, reduced white matter integrity in the corpus callosum has been associated with impaired interhemispheric communication in multiple sclerosis and other neurodegenerative diseases (Basser et al., 1994).

structural MRI is a versatile and powerful neuroimaging tool that has significantly advanced our understanding of brain structure and its alterations in health and disease. Its ability to provide detailed and accurate measurements of brain morphology makes it indispensable for diagnosing and monitoring neurological and psychiatric conditions, studying brain development and aging, and exploring the structural basis of brain connectivity. As sMRI technology continues to evolve, it will undoubtedly continue to play a crucial role in neuroscience research and clinical practice.

2.3.2 Functional Magnetic Resonance Imaging (fMRI)

Functional magnetic resonance imaging (fMRI) is a pivotal neuroimaging technique that measures brain activity by detecting changes associated with blood flow. The fundamental principle behind fMRI is the blood-oxygen-level-dependent (BOLD) signal, which relies on the fact that cerebral blood flow and neuronal activation are coupled. When a brain region becomes more active, it consumes more oxygen, leading to an increase in local blood flow to meet the metabolic demands. This hemodynamic response results in a relative decrease in deoxygenated hemoglobin, which has different magnetic properties than oxygenated hemoglobin, thereby altering the MR signal and allowing the detection of brain activity (Logothetis, 2008).

One of the major advantages of fMRI is its ability to non-invasively map functional activity across the entire brain with high spatial resolution. This capability has revolutionized cognitive neuroscience by enabling researchers to investigate the neural correlates of a wide range of cognitive processes, such as perception, memory, attention, and emotion. For instance, studies using fMRI have elucidated the brain networks involved in working memory, highlighting the roles of the prefrontal cortex and parietal lobes in maintaining and manipulating information (Emch et al., 2019). Similarly, fMRI research has advanced our understanding of the neural basis of emotional processing by identifying key regions such as the amygdala and prefrontal cortex, which are involved in the regulation of emotional responses (Kustubayeva et al., 2023).

The versatility of fMRI extends to its use in studying the functional connectivity of the brain. Functional connectivity refers to the temporal correlation between spatially remote brain regions, indicating that these areas are functionally linked. Resting-state fMRI (rs-fMRI) is a popular approach to studying functional connectivity, as it measures spontaneous brain activity while the subject is not engaged in any specific task. Rs-fMRI has revealed the existence of

intrinsic brain networks, such as the default mode network (DMN), which is active during rest and involved in self-referential and introspective activities. Alterations in the connectivity of these networks have been implicated in various neurological and psychiatric disorders, including Alzheimer's disease, schizophrenia, and depression (Brandman et al., 2021).

fMRI has also been instrumental in clinical research and applications. For example, pre-surgical fMRI is used to map critical functional areas in patients undergoing brain surgery, such as those with tumors or epilepsy. By identifying regions involved in language, motor functions, and sensory processing, surgeons can minimize the risk of impairing essential cognitive and motor abilities. Furthermore, fMRI is increasingly employed in neurofeedback and brain-computer interface (BCI) applications, where real-time feedback of brain activity is used to train individuals to modulate their brain functions, potentially offering therapeutic benefits for conditions like chronic pain, ADHD, and depression (Pilmeyer et al., 2022).

Functional MRI has become an indispensable tool in neuroscience, offering profound insights into the functional architecture of the brain. Its ability to non-invasively map brain activity and connectivity has facilitated the study of complex cognitive processes and the identification of neural abnormalities associated with various disorders. As technology and analytical methods continue to evolve, fMRI is poised to further our understanding of brain function and contribute to the development of novel therapeutic strategies.

2.3.3 Other Imaging Modalities

In addition to structural MRI (sMRI) and functional MRI (fMRI), several other neuroimaging modalities provide complementary insights into brain structure and function. These techniques, including positron emission tomography (PET), electroencephalography (EEG), and

magnetoencephalography (MEG), offer unique advantages that enhance our understanding of the brain's intricate workings.

2.3.3.1 Positron Emission Tomography (PET)

Positron emission tomography (PET) is a powerful imaging modality that provides detailed images of metabolic processes and molecular activity within the brain. PET involves the use of radiotracers—radioactive substances that are injected into the bloodstream and accumulate in specific brain regions based on their metabolic activity. By detecting the gamma rays emitted from these tracers, PET scans can measure various physiological processes, including glucose metabolism, blood flow, and neurotransmitter activity. This technique is particularly valuable for studying the brain's chemical environment and identifying abnormalities in neurotransmitter systems. For example, PET has been used to investigate the dopaminergic system in Parkinson's disease, revealing reduced dopamine activity in the basal ganglia, which correlates with motor symptoms (Loane & Politis, 2011). Similarly, PET studies in depression have identified alterations in serotonin and dopamine pathways, providing insights into the neurochemical basis of mood disorders (Singh et al., 2024).

2.3.3.2 Electroencephalography (EEG)

Electroencephalography (EEG) is a non-invasive technique that measures electrical activity generated by the brain's neurons. By placing electrodes on the scalp, EEG captures the brain's electrical signals, or brain waves, which reflect synchronous neuronal firing. EEG is renowned for its excellent temporal resolution, allowing researchers to track brain activity in real time with millisecond precision. This makes EEG particularly useful for studying dynamic cognitive processes, such as attention, perception, and sensory processing. For instance, event-related potentials (ERPs), derived from EEG data, are used to investigate the timing and sequence

of neural responses to specific stimuli, shedding light on cognitive and sensory processing stages. EEG is also widely used in clinical settings for diagnosing and monitoring neurological conditions such as epilepsy, where abnormal electrical activity patterns can be detected during seizures (Ein Shoka et al., 2023).

2.3.3.3 Magnetoencephalography (MEG)

Magnetoencephalography (MEG) is another technique that measures brain activity, but it detects the magnetic fields produced by neuronal electrical activity rather than the electrical signals themselves. MEG offers a combination of high temporal resolution, similar to EEG, and better spatial resolution, making it a powerful tool for mapping brain function. The magnetic fields measured by MEG are less distorted by the skull and scalp compared to the electrical signals detected by EEG, allowing for more precise localization of neural activity. MEG is particularly valuable for studying brain dynamics and connectivity, providing insights into how different brain regions interact during various cognitive tasks. It is also used in pre-surgical planning for epilepsy patients, helping to identify and preserve critical functional areas during surgery (Barlow, 1983).

Each of these imaging modalities—PET, EEG, and MEG—offers unique advantages that complement the capabilities of MRI. By integrating data from multiple imaging techniques, researchers can obtain a more comprehensive understanding of the brain's structure, function, and neurochemical environment. This multimodal approach is essential for advancing our knowledge of the brain's complexities and developing targeted interventions for neurological and psychiatric disorders.

2.4 Methodologies of Multimodal Imaging Genetic Integration

Imaging genomics, or imaging genetics, is an interdisciplinary field that aims to understand how genetic variations influence brain structure and function. By integrating neuroimaging and

genetic data, researchers can explore the complex interactions between genes and the brain, providing insights into the biological underpinnings of cognitive functions and neuropsychiatric disorders. This section of the literature review discusses the methodologies, findings, and implications of integrating neuroimaging and genetic data.

2.4.1 Univariate Approaches to Imaging Genomics

Univariate approaches to brain imaging genomics are foundational techniques that investigate the relationship between genetic variations and brain imaging phenotypes on a single-variable basis. These methods are often used to identify associations between specific genetic markers (such as single nucleotide polymorphisms, SNPs) and individual imaging measures (e.g., volume of a particular brain region, functional connectivity strength). The univariate approach is advantageous due to its simplicity and interpretability, making it a popular choice in early neuroimaging genetics studies.

2.4.1.1 Voxel Based Morphometry

Voxel-Based Morphometry (VBM) is a neuroimaging analysis technique that enables the investigation of focal differences in brain anatomy. It is widely used in brain imaging genomics to assess the relationship between genetic variations and brain structure. The process involves segmenting the brain into gray matter, white matter, and cerebrospinal fluid, and then comparing these segments across individuals to identify areas where local brain volume or concentration differ significantly (Ashburner & Friston, 2000).

The VBM process typically begins with the acquisition of high-resolution MRI scans, which are then preprocessed to ensure alignment and normalization to a standard brain template. This preprocessing involves steps such as segmentation of the brain into different tissue types (gray matter, white matter, and cerebrospinal fluid), spatial normalization to align individual brains to a

common space and smoothing to enhance the signal-to-noise ratio. These steps are crucial for ensuring that the subsequent statistical analyses are robust and reliable (R. G. Brans et al., 2010; Stein et al., 2010). The resulting preprocessed images can then be subjected to voxel-wise comparisons to identify regions where gray matter concentration correlates with genetic variants (Nemoto, 2017).

One of the key strengths of VBM in brain imaging genomics is its ability to conduct whole-brain analyses without a priori hypotheses about specific regions (Takeuchi & Kawashima, 2017). This unbiased approach allows for the discovery of novel brain-genetic associations that might not be identified using region-of-interest (ROI) methods. For instance, studies using VBM have identified associations between certain single nucleotide polymorphisms (SNPs) and gray matter volume in regions implicated in neuropsychiatric disorders (Stein et al., 2010). These findings provide valuable clues about the biological pathways through which genetic variations may contribute to the risk of developing such disorders (R. G. H. Brans et al., 2010).

Moreover, VBM has been effectively utilized in longitudinal studies to investigate how genetic factors influence brain development and aging (R. G. H. Brans et al., 2010). By comparing brain images from the same individuals at different time points, researchers can track changes in gray matter over time and relate these changes to genetic variations. This approach has revealed important insights into the genetic underpinnings of brain plasticity and the progression of neurodegenerative diseases. For example, VBM studies have shown how specific genetic variants can accelerate or decelerate age-related gray matter loss, highlighting potential targets for therapeutic intervention (R. G. H. Brans et al., 2010).

2.4.1.2 Region of Interest Analysis

Region of Interest (ROI) analysis is a pivotal method in the field of brain imaging genomics, offering a focused approach to understanding the relationships between genetic variations and specific brain structures or functions. Unlike whole-brain analyses, which examine the entire brain simultaneously, ROI analysis concentrates on predefined regions based on prior knowledge or hypotheses about their involvement in particular cognitive functions or neurological conditions (Fischl et al., 2002). This targeted approach allows for a more detailed and statistically powerful investigation of these regions, making it particularly useful in studies where the regions of interest are well-defined and hypothesized to be affected by genetic variations.

ROI analysis in structural MRI involves several key steps to ensure precise and reliable measurements. Initially, high-resolution T1-weighted MRI scans are acquired, offering detailed images of brain anatomy. These images undergo preprocessing steps, including skull stripping, bias field correction, and spatial normalization to a standard brain template, such as the Montreal Neurological Institute (MNI) template. The preprocessing ensures that individual brain images are aligned in a common space, facilitating accurate comparison across subjects (Ashburner & Friston, 2000).

Following preprocessing, the ROIs are delineated, either manually or using automated parcellation methods. Manual delineation involves an expert tracing the regions of interest based on anatomical landmarks, which can be time-consuming and subject to inter-rater variability. Automated methods, such as the use of atlases or machine learning algorithms, provide a more standardized approach, reducing subjectivity and enhancing reproducibility (Fischl et al., 2002). These methods can segment the brain into various regions, such as the hippocampus, amygdala, and prefrontal cortex, which are commonly studied in neurological and psychiatric research.

Once the ROIs are defined, the structural properties of these regions, such as volume, thickness, and surface area, are extracted and subjected to statistical analysis. These measures can then be correlated with behavioral data, clinical variables, or genetic markers to identify associations. For instance, ROI analysis has been pivotal in identifying volumetric reductions in the hippocampus in patients with Alzheimer's disease and in linking genetic polymorphisms to variations in cortical thickness (Raz et al., 2007).

The strength of ROI analysis lies in its ability to test specific hypotheses with high anatomical precision. By focusing on predefined regions, researchers can achieve greater statistical power to detect effects, especially in studies with limited sample sizes. Additionally, ROI analysis can be tailored to the research question at hand, whether it involves investigating disease-related atrophy, developmental changes, or genetic influences on brain structure. However, the method is not without limitations; it requires a priori selection of regions, which may bias the results if critical areas are overlooked. Despite this, ROI analysis remains an essential tool in the field of structural neuroimaging, providing valuable insights into the localized brain changes associated with various conditions and genetic factors

2.4.1.3 Statistical Parametric Mapping (SPM) Analysis

Statistical Parametric Mapping (SPM) is a comprehensive framework widely used in neuroimaging to analyze brain imaging data, particularly structural MRI (sMRI) images. Developed originally for functional MRI, SPM has been adapted for structural MRI to facilitate the investigation of brain morphology and its association with various clinical and cognitive variables. The primary advantage of SPM lies in its ability to perform voxel-wise statistical analysis across the entire brain, allowing researchers to identify subtle structural differences and their potential causes or correlates.

The SPM process for structural MRI analysis begins with the acquisition of high-resolution T1-weighted images, which provide detailed anatomical information (Khadka et al., 2016). These images undergo several preprocessing steps to ensure they are suitable for statistical analysis. The preprocessing pipeline typically includes bias correction to correct for intensity non-uniformities, skull stripping to remove non-brain tissues, and spatial normalization to align the brain images to a standard anatomical space, such as the Montreal Neurological Institute (MNI) template. This normalization ensures that brain structures are in the same coordinate system across all subjects, facilitating voxel-wise comparisons (Khadka et al., 2016).

Following preprocessing, the normalized brain images are smoothed using a Gaussian kernel. Smoothing enhances the signal-to-noise ratio and accommodates anatomical variability between subjects by averaging voxel intensities with their neighbors (Smith et al., 2022/04/25). This step is crucial for ensuring that the subsequent statistical tests are robust and reliable. The choice of the smoothing kernel size can affect the sensitivity of the analysis; larger kernels increase sensitivity to larger structures, while smaller kernels are more sensitive to finer details (Worsley et al., 1992).

The core of SPM analysis involves constructing a general linear model (GLM) at each voxel to test hypotheses about the relationship between brain structure and various explanatory variables, such as age, disease status, or genetic variants. The GLM allows for the inclusion of covariates, making it possible to control for confounding factors. After fitting the model, statistical tests are performed at each voxel to generate statistical parametric maps, which display the significance of the associations across the brain. These maps are then thresholded to correct for multiple comparisons, typically using family-wise error (FWE) correction or false discovery rate (FDR) methods, to ensure that the identified regions are not due to chance (Friston et al., 1994).

One of the key applications of SPM in structural MRI is the investigation of brain changes associated with neurological and psychiatric disorders. For example, SPM has been used to identify regional atrophy in Alzheimer's disease, schizophrenia, and depression. By comparing the brain images of patients with those of healthy controls, researchers can pinpoint specific regions that show significant structural differences. Additionally, SPM has been instrumental in studying the effects of genetic variations on brain morphology. Genome-wide association studies (GWAS) combined with SPM have revealed how certain genetic polymorphisms are linked to changes in brain structure, providing insights into the genetic basis of brain development and disease (Stein et al., 2010/11/11).

Despite its powerful capabilities, SPM analysis also has limitations. The reliance on spatial normalization and smoothing can introduce biases, especially when dealing with populations that have significant anatomical variability. Moreover, the interpretation of SPM results requires careful consideration of the underlying biological processes, as the relationship between voxel intensity and brain structure is complex. Nevertheless, SPM remains a pivotal tool in the field of neuroimaging, offering a robust framework for exploring the intricate relationships between brain anatomy and various biological and clinical factors.

2.4.1.4 Single Nucleotide Polymorphism (SNP) Analysis

Single Nucleotide Polymorphism (SNP) analysis is a fundamental technique in the field of genomics that focuses on identifying genetic variations associated with phenotypic traits, including brain structure and function. SNPs are the most common type of genetic variation among people, consisting of single base-pair changes in the DNA sequence. In brain imaging genomics, SNP analysis aims to uncover how these genetic variations influence brain morphology and function, offering insights into the genetic underpinnings of neurological and psychiatric conditions.

SNP analysis in brain imaging genomics typically begins with the collection of genetic data through genome-wide genotyping arrays or whole-genome sequencing. Concurrently, high-resolution structural MRI (sMRI) scans are obtained to capture detailed images of the brain. The genetic data and imaging data are then integrated to explore associations between specific SNPs and various brain phenotypes, such as gray matter volume, cortical thickness, and white matter integrity (Visscher et al., 2012).

One of the primary methods for SNP analysis in brain imaging is the Genome-Wide Association Study (GWAS). GWAS involves scanning the entire genome to identify SNPs that are significantly associated with brain imaging traits. This approach is hypothesis-free, allowing for the discovery of novel genetic associations without prior assumptions. The process involves quality control steps to filter out poorly genotyped SNPs and individuals with excessive missing data, followed by statistical tests to examine the association between each SNP and the imaging phenotype. Corrections for multiple comparisons, such as the Bonferroni correction or false discovery rate (FDR) adjustment, are applied to account for the large number of tests performed (Elliott et al., 2018).

The integration of SNP analysis with brain imaging has led to significant discoveries in the field. For example, studies have identified SNPs associated with variations in hippocampal volume, providing insights into genetic factors contributing to cognitive aging and neurodegenerative diseases (Stein et al., 2012). Additionally, SNP analysis has been used to explore the genetic architecture of psychiatric disorders, revealing genetic variants that affect brain regions implicated in conditions such as schizophrenia, bipolar disorder, and autism spectrum disorder (Ripke et al., 2013). These findings highlight the potential of SNP analysis to uncover the biological pathways through which genetic variations influence brain structure and function.

Despite its powerful capabilities, SNP analysis also faces several challenges. The detection of true associations requires large sample sizes due to the small effect sizes of individual SNPs. Moreover, the interpretation of significant SNPs can be complex, as they often reside in non-coding regions of the genome and may influence gene expression through regulatory mechanisms. Functional validation studies are needed to elucidate the biological impact of these SNPs on brain structure and function. Nevertheless, advances in statistical methods and the increasing availability of large, well-characterized datasets are enhancing the ability of SNP analysis to contribute to our understanding of brain imaging genomics.

2.4.2 Multivariate Approaches in Structural Imaging Genomics

Multivariate approaches in structural imaging genomics are essential for handling the complex and high-dimensional data that arise from integrating genetic information with neuroimaging measures. These approaches enable researchers to uncover relationships between multiple genetic variants and brain structures, providing a more comprehensive understanding of the genetic influences on brain morphology. Here are some of the key multivariate approaches used in structural imaging genomics.

2.4.2.1 Sparse Canonical Correlation Analysis (sCCA)

Sparse Canonical Correlation Analysis (sCCA) is a powerful multivariate statistical technique designed to identify and quantify the relationships between two sets of variables. This method extends traditional canonical correlation analysis (CCA) by incorporating sparsity constraints, which allow for the selection of a subset of relevant features from each dataset. This makes sCCA particularly well-suited for high-dimensional data, such as those encountered in imaging genomics, where the number of variables (e.g., genetic markers and brain imaging measures) can far exceed the number of observations (Witten & Tibshirani, 2009).

The primary objective of CCA is to find linear combinations of the variables in each dataset that are maximally correlated with each other. Given two datasets, $X\ and\ Y$, CCA seeks to identify vectors a and b such that the correlation between X_a and Y_b is maximized. Mathematically, this can be expressed as:

$$(a, b)\ = argmax_{(a,b)}\ corr(X_a, Y_b) \tag{2.1}$$

In sCCA, sparsity constraints are added to this optimization problem to ensure that the resulting vectors a and b have only a few non-zero elements. This is achieved by adding penalty terms to the objective function, typically using l_1-norm regularization. The optimization problem for sCCA can be formulated as:

$$(a, b) = argmax_{a,b}\ corr(X_a, Y_b)\ subjecct\ to\ ||a||_1 \leq \lambda_1, ||b||_1 \leq\ \lambda_2 \tag{2.2}$$

where λ_1 and λ_2 are regularization parameters that control the degree of sparsity. By enforcing sparsity, sCCA can effectively handle the curse of dimensionality and identify meaningful associations between the two datasets.

sCCA is particularly valuable in imaging genomics, where researchers aim to uncover the relationships between genetic variations (e.g., SNPs) and brain imaging phenotypes (e.g., cortical thickness, gray matter volume). The high-dimensional nature of these datasets poses significant challenges for traditional analytical methods, but sCCA's ability to perform feature selection makes it well-suited for this context. For instance, in a study examining cortical thickness, researchers might employ sCCA to correlate a set of single nucleotide polymorphisms (SNPs) with measurements of cortical thickness across different brain regions. By imposing sparsity constraints, sCCA ensures that only the most relevant genetic variants and brain regions are highlighted, thereby simplifying the interpretation and reducing the likelihood of spurious findings (Jang et al., 2017).

Several studies have successfully utilized sCCA to reveal genetic influences on brain structure. For example, Shen et al. (2010) applied sCCA to integrate SNP data with voxel-based morphometry measures from MRI scans in a cohort of Alzheimer's disease patients and healthy controls. Their analysis identified specific genetic variants associated with brain atrophy patterns characteristic of Alzheimer's disease, providing insights into the genetic underpinnings of this neurodegenerative disorder. Such findings underscore the potential of sCCA to pinpoint genetic factors that contribute to structural brain changes in various conditions (Shen & Thompson, 2020).

In another study, Ge et al. (2012) used sCCA to investigate the genetic basis of cortical thickness in a large sample of healthy individuals. They identified significant associations between several SNPs and cortical thickness in regions implicated in cognitive functions, such as the prefrontal cortex and parietal lobes. These results not only highlighted the genetic architecture of cortical development but also provided a basis for understanding how genetic variations contribute to individual differences in cognitive abilities (Ge et al., 2012).

The application of sCCA in imaging genomics extends beyond identifying genetic influences on normal brain structure to understanding the genetic basis of neuropsychiatric disorders. For example, research utilizing sCCA has identified genetic variants that correlate with structural brain abnormalities in schizophrenia, such as reduced gray matter volume in the prefrontal cortex and temporal lobes. These findings support the hypothesis that schizophrenia involves widespread disruptions in brain structure influenced by genetic risk factors (Glahn et al., 2007).

Sparse Canonical Correlation Analysis (sCCA) has proven to be a valuable tool in understanding the genetic underpinnings of neuropsychiatric disorders. These disorders, such as schizophrenia, bipolar disorder, and major depressive disorder, are characterized by complex and

heterogeneous symptoms that are influenced by both genetic and environmental factors. By integrating genetic data with neuroimaging measures using sCCA, researchers can identify specific genetic variants that contribute to brain abnormalities associated with these conditions, thereby elucidating the biological mechanisms underlying these disorders.

Schizophrenia, for instance, has been extensively studied using sCCA to uncover the relationships between genetic variations and structural brain changes. Studies have consistently found that patients with schizophrenia exhibit reduced gray matter volume in regions such as the prefrontal cortex, temporal lobes, and hippocampus. These structural abnormalities are thought to be influenced by genetic risk factors. For example, a study by Meda et al. (2012) applied sCCA to integrate genome-wide SNP data with voxel-based morphometry (VBM) measures in a cohort of schizophrenia patients and healthy controls. The analysis identified several genetic variants associated with reduced gray matter volume in the prefrontal cortex, providing insights into the genetic basis of the structural brain changes observed in schizophrenia (Song et al., 2022).

In bipolar disorder, sCCA has also been used to explore the genetic factors contributing to brain structure alterations. Research has shown that individuals with bipolar disorder often exhibit abnormalities in brain regions involved in emotional regulation, such as the amygdala and prefrontal cortex. By applying sCCA to integrate genetic and neuroimaging data, researchers have identified genetic variants associated with these structural changes. For instance, an sCCA study identified SNPs in genes related to synaptic function and neural plasticity that were linked to reduced gray matter volume in the prefrontal cortex of bipolar disorder patients. These findings suggest that genetic variations affecting synaptic pathways may play a crucial role in the neurobiological basis of bipolar disorder (Leonenko et al., 2018).

Major depressive disorder (MDD) is another neuropsychiatric condition where sCCA has been instrumental in revealing genetic influences on brain structure. Patients with MDD often exhibit structural abnormalities in the hippocampus and prefrontal cortex, regions critical for mood regulation and cognitive functions. sCCA studies have identified genetic variants associated with these brain changes, providing insights into the genetic predispositions that may contribute to MDD. For example, a study by Shen et al. (2010) used sCCA to integrate SNP data with sMRI measures, identifying variants in the BDNF gene associated with reduced hippocampal volume in MDD patients. This highlights the role of genetic factors in the neuroanatomical alterations linked to depressive symptoms (Buch & Liston, 2021).

Moreover, sCCA has facilitated the identification of biomarkers for neuropsychiatric disorders, aiding in early diagnosis and personalized treatment strategies. By uncovering specific genetic and brain imaging features that distinguish patients from healthy individuals, sCCA helps in developing predictive models that can be used in clinical settings. For instance, combining genetic risk scores with neuroimaging markers identified through sCCA can improve the accuracy of early diagnosis for disorders like schizophrenia and bipolar disorder. This approach not only enhances our understanding of the genetic and neurobiological basis of these disorders but also paves the way for targeted therapeutic interventions that address the underlying genetic and structural abnormalities.

2.4.2.2 Independent Component Analysis (ICA)

Independent Component Analysis (ICA) is a computational technique widely used in imaging genomics to disentangle complex and mixed signals into statistically independent components. This method is particularly valuable for analyzing neuroimaging data, where it can

separate signals originating from different brain sources, and for integrating these data with genetic information to uncover underlying genetic influences on brain structure and function.

ICA is based on the assumption that observed data are linear mixtures of independent source signals. The goal of ICA is to identify these source signals and the mixing matrix by maximizing the statistical independence of the components. Given a matrix of observed signals X, ICA seeks to find a matrix W such that:

$$S = WX \tag{2.3}$$

where S represents the matrix of independent components. Unlike traditional methods such as Principal Component Analysis (PCA), which assumes orthogonality of components, ICA does not require orthogonality, making it more flexible in capturing complex and biologically meaningful patterns in the data.

One of the primary applications of ICA in imaging genomics is the decomposition of neuroimaging data, such as functional MRI (fMRI) and structural MRI (sMRI), into independent components. This allows researchers to isolate signals related to specific brain functions or structures. For example, ICA has been used to identify resting-state networks in fMRI data, such as the default mode network (DMN), which are then analyzed for genetic associations (Beckmann & Smith, 2004).

By integrating ICA-derived components with genetic data, researchers can investigate how genetic variations influence specific brain networks. For instance, an ICA study might reveal that certain genetic variants are associated with alterations in the connectivity of the DMN, providing insights into the genetic basis of cognitive and behavioral traits. A study used ICA to identify independent components of brain activity that were then linked to genetic variants, revealing

associations between specific SNPs and functional brain networks in schizophrenia patients (Salman et al., 2019).

ICA is also employed in multimodal data integration, combining information from different imaging modalities and genetic data. Parallel Independent Component Analysis (pICA) extends ICA to jointly analyze multiple datasets, identifying shared independent components that capture the common variance across modalities. For example, pICA can be used to integrate fMRI and sMRI data with genomic information, uncovering genetic variants that simultaneously affect brain structure and function (Meda et al., 2010).

ICA has been instrumental in studying neuropsychiatric disorders, where it helps to identify brain abnormalities associated with genetic risk factors. In bipolar disorder and schizophrenia, ICA has revealed altered functional and structural brain components that correlate with genetic variations, offering insights into the neurobiological mechanisms of these disorders. For example, Calhoun et al. (2012) applied ICA to fMRI data from schizophrenia patients, identifying independent components of brain activity that were significantly associated with genetic risk scores (Calhoun & Adalı, 2012).

The key advantage of ICA in imaging genomics is its ability to isolate independent signals from complex, mixed data. This makes it particularly useful for identifying specific brain networks and their genetic associations, which might be obscured by noise and confounding factors in traditional analyses. Additionally, ICA's flexibility in dealing with non-Gaussian and non-orthogonal components enhances its applicability to real-world neuroimaging data.

However, ICA also presents challenges. The identification of independent components depends on the initial assumptions and the specific algorithm used, which can lead to variability in the results. Moreover, the interpretation of ICA-derived components requires careful

validation, as the components may not always correspond to anatomically or functionally distinct brain regions. Selecting the appropriate number of components is also critical, as over- or under-estimation can affect the quality of the results (Sui et al., 2012).

3 EVALUATING THE NEUROIMAGING-GENETIC PREDICTION OF SYMPTOM CHANGES IN INDIVIDUALS WITH ADHD

3.1 Introduction

Attention-deficit/hyperactivity disorder (ADHD) is one of the most common neurodevelopmental disorders of childhood. It is usually first diagnosed in childhood and could persist into adulthood (Duan et al., 2018). Children with ADHD may have trouble paying attention, controlling impulsive behaviors (may act without thinking about what the result will be), or be overly active (Jiang et al., 2020), and may also have various types of cognitive impairments (Liu et al., 2020). A meta-analysis of follow-up studies has shown that in about 15% children with ADHD the disorder persists into adulthood, and the persistence percentage increases to 65% if partially remitted patients are considered (Jiang et al., 2020). Although the classification of ADHD and the persistence of ADHD are binary, highly dependent on the threshold used by the clinicians following the Diagnostic and Statistical Manual of Mental Disorders (DSM) or International Classification of Diseases (ICD), the symptoms themselves are continuously distributed among individuals, as are the symptom changes. Predicting the trajectories of ADHD symptoms along the disorder progression can have huge impact in the development of effective prevention and treatment; it can classify individuals whose symptoms aggravate in the future, and thus early intervention can be provided in time.

Many longitudinal studies have been devoted to uncovering the factors influencing the course of ADHD symptoms and to improve the prediction of symptom trajectories (Sasser et al., 2016). As reviewed by Caye, et al. a meta-analysis summarized the consistent predictors of symptom trajectory including characteristics of the clinical syndrome, ADHD symptom severity, treatment, comorbidities, and parental mental health problems, etc. (Caye et al., 2016). However,

little is known about the relation between brain structure and function factors and the symptom trajectory, despite abundant evidence supporting association of brain anomalies with ADHD and its symptoms. Structural MRI studies have suggested that gray and/or white-matter structural underdevelopment in frontal lobe, thalamus, and striatum significantly contribute to the emergence of ADHD during childhood (Cupertino et al., 2020; Damatac et al., 2022; Ellison-Wright et al., 2008; Xia et al., 2012). Furthermore, persistence of ADHD symptoms is linked to reduced regional cortical gray matter thickness in frontal and parietal cortices (Almeida Montes et al., 2013; Batty et al., 2010). Our team also found frontal, and cerebellum gray matter variations consistently associated with working memory deficit and inattention symptoms in both adolescents and adults with ADHD (Duan et al., 2018; Jiang et al., 2020; Liu et al., 2020). Functionally, lower connection efficiency in right inferior frontal gyrus and left-side frontal-parietal functional interactions were observed in both adult remitters and persisters, and unique lower connection efficiency in right middle frontal gyrus and hyper-interactions between bilateral middle frontal gyrus in persisters (Francx et al., 2015; Luo et al., 2018). How brain structural and functional alterations relate to symptom trajectory is yet to be studied (Sudre et al., 2021)

The heritability of ADHD Is estimated between 30%- 80% in twin and family studies (Pettersson et al., 2019). Strongly increased risks for ADHD (57%) among the offspring of adults with ADHD have been reported (Biederman et al., 1995). Longitudinal studies that investigated the genetic contributions to the long-term ADHD suggested while persistence of ADHD symptoms is predominantly due to the same genetic influences as its onset, changes of symptoms are to a large extent due to new genetic effects beginning in early adolescence, as well as environmental factors (Larsson et al., 2004). More recently, large sample genome-wide association studies (GWAS) have reported several genetic risk loci for ADHD [18]. Polygenic risk score (PRS) based

on GWAS risk profile, estimating an individual's genetic liability for a particular disorder or trait, were able to explain significant variance (5.5%) in ADHD (Demontis et al., 2019). Genetic risk for ADHD is highly correlated to the risk to other disorders or traits, and one of the highest correlations are from genetics for college completion (Demontis et al., 2019). To what extent genetics could influence the course of ADHD symptoms is largely unstudied.

Although various genetic, cognitive, and neural factors have been associated with ADHD, very little is known about their combined ability to predict the symptom trajectory. In this study we leveraged longitudinal data collected from individuals with ADHD and investigated the prediction power of brain structure and genomic features, as well as cognition assessments, for future symptom changes. Based on the previous findings we hypothesize that the interplay of the examined factors might better explain the trajectory of symptoms in both domains (inattention and hyperactivity) than any individual feature set. Assessing the neural, genetic, and cognitive factors of subjects can enrich our understanding of the symptom trajectory and thereby aid in creating personalized prevention and treatment.

3.2 Materials and Methods

3.2.1 Participants

We employed a subset of data from NeuroIMAGE project (von Rhein et al., 2015). The NeuroIMAGE is a multi-site prospective cohort study designed to investigate the course of ADHD, its genetic and environmental determinants, its cognitive and neurobiological underpinnings, and its presentations in adolescence and adulthood. The study was approved by the regional ethics committee and the medical ethical committee of the VU University Medical Center. All participants provided a written consent form. From all participants, we selected 77 participants, including 43 male and 34 female, who 1) met the ADHD diagnostic criteria based on DSM-IV at

one time point (here named baseline), 2) provided good quality neuroimaging and genetic data at baseline, and 3) had cognitive and symptom assessments at both baseline and follow up time points. The average age of the participants was 16.30 and 19.97 years old for the baseline and follow up timepoint respectively.

Symptoms were measured in both domains: inattention and hyperactivity/impulsivity. Symptom change between the two time points reflects the progression of disorder and is the variable we want to predict. WAIS Digit Span test (maximum forward and maximum backward scores) was utilized to gauge working memory capacity, as it showed persistent impairment in adolescents and adults with ADHD (Schoenmacker et al., 2019). Base-line working memory scores are the features tested for prediction.

3.2.2 Neuroimaging Data and Features

T1-weighted MRI images after quality control were normalized, modulated, segmented, and smoothed with 6mm Gaussian kernel using SPM12, and the resultant gray matter maps were further regressed out age, sex, and site effects. Independent component analysis was then applied to the whole brain voxels with gray matter density >0.2, resulting in 24 components. The details of the preprocess can be seen in (Duan et al., 2018).

Each component is a brain network, and the relative gray matter density of this network is measured by the component loadings. Also, we added 5 more components we identified in our previous studies that are associated with adult ADHD symptom and cognitive impairment (Duan et al., 2018). These 29 gray matter components' loadings were the input features for prediction model.

3.2.3 Genomic Data and Features

From genomic SNP data after imputation, we computed two sets of genetic scores: Quantative Genetic Score (QGS) (Schoenmacker et al., 2019), and Polygenic Risk Score (PRS) (Choi et al., 2020). QGS assigns a numeric value $0 \leq QGS \leq 1$ to any preselected genetic region, based on the average difference between an individual's genetic information (in the form of genotypes) and that of a reference population (i.e., the same reference used to impute genetic information to said individual). QGS can be interpreted as a measure of individual's genetic "distance" to the reference population: a lower score indicates higher similarity to the reference population, whereas a high score indicates a lower similarity (Schoenmacker et al., 2019). We selected 29 genes whose QGS scores were stably associated with the five gray matter components underlying adult ADHD symptoms and working memory impairments. See details of QGS method in (Schoenmacker et al., 2019). PRS is the weighted summary score of individual SNPs' risk to a specific disease or trait based on genome-wide association study results. We computed PRS for education attainment (Lee et al., 2018), intelligence (Jansen et al., 2020), ADHD (Demontis et al., 2019), and major disorder (Wray et al., 2018) using pRsice2 (Choi et al., 2020).

3.2.4 Data Analysis

In this study we focused on using baseline brain images, working memory tests, and genetic scores to predict symptom changes in both inattention and hyperactivity/impulsivity domains. Specifically, tested predictors include age, sex, baseline 29 gray matter components, QGS of 29 genes, four PRS, baseline working memory scores, and the interval between two timepoints. To build a reliable prediction model, we implemented stepwise linear regression with forward feature selection, LOOCV, stability selection with resampling (two resampling strategies: subsamples and

bootstrapping with replacement), permutation test. We combined stepwise linear regression feature selection with LOOCV (FS-LOOCV), which is useful when a small sample size cannot afford withholding data from the training set (Hawkins et al., 2003). As shown in Figure 3.1, we performed FS-LOOCV in full training samples. To further reduce overfitting, we performed stability selection with resampling, and permutation tests with different feature sets. Finally, we performed a validation test on independent holdout samples. The details of each step are explained next.

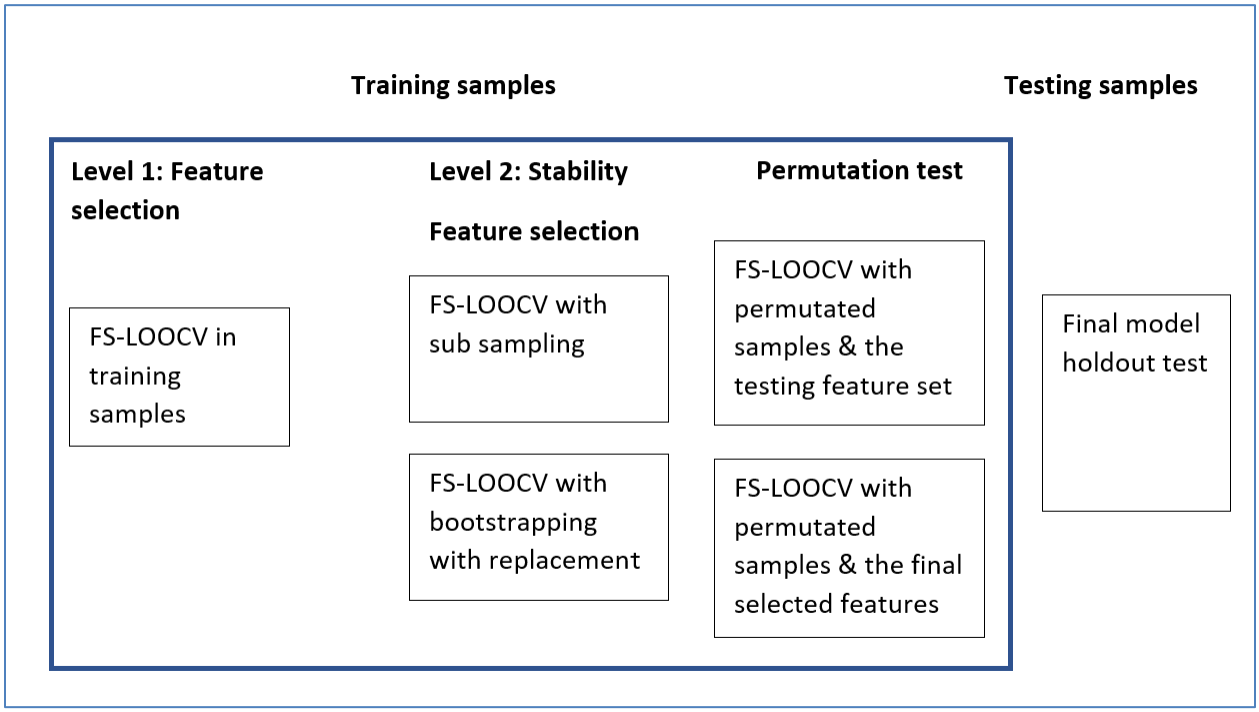

Figure 3.1 Analysis performed on the ADHD data.

FS-LOOCV: The performance of any machine learning model is sensitive to the set of features that are used in the training of the model. Determining the best set of features for the final model is called feature selection. Here we used forward stepwise regression, a procedure that selects the best set of features iteratively. Specially for a prediction model, starting with no predictors in the working set, at each iteration the algorithm tests model accuracies for individual

predictors when added to the working set, and selects only one predictor with the best model fit to the working set. We used LOOCV R2 to measure model fit. All training samples except one were used to build a linear regression model, which was then used to predict the value of the one sample not used. Repeat this procedure for N times (N = size of training samples) to generate predicted values for all training samples. LOOCV R2 is then computed as

$$\text{LOOCV}R^2 = 1 - \frac{SS_{res}}{SS_{tot}} \tag{3.1}$$

where, $SS_{res} = \sum_i (y_i - f_i)^2$; $f_i =$ predicted value and y_i is true value; $SS_{tot} = \sum_i (y_i - \bar{y})^2$; y_i is the true value and $\bar{y}$ is the mean of true values

The pseudocode of the FS-LOOCV stepwise regression is as follows:

1) Starting with an empty working set, S, and all available predictors, Predictors Set
2) Iterate over available predictors in the Predictors Set
    a) Add each predictor to the working set S
    b) Test the model estimate using LOOCV when the predictor is added.
    c) Remove the added predictor from S
3) Add the best predictor to the working set S
4) Remove the best predictor from Predictors Set
5) Repeat Step 2, 3 and 4.

To further reduce possible overfitting, we performed stability selection with resampling for the feature set after FS-LOOCV. Stability selection identifies the most stable predictors by assuming that the same algorithm should yield similar results on similar datasets if the results are "stable" (Meinshausen & Bühlmann, 2010). To generate similar data, we implemented subsampling and bootstrapping strategies. For sub-sampling, sample sizes of 50, 55, 60, and 65 were selected. 64 sub-samples, including 16 random sub-samples of each sample size, are

generated and FS-LOOCV is applied. The features selected from each sub-sample are aggregated. The frequency of each feature being selected indicates its stability. Whereas for bootstrapping, in each iteration, an instance is drawn from the same original dataset such that certain instance may appear more than once in a bootstrap sample (Efron, 1979). We applied FS-LOOCV to each of the bootstrap samples, aggregate the features selected, and compute the feature frequency. For both resampling strategies, a preset threshold is used to select stable features, i.e., features with frequency higher than the threshold will be selected as stable features.

3.2.5 Permutation Tests

To select the best threshold for stability frequency and empirical significance, we performed a permutation test. We performed two permutation tests using, 1) all the 65 features in the dataset to set up the best threshold on stability selection and to test the power of samples to select the features, and 2) the selected features from the selected threshold to test the empirical significance of model prediction on symptom change.

For the permutation test using the full 65 features, we generated 100 datasets by randomly permuting the sample symptom scores of the full training data. For each dataset, the analysis methods used on the original data were applied, i.e., FS-LOOCV stepwise regression followed by stability selection. On the aggregated features derived from multiset resampling, different thresholds (50% to 100% in steps of 5) were applied to select stable features, and then using selected features the model was trained and tested using LOOCV. The model's performance was measured by R^2. For each threshold, we calculated p-value as the probability of obtaining the R2 on permuted samples equal to or greater than the observed R2 in the original data at the same

threshold. For example, a p-value of 0.23 at threshold 90% indicates a 23% chance of getting higher LOOCV explained.

variance (R^2) in the randomly permuted samples than the observed explained variance in original data with the features selected at the same threshold of 90% (R^2 calculated using the same analysis method). The threshold that gave the best p-value (smallest *p*-value) was used to set the threshold for selecting final features.

Another permutation test was performed in the same manner but only using the selected features of all training samples. The null hypothesis is the selected features cannot predict dependent variable. Analysis was performed on data with the selected features and permuting the symptom scores (Ojala & Garriga, 2009) to test the empirical significance.

3.2.6 Holdout Test

Finally, we used the 6 hold out samples to verify the final prediction model, which is estimated using the linear regression on all 71 samples with the final selected features. We calculated the model estimate on the holdout dataset using the linear model trained on all 71 samples with the final selected features. We used 6 datapoints that were not included in the original dataset.

3.3 Results

First, using feature selection we reduced the feature space from 65 to 25 features in inattention domain (14 in the hyperactivity domain). Further, using stability selection with subsampling, to counter overfitting, we further reduced the feature space to 7 features. In the bootstrap method of stability selection, the resulting frequencies of each aggregated feature are very low. Standard data analysis was performed (training, testing, and holdout testing) and selected

features explained significant variance in training and testing in both domains. However, the holdout testing in both the domains was not significant.

3.3.1 Inattention Domain

Using the FS-LOOCV stepwise regression we selected 25 features that gave maximum LOOCV R^2. Figure 3.2(a) plots the R^2 of the linear model trained with all the samples and LOOCV R^2 at each iteration of stepwise regression. After the 25^{th} iteration with 25 features the LOOCV R^2 reaches the highest values and with each additional iteration R^2 value starts diminishing.

Table 3-1: Performance of the model on the inattention symptom change prediction.

Phase	R-square	Correlation
Training	0.41	0.64
LOOCV Testing	0.26	0.53
Holdout Testing	-0.018	0.46

Using stability selection with 64 sub-samples, we computed the frequency of the 25 features from the stepwise regression. Figure 3.2(b) shows the frequency distribution of the features. There are 5 features which were included by all the stability models i.e., these features are strongly associated with symptom change. 19 features were selected at least by 50% of the subsample models. In contrast, Figure 3.2(c) shows the frequency distribution of features computed using bootstrapping (subsampling with replacement). The maximum frequency attained by the bootstrap method is 33%. Most of the features are selected only by 20% of the bootstrap

models.

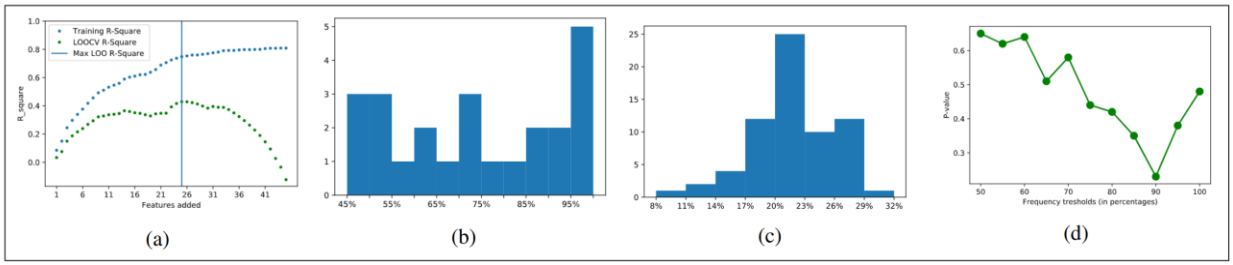

Figure 3.2: Results from prediction of inattention symptom change.

Figure 3.2(d) shows the frequency thresholds and their respective p-values calculated using permutation tests (tests performed using the full feature set). The p-value is highest at 50% threshold and starts decreasing while the threshold increases. The most significant result among all feature sets is p-value of 0.23 achieved by the features thresholding at frequency of 90%. Of the 25 features selected in stepwise regression with forward selection, 7 features had frequency greater than 90%.

The 7 features include Age, gene OSBPL1A, CTNNB1, GM in Insula region (Figure 3.3) which are negatively correlated to the symptom change, while genes PRPSAP2, ACADM, and PRS of education attainment were positively correlated to the symptom change. The permutation test performed using these 7 selected features has a p-value < 0.05. Table 1 summarizes the model training, testing, and holdout results in the inattention domain. The training model fits using all points with these 7 selected features has $R^2 = 0.418$ whereas the LOOCV testing $R^2 = 0.26$. Also, the correlation between the predicted values and true value in both the phases, training, and testing, is 0.64 and 0.53 respectively. On the other hand, in the holdout test, the R^2 is negative (-0.018) while the correlation is positive (0.46). The empirical p-value obtained by the permutation tests with these selected 7 features is less than 0.05.

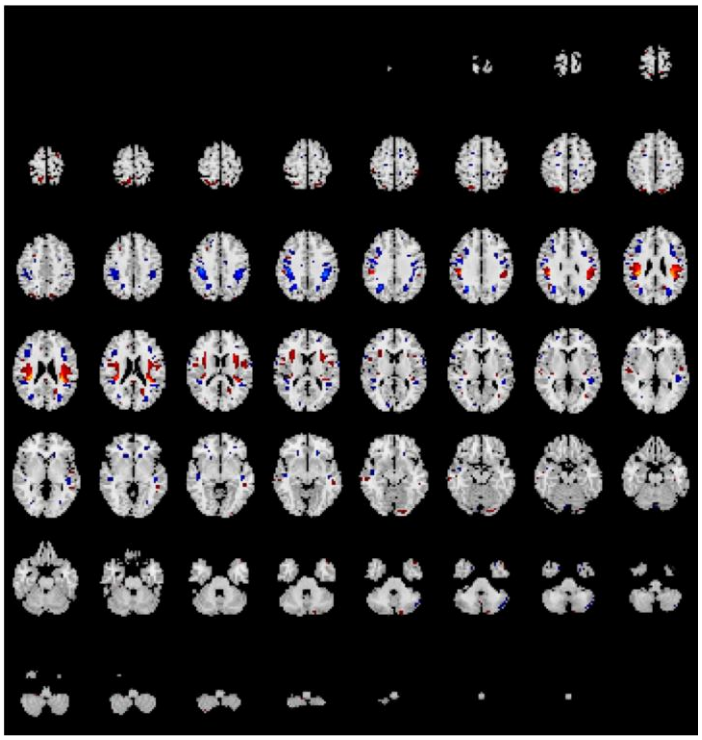

Figure 3.3: Grey matter component from the insula region

3.3.2 Hyperactivity Domain

Similar to inattention domain, in the hyperactivity domain, using FS-LOOCV stepwise regression we selected 14 features that gave LOO R^2. The plot shown in Figure 3.4 (a) compares the training R^2 vs the LOOCV testing R^2. The LOOCV R2 is maximum after 15 iterations and starts decreasing when further features are added. Moreover, the R2 becomes negative on further iterations.

Using stability selection with 64 sub-samples, we computed the frequency of the 14 features from the stepwise regression. Figure 3.4(b) shows the frequency distribution of the features. There are 5 features which were included by all the stability models i.e., their frequency is greater than 95%. 11 features were selected at least by 50% of the subsample models. On the other hand, Figure 3.4 (c) shows the frequency distribution of features computed using

bootstrapping (subsampling with replacement). The maximum frequency attained by the bootstrap method is 32%. Most of the features are selected with equal frequency.

Figure 3.4 (d) shows the frequency thresholds and their respective p-values calculated using permutation tests (tests performed using the full feature set). The p-value is highest at 50% threshold and starts decreasing while the threshold increases. The most significant result among all feature sets is p-value of 0.33 achieved by the features that are threshold at frequency of 80%. Of the 14 features selected in stepwise regression with forward selection, 6 features had frequency greater than 80%.

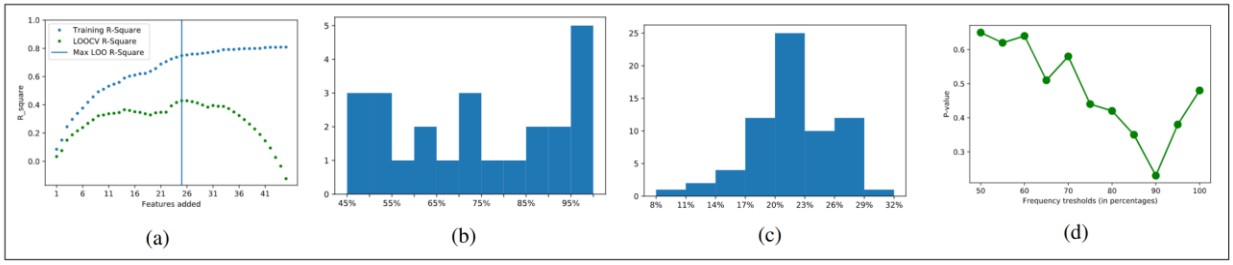

Figure 3.4: Results from prediction of inattention symptom change.

At threshold of 80%, we selected 6 features that include genes CTNNB1, DYNC1I1, GM component (negatively correlated), genes PRPSAP2, LING02, and AC104662 2 (positively corelated) were selected. The permutation test performed using these 6 features has a p-value < 0.05. Model fit with all data points with these features has an R^2 of 0.31 and in the LOOCV testing the R2 is 0.17. But the permutation *p*-value is 0.38. The holdout test result showed correlation r= 0.017 whereas R^2 = -2.82.

Table 3-2: Performance of the model on hyperactivity symptom change prediction.

Phase	**R-square**	**Correlation (r)**
Training	0.31	0.56

LOOCV Testing	0.17	0.43
Holdout testing	-2.82	0.025

3.4 Discussion

In this study, we investigated the ability to predict the trajectory of the symptoms in both domains——inattention, and hyperactivity——using features from sMRI images and genomics of ADHD cohort of 77 subjects. Using stepwise regression with forward selection, we selected features that explain maximum variance in the symptom change. But testing results indicated the model to be overfitting. Using stability selection coupled with permutation tests, we further reduced the feature space. Permutation tests suggested we do not have the power for selecting features. But given the final selected features, for inattention, the prediction performance is very promising within our samples. In inattention domain, we identified age, genes OSBPL1A, CTNNB1, PRPSAP2, ACADM, and one GM component in the insula region associated with symptom change.

In both symptom domains, using the stepwise regression with forward selection we selected the set of features that has maximum testing LOOCV R^2. Even though this is a standard approach for feature selection and model training, however, as shown in the Figures 2(a) and 4(a), the improvement of testing LOOCV R^2 from a lower feature set (16 for inattention and 10 for hyperactivity) to the top feature set is small compared to the gap between training R^2 and testing LOOCV R^2. These results indicate that 1) the set of features that gave maximum LOOCV R2 are overfitting, and 2) a smaller set of features can explain similar variance.

Thus, we applied stability selection in combination with permutation tests to further reduce feature set to alleviate overfitting. Two sampling strategies were used for stability selection. In most studies the threshold value for stable feature selection has been a tuning parameter i.e., no objective way to determine the value. In this study, we used permutation tests to determine the threshold such that the variance explained by features selected at the threshold is significant (or the most significant) compared to the null distribution simulated by permuted samples using features selected at same threshold. The difference between the training and testing R2 results summarized in Table 1 and Table 2 show that the smaller set of features has reduced overfitting.

However, the best p-value obtained using the permutation tests to identify the threshold of frequency, are 0.23 and 0.36 in the inattention and hyperactivity domains respectively. These results indicate that the selection of features using the threshold are non-significant; we do not have the power to select the features. On the contrary, the permutation tests performed using the selected features has empirical p-value < 0.05 which indicate that these features are significantly associated with the symptom changes within our training samples, but we do not know whether this is true for other independent samples.

On the other hand, the bootstrap method for stability selection was unable to select stable features due to heterogeneity in the data sample. We observed each data sampling produces a model with similar performance (R^2) but different feature sets. We speculate that within our small samples there are large heterogenous properties, so that each bootstrapping sampling has a different property distribution, leading to a different feature set and model. Compared to subsampling strategy, common samples between any two samplings in bootstrapping are less, leading to low frequencies as shown in figure 2d and 4d.

The LOOCV testing results in both the domains were promising. However, LOOCV is known to have inferior performance for model estimation, risk for overfitting (Pontil, 2002). The additional validation test results are not significant and suggest the features selected lack generalizable power to significantly explain the symptom changes. Though the validation R2 is small in the inattention domain, the correlation between the true value and the predicted value is high (r=0.46) and at the same level as training and testing results. The consistent effect size provides very promising indication of strong association among the features selected and the symptom change. This non-significance might be the result of small sample size of validation sets. We speculate that with large sample size these features may be proven significantly associated with symptom changes. On the other hand, the results in the hyperactivity domain indicate no association of features with the symptom change.

The features identified in the inattention domain include genes OSBPL1A and PRPSAP2 that have been previously reported to be associated with ADHD (Xu et al., 2001). The gene CTNNB1 was discovered recently to be responsible for developmental delay/intellectual disability (Kharbanda et al., 2017). CTNNB1 is important in the development and maturation of the brain and loss of its function causes learning and memory problems (Kharbanda et al., 2017). Aging effects on ADHD has been researched extensively (Biederman & Faraone, 2005; Holland & Sayal, 2019). Furthermore, the GM components reported in our results —component in the insula region, are also previously reported to be associated with ADHD problem (Lopez-Larson et al., 2012). However, the effect of postcentral gyrus on ADHD is yet to be studied.

The small sample size of 77 hinders our statistical analyses from being generalizable to other data. This is demonstrated by the inability to obtain significant results using validation testing. To sum up, in this study we aimed to predict the trajectory of the ADHD symptoms in both

the domains – inattention, and hyperactivity using genetics and neuroimaging data. Using data of 77 subjects from two time points (6 subjects used for holdout testing) we performed variable selection using stepwise regression using forward selection, leave one out cross validation. The selected variables were still overfitting, to further reduce overfitting we performed stability selection in combination with permutation tests and selected top features. In both the domains, the features selected were unable to explain the symptom change in the test samples. However, in the inattention domain, the features selected do have a strong association with the symptom change and can be studied further to predict the trajectory of ADHD symptoms.

4 EFFECTIVE TRAINING STRATEGY FOR NN MODELS OF WORKING MEMORY CLASSIFICATION WITH LIMITED SAMPLES

4.1 Introduction

Working memory refers to the amount of information retained in memory for a short duration, which can be recalled for cognitive tasks. Previous studies have shown that an average adult can retain about three or four random items, abstract or concrete, in their working memory (Cowan, 2001) and up to seven items when associated with a pattern (Miller, 1956). Working memory capacity in an individual affects their cognitive development, learning, and attention (Pascual-Leone & Smith, 1969). For cognitive development, working memory capacity is directly proportional to the ability to comprehend ideas of various complexity. In addition, staying focused on a task is essential to learning. Individuals who test well on working memory tasks have been shown to focus better on the task at hand and learn effectively (Kane et al., 2001).

In the recent past, immense research efforts have been made in the statistical modeling of brain imaging to uncover the neuronal underpinnings of working memory. Investigations of neural correlates of age-related working memory deficit among 56 older adults using general linear models showed a significant difference in the cortical surface area of the right frontal lobe between high and low-memory performers (Nissim et al., 2016). In another study, Gorbach et al. examined the correlations of structural changes to the cognitive trajectories in the aging of 155 subjects. They observed that atrophy in the hippocampus was related to episodic-memory decline (Gorbach et al., 2017). The number of samples available for analysis limits both these studies and utilizes ROI (Region of Interest) extracted to perform the analysis.

Contrary to the existing studies, we hypothesized that we might be able to differentiate individuals with higher and lower working memory capacity by utilizing hierarchical information

directly from minimally processed structural MRI(SMRI) images through deep learning. Moreover, we analyzed a relatively larger dataset from Uk biobank; the details are presented in the next section. To our knowledge, this is the first study that employed statistical modeling—either machine learning or deep learning techniques that utilize voxel-wise data of structural MRI scans to differentiate between the lower and higher working memory capacity.

Convolutional Neural Networks (CNNs) have shown tremendous medical image analysis breakthroughs (Litjens et al., 2017). They can extract discriminating, non-linear, higher-level features from the images that effectively and accurately represent the data for the problem. A CNN model generally has a very flexible configuration, consisting of a few convolutional layers followed by one or more fully-connected (FC) layers.

To determine the optimum number of convolutional layers, FC layers, as well as learning rate, requires model tuning, referred to as hyper-parameter tuning. CNN model has been applied to brain MRIs and has shown its effectiveness. For instance, 3D convolutional neural networks based on MRI (Magnetic resonance images) scans of the brain to predict cognitive impairment. However, to accurately capture the non-linearity of the data, CNNs require vast amounts of data often unavailable for medical image analysis. The transfer learning technique is commonly used to overcome the data scarcity impediment. Using transfer learning, the CNNs are pre-trained on a large sample on a source task that closely resembles the target task. Later, these pre-trained model weights are refined or reused for the target CNN models. Because the publicly available pertained models, such as VGG-16 (Simonyan & Zisserman, 2014), are not trained on biomedical images, the knowledge being transferred is limited, hindering the power of direct transfer learning from such models. In this study, we propose an effective training strategy under limited samples, which leverages self-transfer learning ability.

4.2 Materials and Methods

In the present study, we analyzed data from UkBiobank, a large-scale biomedical database that contains health information of over a million UK participants and over 40,000 brain imaging MRI data (Alfaro-Almagro et al., 2018). Informed consent was obtained from all UKB participants. Ethics and Guidance Council (http://www.ukbiobank.ac.uk/ethics) has developed UKB Ethics and Governance Framework with IRB approval from the Northwest Multi-center Research Ethics Committee. We analyzed the T1-weighted structural MRI data of 5469 subjects to classify short-term memory ability. The memory scores indicate the maximum number of digits recalled correctly by the individual. The test starts with two digits being displayed for a short while for participants to remember. The number became one digit longer each time they remembered correctly (up to a maximum of 12 digits). For our task of classifying the subjects with high or low scores, we divided these 5469 subjects into two groups: i) subjects with memory scores ranging from 2-5 and ii) subjects with scores of 9-12. The demographic details of the two groups are shown in.

Table 4-1: Demographic of the two groups used for working memory classification.

	Low Memory	**High Memory**
No. of Participants	*3501*	1968
Male/Female	1435/2066	1108/860
Age	55.85 ±7.58	52.28 ± 7.08

T1-weighted MRI images were collected at three imaging centers with identical scanners, free from major significant software or hardware updates throughout the study (Alfaro-Almagro

et al., 2018). The images were segmented into six types of tissues (gray matter, white matter, etc.) using SPM 12. Subsequently, gray matter images were normalized into Montreal Neurological Institute space, modulated, and smoothed with a 6×6×6 mm Gaussian kernel. Further quality control was conducted to retain samples with a correlation greater than 0.9 with the mean gray matter map across all the individuals, yielding 5469 subjects. Each map has a 3D voxel matrix of 128 × 141 × 128 as inputs for the following analyses.

4.2.1 Model Configuration

In this study, we modified the SFCN, Simple Fully Convolutional Network, architecture by removing the sixth block and replacing the final seventh block with FC layers for brain age prediction. SFCN is a convolutional neural network model proposed by Peng et al. for accurate brain age prediction using T1-weighted structural MRI data. As shown in Figure 4.1, our neural network architecture consists of 5 convolutional blocks followed by FC layers. Each convolutional block consists of a 3D convolutional layer, a batch normalization layer, a max pooling layer, and finally, a ReLU activation layer. We used 32, 64, 128, 256, and 256 channels (filters) of shape 3 × 3 × 3, respectively, for each convolutional layer. The final FC layer has an output shape of 2. In addition, we added dropout (p=0.20) after each convolution block to account for generalizability.

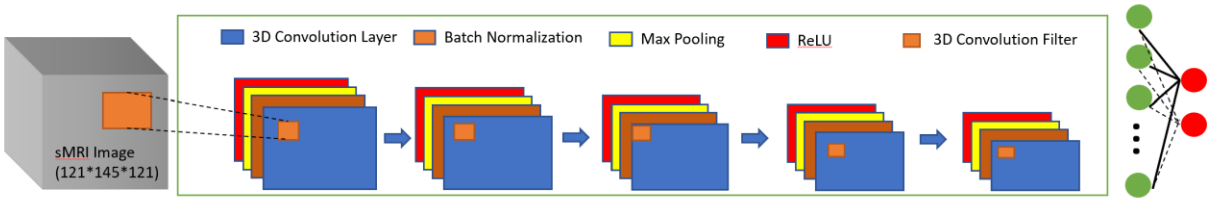

Figure 4.1: Modified SFCN architecture used for classifying working short-term memory task.

4.2.2 Self-Transfer-Training Strategy (STT)

This framework is motivated by the observation that CNN, when trained on a small sample size, is stuck in a suboptimal minimum and hyperparameter tuning (finding the best set of model layers, number of channels, learning rate, batch size, dropout, random weight initialization, and different optimization techniques such as ADAM etc.), often results in low to no improvement in the prediction. Previous studies have shown that the initial layers of a CNN capture generic imaging features and quickly reach near-optimality after a certain number of epochs. In contrast, deep layers of CNN provide more task-specific information. Thus, we design a practical yet effective hierarchical self-transfer-training strategy, where the model's different layers are trained hierarchically, and transfer learning techniques are leveraged where the source and target tasks are the same to promote self-transfer. We applied this STT strategy to brain structural MRI data to classify memory capacity to demonstrate its effectiveness. STT consists of two steps. First, we train a CNN for the task and perform hyperparameter tuning to find the optimal model. Second, using the optimal model performance as the baseline, we retrain the optimal model by freezing the first and refining the latter layers. The number of layers to freeze is part of hyper-parameter tuning.

4.2.3 Statistical Analysis

First, we performed a stratified data split into training (90%) and holdout (10%) sets. To optimize the hyperparameters– learning rate, dropout probability, and the number of FC layers, we performed stratified 5-fold cross-validation using the training set on each set of hyperparameters. Initially, we started training the model with one FC layer and optimizing the model for learning rate, momentum, and dropout probability. Then, we varied the number of FC layers from two to four and optimized the model for other hyperparameters. On each fold, we trained the model for

75 epochs with exponential decay of the learning rate if the training loss did not change for three consecutive epochs. We used Stochastic Gradient Descent as an optimizer and computed the Binary Cross Entropy loss (BCE). After identifying the best setting, we tested the performance of the best model (epoch where the model is neither overfitting nor underfitting) from every fold on the holdout set. We used balanced accuracy as our metric to judge the model. Balanced accuracy is measured as the means of sensitivity and specificity and helps estimate the performance of a model when dealing with an imbalanced dataset.

Second, we further trained the best model from the previous step using 5-fold cross-validation using the same data split by freezing various layers. Initially, we started by freezing all the convolution layers except the final FC layer, i.e., reusing all the higher-level brain imaging features for prediction. And then, we unfreeze the convolution layers one by one, moving from the final (higher) layer to the initial (lower) one in each subsequent analysis. Under each condition, we performed hyperparameter tuning to find the best combination of the learning rate, dropout, and momentum. We tested the performance on the holdout set using the best model from each fold for each experiment. We reported the balanced accuracy averaged across five folds for all the experiments.

4.3 Results

In Table 4-2, we show the best inter-fold balanced accuracy obtained for the models with a different number of FC layers without self-transfer training. Among the different trained models, the model with one FC layer and a dropout of 0.20 between the convolutional layers performed better with a mean balanced accuracy of 67.80, 64.42, and 70.41 for training, validation, and testing, respectively. Although the model with two FC layers has a mean balanced accuracy of 67.43 with a standard deviation of 0.59 in training, the variation of validation accuracy indicates

that some of the folds are not generalized, i.e., either overfitting or underfitting. The performance of the models with three or more FC layers is low compared to those with a smaller number of FC layers, indicating insufficient samples for more complex models.

Table 4-2: Inter-fold balanced accuracy of model with fully-connected layers.

Number of fully-connected layers	***Balanced Accuracy***		
	Train	Validation	Holdout
1	67.80 ± 0.69	64.42 ± 0.51	70.41 ± 0.86
2	67.43 ± 0.59	60.45 ± 3.45	62.12 ± 0.89
3	59.26 ± 2.45	58.32 ± 1.89	59.62 ± 2.69
4	57.25 ± 2.43	55.32 ± 1.25	56.45 ± 1.45

Table 4-3shows the model's performance with the best hyperparameters (model with one FC layer, dropout of 0.2 between convolutional layers) when further trained using step two of self-transfer-training. The model performed better when the initial convolutional layers were frozen, and the final few layers were open to train. When trained by freezing only the two convolutional layers, the model performed best with the mean balanced accuracy of 73.12, 70.20, and 76.15 on training, validation, and holdout sets, respectively.

Table 4-3: Inter- fold balanced accuracy achieved by the model.

Layers trained	***Balanced Accuracy***		
	Train	**Validation**	**Holdout**
Fully-connected layer	68.24 ± 0.46	68.42 ± 3.13	66.15 ± 0.39
5th Convolutional layer and FC layer	69.77 ± 0.41	67.77 ± 2.82	70.21 ± 0.73
4th and 5th conv and FC layers	72.53 ± 1.58	69.83 ± 3.61	73.80 ± 3.41

3rd, 4th, and 5th conv and FC layers	73.12 ± 2.08	70.20 ± 2.77	76.15 ± 1.96
2nd, 3rd, 4th, and 5th conv and FC layers	71.90 ± 1.14	69.39 ± 2.39	75.15 ± 1.20

4.4 Discussion

Our present study modified the SFCN architecture to classify the working memory. We grouped the working memory scores as high and low, which induced data imbalance. Our results indicate that the model with fewer fully connected layers performed better. Adding more non-linearity to the model by increasing the number of FC layers hindered its generalizability, indicated by the massive difference between training and validation balanced accuracy. Moreover, with the current best practice of initialization and adaptive learning (ADAM), the model performance saturated at a suboptimal solution.

However, we improved the model performance by adopting self-transfer-training– early stopping when the model hits suboptimal solution and retraining by freezing the initial convolutional layers. Model training on a small sample size with data imbalance saturated the model after a few epochs. Freezing some of the layers from the saturated model and training the rest of the layers helped the later layers to learn the non-linearity of the features and decision function better and faster. Another reason behind the success of the self-transfer-training strategy is that we assume features in initial layers in CNN models represent more local, generic features. In contrast, deep layers provide more task-specific features. Thus, the model could provide better task performance by focusing on training later layers.

Using this empirical self-transfer-training strategy for classifying the working memory, we showed that the strategy works with a relatively small imbalanced dataset. The underpinning

of this strategy is the observation that the initial convolution layers extract the generic imaging features common to many prediction tasks in CNNs. These initial layers reach near optimality quickly, which can be inferred by the model's performance improvement after freezing the initial two convolutional layers. On the other hand, the deep layers of CNN are task-specific, and fine-tuning them improved the performance of our current task.

4.5 Conclusion

In conclusion, we have shown that the same model architecture, when trained differently, could produce improved results to predict the working memory with limited unbalanced data. The empirical Self-Transfer-Training strategy aids in improving the performance of the model by freezing the initial layers of the CNN and training the deep layers for our task. In addition, this finding indicates that the same brain features with different non-linear connections can predict different variables.

Based on our finding that different tasks share the same brain features, we speculate that transfer learning techniques might help us improve the model's decision-making, mainly when applied to medical imaging. In addition, we also speculate that any dataset with class imbalance will benefit from our self-transfer-training strategy.

5 TRANSFER STRUCTURAL MRI BRAIN AGE MODEL TO WORKING MEMORY PREDICTION IN UK BIOBANK COHORT

5.1 Introduction

Working memory (WM) functioning is a cognitive process responsible for temporarily holding and manipulating information in our minds during complex cognitive tasks (Baddeley, 2000; Baddeley & Hitch, 1974; Cowan, 2014). Understanding working memory functioning is essential for comprehending how our brains hold, reason and execute information (D'Esposito & Postle, 2015; Miyake & Shah, 1999). WM plays a crucial role in a wide range of cognitive activities, including learning, problem-solving, decision-making, attention control(Unsworth & Spillers, 2010) and language comprehension (Oberauer, 2019), highly correlated to overall intelligence(Ackerman et al., 2005). The impairment of working memory has been associated with a large number of mental disorders including ADHD (Duan et al., 2021), autism spectrum disorders (Rabiee et al., 2020), major depression (Nikolin et al., 2021), schizophrenia (Forbes et al., 2009), and more (Henseler & Gruber, 2007). More particularly, working memory deficits are apparent in older individuals, not only presenting as age related decline (Bopp & Verhaeghen, 2005) but also as susceptibility to cognitive deterioration such as Alzheimer's disease related dementia (BADDELEY et al., 1991), and mild cognitive impairment (A.-M. Kirova et al., 2015).

Understanding working memory capacity and its changes in the older population is of great importance, according to the WHO report on aging and health [18], as globally there is a shift towards older populations in more countries. Age-related cognitive decline and memory impairment have become significant concerns worldwide (Association, 2015; Tomaszewski Farias et al., 2009). Working memory is more sensitive to ageing than other spectrum of memory; its capacity in the older population decreases to 74% compared to younger adults

(Bopp & Verhaeghen, 2005). Furthermore, pathological working memory deficits in the older population serves as an essential diagnostic and prognostic marker for cognitive impairments and neurodegenerative disorders (Bleckley et al., 2003; Kane et al., 2001). Thus, it is crucial to delineate neuronal mechanisms of working memory functioning decline in older population.

Neuroimaging studies have been instrumental in the investigation of working memory, providing insights into the underlying brain mechanisms and networks involved. Using Voxel Based Morphometry (VBM) analysis, studies have found that older adults with larger volumes in the prefrontal cortex, anterior cingulate cortex, and parietal cortex performed better on working memory tasks (Nyberg et al., 2010). Older populations with cognitive impairment were observed to have reduced grey matter (GM) volume in the prefrontal cortex, hippocampus, caudate, and cerebellum (Dennis & Cabeza, 2011; Nyberg et al., 2010; Raz & Rodrigue, 2006). A functional MRI study of 163 subjects revealed lower connectivity within the fronto-parietal network (FPN) as well as between FPN and striatum in subjects with lower working memory capacity (Salami et al., 2018). More recently, a study of the working memory deficits in schizophrenia patients found disfunction in Heschl gyri, insular and amygdala, in addition to superior frontal gyrus and superior temporal gyrus, are associated with working memory deficit of patients(Chatterjee et al., 2019). A meta-analysis of 42 studies of neural-correlates of verbal working memory highlighted the activation in a large network including fronto-parietal areas, right cerebellum, insular and basal ganglia structures (Emch et al., 2019). Angular gyri as part of default mode network interacting with other brain networks serves as an indicator of reaction times to n-back tests, implying a role in working memory (Vatansever et al., 2017). Another study which examined the temporal dynamics of visual working memory found more pronounced activations in inferior frontal cortex that were more pronounced during maintenance than in encoding (Sobczak-Edmans et al., 2016).

Gender differences in neural networks underlying working memory have been documented in a meta-analysis with females activating more limbic system (hippocampal and amygdala), males activating more distributed network (Hill et al., 2014).

Until recently, neuroimaging studies were limited in sample size (Suresh et al., 2021), precluding the use of predictive learning models such as deep learning, which have proven useful in many other fields. This changed as larger cohorts of neuroimaging resources, such as UK biobank, Adolescent Brain Cognitive Development (ABCD), and Alzheimer's Disease Neuroimaging Initiative (ADNI), have been made available (Petersen et al., 2010; Saragosa-Harris et al., 2022; Sudlow et al., 2015). Even so, these numbers are still suboptimal for the data-hungry deep learning models to be used to their full potential. For example, more than 14 million natural images in ImageNet dataset (Deng et al., 2009) are available for deep learning models to recognize objects with high levels of accuracy. To mitigate the limitation of smaller sample sizes, the transfer learning technique enables researchers to leverage a model trained with big data for a source task and then fine-tune the model on a smaller dataset for a target task (Ardalan & Subbian, 2022; Weiss et al., 2016). This approach has been shown to lead to improved performance particularly for the homogeneous transfer within the same domain (Raza et al., 2023; Weiss et al., 2016), as the pre-trained models already have a strong initial understanding of the data. We propose, in this study, a transfer learning within neuroimaging domain, instead of commonly implemented across natural image and neuroimage domains, and transferring knowledge learned from related source task (brain age) to a target task (working memory capacity).

Brain age prediction done by deep learning models has improved significantly over the past decade (Han et al., 2021; Ray et al., 2021). In an older population of the UK biobank cohort, a simply fully connected convolutional network (SFCN) (Han et al., 2021) architecture introduced

by Peng et. al at Predictive Analysis Challenge 2019 has achieved an accuracy of about 2 years for subjects ranged 40-70 years of age when trained with relatively large dataset. During training, the learned features capture important structural characteristics of the brain that are related to aging. We believe by leveraging the pre-trained features related to ageing, transfer learning will enable efficient feature extraction for our task of working memory capacity classification, therefore reducing the need for large, labeled data. Currently, deep learning methods that have only trained using working memory capacity and sMRI have much lower mean balanced accuracy of 73.12 (Pranav Suresh, 2023). To improve this, we will first build a brain age prediction model trained with the sMRI images of 39,755 subjects, and then transfer the learned brain features from the brain age model to the deep neural networks that we will use on the sMRI images of the subset of 5,469 subjects to classify them into high or low memory categories. Our aim is to demonstrate the higher accuracy of deep neural networks trained first on brain age models and reveal a more complete picture of the neuronal underpinnings of working memory capacity differences.

5.2 Materials and Methods

Data used for this study was obtained from UK Biobank (Sudlow et al., 2015). UK Biobank is a large-scale biomedical database containing in-depth genetic and health information from half a million UK participants, over 40,000 of whom also had brain MRI imaging data. Informed consent was obtained from all UKB participants. Ethics and Guidance Council (http://www.ukbiobank.ac.uk/ethics) has developed UKB Ethics and Governance Framework with IRB approval obtained from the North-West Multi-center Research Ethics Committee. We focused on T1-weighted sMRI data in this study. After quality control as described later, there were valid data from 39,755 participants who had a mean age of 54.81 years old and a standard deviation of 7.46, range 40-70 years.

WM was assessed by recording the maximum digits remembered correctly during a backward digit span task. The test starts with two digits being displayed for a short period for participants to memorize. For each test, if subjects memorized the number correctly in the reverse order, then for the subsequent test the length of the number increased by one digit (up to a maximum of 12 digits). The working memory scores from 26,534 participants roughly follow a normal distribution as shown in supplementary Figure 1. For our task of classifying the participants with high memory capacity vs. low memory capacity, of 26,534 participants we selected subpopulation of 5469 and divided into two groups: i) subjects with memory scores ranging from 2-5 and ii) subjects with scores of 9-12. The segregation was based on the Miller's Law of clinical psychology which states that individuals, on average, can hold about 7 ± 2 items at a time in their working memory (Miller, 1956). However, based on the distribution of our dataset we presumed 7 ± 1 as the average capacity. Table 5-1 shows the demographic distribution of the subjects with low memory scores and high memory scores.

Table 5-1: Demographic data of the two groups used for working memory classification.

	Low Memory	**High Memory**
No. of Participants	*3501*	1968
Male/Female	1435/2066	1108/860
Age (*p* = 3.02e-14)	55.85 ±7.58	52.28 ± 7.08
Memory score	4.6 ± 0.6	9.22 ± 0.48

T1-weighted MRI images were collected at three imaging centers with identical scanners, free from major software or hardware updates throughout the study (Alfaro-Almagro et al., 2018). The images were segmented into six types of tissues (gray matter, white matter, etc.) using SPM

12. Subsequently, gray matter images were normalized into Montreal Neurological Institute space, modulated, and smoothed with a $6 \times 6 \times 6$ mm^3 Gaussian kernel. Each map consists of a 3D voxel matrix of 128 × 141 × 128. Further quality control was conducted to retain samples with a correlation larger than 0.9 with the mean gray matter map across all the individuals, yielding 39,755 subjects.

5.2.1 Classification of working memory using SVM

To establish a baseline for our task of working memory classification, we have fitted a model using a standard machine learning method. A L1 regularized support vector machine classifier (SVC) with radial basis function as the non-linear kernel was used to learn the underlying gray matter patterns to classify the subjects as high or low working memory. Previous work has shown that feature reduction plays an important role in boosting performance of the machine learning models (Suresh et al., 2021). After quality control, using the subjects from the training set, we computed the mean gray matter image and removed the voxels with gray matter volume less than 0.2 resulting in dataset with shape of 4423 X 472,035. Next, we performed principal component analysis (PCA) to extract 741 components that explain 80% of the variance. The PCA transformed matrix was used to train the regularized SVC. Finally, the trained SVC's performance was computed on the holdout set. We've also tested the performance of SVC using a different number of PCA components. In addition, to examine the effect of age on the baseline classifier we have trained the baseline classifier with age as a predictor along with the PCA components.

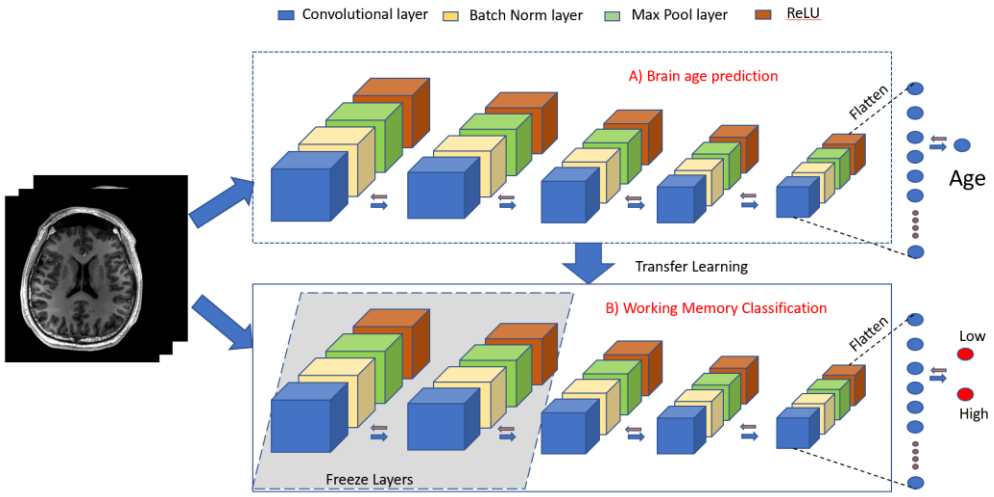

Figure 5.1: Overview of the analyses performed.
Top) CNN for predicting brain age. CNN consists of five convolutional blocks and each block consists of a Convolutional layer, a batch norm layer, a max pool layer, and ReLU layer. Bottom) CNN model transferred from brain age to classify the working memory. The two CNN blocks in the grey shaded region are frozen with parameters transferred from brain age model while learning to classify working memory groups.

5.2.2 Transfer Learning Model

We previously classified working memory capacity on the same dataset using directly trained deep learning models on structural images achieving a modest mean balanced accuracy of 73.12% (Pranav Suresh, 2023) and the reason could be attributed to the limited sample size. In contrast, brain age models have demonstrated better performance with large samples to learn from (Han et al., 2021). The effect of aging on working memory has been extensively studied in the field of cognitive neuroscience. Accumulated evidence revealed that working memory has steeper decline as age progresses (Fournet et al., 2012), and the decline could be a linear function of age (Bopp & Verhaeghen, 2005; Pliatsikas et al., 2019). Together, we are motivated to propose a transfer leaning model as in **Error! Reference source not found.**.

Error! Reference source not found. shows the overview of the analysis performed for the classification task. First, we built a neural network model for brain age prediction using all

available gray matter data from 39,755 participants. Then another neural network model was trained using a transfer learning technique for classification of working memory capability for the 5469 participants. In particular, we implemented a heuristic training strategy (Pranav Suresh, 2023) coupled with transfer learning from brain age model, which improved the prediction accuracy of the model. Finally, to understand the brain regions that have significant contribution to the prediction, we employed model interpretability using region occlusion approach to generate sensitivity maps.

5.2.3 Brain Age Prediction

In this study, we modified the SFCN model (Han et al., 2021) by removing the sixth block and replacing the final seventh block with fully-connected layers for brain age prediction. Our final neural network architecture for brain age prediction, shown in **Error! Reference source not found.**, consists of 5 convolutional blocks followed by one fully-connected layer. The model takes 128 × 141 × 128 3D brain image data and contains 5 convolutional blocks followed by one fully-connected layer. Each of the 5 consecutive blocks consists of a 3 × 3 × 3 3D convolution layer, a Batch Norm layer, a 3D Max Pooling layer and a ReLU. Each of the convolutional layers used 32, 64, 128, 256, 256 channels, respectively, with stride of one and no padding was used. The output images from the final convolutional block are flattened and passed to the fully-connected layer which takes 1024 inputs and outputs the predicted brain age. The fully-connected layer has a dropout rate of 0.2.

5.2.4 Transfer Learning for Working Memory Classification

For prediction of working memory capacity, we applied the concept of transfer learning in combination with our heuristic self-transfer-training method (Pranav Suresh, 2023). The best trained model (source) for brain age was used to initialize the target model for the prediction of

the working memory. We replaced the fully-connected layer from the source model to accommodate for the classification task. The model architecture is shown in **Error! Reference source not found.**. Each of the 5 consecutive blocks consists of a 3 × 3 × 3 3D convolution layer, a Batch Norm layer, a Max Pooling layer and a ReLU. The fully-connected layer takes 1024 inputs with a dropout rate of 0.2, and its two outputs are passed on to the soft-max function to calculate the probabilities of each label.

5.2.5 Model Training

During the training process, we used Stochastic Gradient Descent (SGD) as our optimizer to minimize the Mean Absolute Error (MAE) for brain age model and Binary Cross Entropy (BCE) for working memory classification model. All models were trained in batches of 15 images per GPU, with the learning rate initialized to 0.001 for each individual layer. For each model, we performed hyperparameter tuning to determine the optimal set of learning rate for each layer, dropout rate, and the number of fully-connected layers. To reduce overfitting, two data augmentation methods were applied during the training phase. In every epoch, the training input is 1) randomly shifted by 0, 1 or 2 voxels along every axis; 2) has a probability of 50% to be mirrored about the sagittal plane.

We used the same setup for training both the brain age model and the working memory classification model. The whole dataset was split into a training set (90%) and a holdout set (10%). The training set was used in the 5-fold cross-validation to select the best model configuration. For each training fold, we trained a total of 75 epochs, where training each epoch with model replicated on each of the 4 GPUs using PyTorch Data Parallel (Li et al., 2020). The learning rate was multiplied by 0.1 if the change in loss between two consecutive epochs was less than 0.0001. For each fold, the epoch with the least MAE in the case of the brain age model, and highest sensitivity

score on the validation set for the working memory classification model, was selected, and tested on the holdout dataset. The model configuration that gave the best results for brain age model was used as source for transfer training working memory classification model. To avoid data leakage from brain age model into the working memory model, the holdout set for the later task was selected to be a subset of the former task's holdout set.

During training of classification model, we started from the best trained brain-age model (base), replaced the fully-connected layer to adapt for classification, and retrain the model with all parameters in all layers free to be updated, conducted as the typical transfer learning approach. Furthermore, we trained the models by freezing selected individual blocks (setting learning rate to 0) and updating the rest, starting from freezing all convolutional blocks and updating the fully connected layer, then freezing the first 4 convolutional blocks and updating the last and fully connected layer, to freezing only the first convolutional blocks and updating all other layers.

Finally, we test the contribution of age to the overall prediction of the CNN model. We added age to the flattened features from the final convolutional layer and trained only the fully connected layer. Moreover, to test if the working memory CNN model has learnt to classify the subjects based on the memory capacity or based on their age, we created ten subsamples of size four hundreds using stratified bootstrapping with replacement from the holdout set. Each of these subsamples consisted of age matched samples from high and low memory groups. Further, on each of these subsamples, using average age of the holdout set, 56, as the pivot, we encoded the age of the sample as 0 if the actual age was less than 56, and 1 if the actual age was greater than or equal to 56. Then, we tested the performance of the working memory model by computing the balanced accuracy of the prediction of the encoded age as compared to the accuracy of the memory classification.

5.2.6 Model Interpretation

To understand the brain regions that are significant for the classification task, we have explored three gradient based approaches, gradient * input, DeepLift, integrated gradients method (Ancona et al., 2017) and occlusion based method. All three gradient based methods seek to create attention maps by assigning a contribution score to each voxel indicating the importance of the voxel to the classification. Our experiments showed all interpretation methods highlighted similar regions that were obtained using occlusion method. In here, we have reported the experiments and observations from network occlusion method.

Network occlusion sensitivity is a simple technique for understanding which parts of an image are most important for a deep network's classification (Zeiler & Fergus, 2014). We used the AAL3 (Rolls et al., 2020) brain atlas with 116 regions to perform region occlusion. Using region occlusion, the contribution score of each region to the overall prediction is the difference between the probability score of the original image and the probability score of the region occluded image. For occluding a region, we replaced original values in the region with the mean value of the region across all holdout subjects.

Finally, to determine the contribution significance of each region, a one sample *t*-test is applied to the contribution scores of all correctly classified subjects. The *p*-value obtained for each region indicates the likelihood that the region’s mean contribution score across subjects is different from zero by chance. Multiple comparisons correction using Bonferroni correction was applied to correct for 116 tests. Regions that passed the multiple comparisons correction and with positive mean contribution values were identified to significantly contribute to memory prediction. Furthermore, to quantitatively examine differences in regional contribution across groups (i.e., low memory, or high memory) and sex, and relationship with age, ANCOVA model was used for each

significantly contributing region with age, sex, group as variates. Similarly, Bonferroni correction was applied to detect the significant influence of each variate on regional contribution. Statistical significance was considered at $\alpha = 0.05$.

5.3 Results

5.3.1 Baseline model using Support Vector Classifier

As the benchmark comparison for the transfer learning model, we first tested an SVC model for WM classification**.** To specifically mitigate the bias induced by relative smaller input variables to the baseline SVR model, compared to CNN model, we tested a range of number of input variables (from 50 to 750 PCA components), the best performed model was selected for comparison. Table 5-2 shows the balanced accuracy achieved by the SVC models on the training, validation, and the holdout set using different numbers of PCA components. The accuracy of the SVC increased gradually with the increase of the number of components and peaked at 150 components (68.57%) during the training, and validation and testing accuracies are saturated at 64.33% and 64.85%. With the inclusion of age as a predictor, we observed the model peak performance with mean balanced accuracy of 71.29% on training, 67.25% on validation, and 66.96% across five folds when trained using 250 PCA components, shown in Table 5-3. Overall, there is about 3% increase of accuracy after including age.

Table 5-2: Balanced accuracies achieved by the regularized SVC on PCA components

Number of components	Training (%)	Validation (%)	Testing (%)
50	63.73 ± 0.49	61.30 ± 0.43	63.63 ± 0.64
100	68.32 ± 0.87	64.47 ± 0.77	65.60 ± 1.26
150	**68.57 ± 0.97**	**64.33 ± 0.59**	**64.85 ± 0.75**
200	68.15 ± 0.72	63.64 ± 0.99	64.44 ± 0.56

250	68.50 ± 0.31	63.56 ± 0.50	64.89 ± 0.37
300	67.02 ± 0.71	62.44 ± 0.60	63.52 ± 0.73
350	65.56 ± 0.75	61.01 ± 0.81	62.12 ± 0.78
400	65.10 ± 0.59	60.67 ± 0.73	61.83 ± 0.49
450	63.43 ± 0.46	59.61 ± 0.51	60.02 ± 0.54
500	62.86 ± 0.47	58.69 ± 0.54	59.33 ± 0.78
550	62.07 ± 0.39	58.26 ± 0.41	58.74 ± 0.53
600	61.26 ± 0.50	57.75 ± 0.59	57.92 ± 0.64
650	60.87 ± 0.54	57.36 ± 0.52	57.90 ± 0.62
700	60.48 ± 0.44	57.23 ± 0.37	58.03 ± 0.58
741	59.75 ± 0.45	56.58 ± 0.12	57.20 ± 0.65

Table 5-3 Balanced accuracies achieved on by the regularized SVC function fit on age.

NUMBER OF COMPONENTS	**TRAINING (%)**	**VALIDATION (%)**	**HOLDOUT (%)**
50	65.38 ± 0.55	63.59 ± 0.73	65.26 ± 0.42
100	69.93 ± 0.95	67.15 ± 0.54	67.48 ± 0.97
150	70.63 ± 0.90	67.02 ± 0.78	67.17 ± 0.49
200	70.84 ± 0.66	66.88 ± 0.68	67.15 ± 0.35
250	**71.29 ± 0.61**	**67.25 ± 0.52**	**66.96 ± 0.71**
300	70.21 ± 0.75	66.17 ± 0.72	65.90 ± 0.56
350	69.12 ± 0.58	65.02 ± 0.70	65.02 ± 0.66
400	68.13 ± 0.68	64.20 ± 0.77	64.18 ± 0.57

450	66.72 ± 0.67	62.87 ± 0.76	63.00 ± 0.53
500	66.04 ± 0.79	61.98 ± 0.58	62.42 ± 0.66
550	65.43 ± 0.57	61.64 ± 0.33	61.37 ± 0.71
600	64.33 ± 0.52	60.83 ± 0.54	60.43 ± 0.69
650	63.35 ± 0.62	59.83 ± 0.51	59.98 ± 0.70
700	63.08 ± 0.56	59.59 ± 0.61	59.96 ± 0.91
741	62.34 ± 0.39	59.12 ± 0.34	59.01 ± 0.63

5.3.2 Brain Age Prediction

As stated earlier, we used data of 39,755 subjects for brain age prediction. We achieved the best results (MAE of 2.82 ± 0.04 on training, 2.88 ± 0.05 on validation, 2.47 ± 0.2 on holdout set) when the network was trained with one fully-connected layer, learning rate of 0.001, a dropout rate of 0.2. This accuracy is comparable to that reported in the original brain age study using UK biobank data with MAE of 2.14 years (Han et al., 2021).

5.3.3 Working Memory Classification

The best model from the brain-age prediction was transferred for working memory classification. Table 5-4 shows the balance accuracy (averaged accuracy for high memory and low memory groups) while training the model by freezing different numbers of layers. Best results were obtained when the model was trained only for the high-level representations (layers 3 to 5) and used the low-level representations (first and second convolutional layer) learnt from the brain age model. Table 5-5 shows the balanced accuracy, accuracy for high memory group (sensitivity), and accuracy for the low memory group (specificity) across all five-folds of the models trained while freezing first two convolutional layers and training the rest.

Table 5-4: Balanced accuracy trained by freezing different number of layers.

Layers trained	***Balanced Accuracy***		
	Train	Validation	Holdout
All layers	67.80 ± 0.69	64.42 ± 0.51	70.41 ± 0.86
Fully-connected layer	68.73 ± 1.52	70.83 ± 1.37	68.25 ± 1.36
5th Convolutional layer and FC layer	71.77 ± 0.21	68.77 ± 2.42	70.21 ± 0.73
4th and 5th conv and FC layers	73.63 ± 1.04	70.24 ± 0.61	72.16 ± 1.41
3rd, 4th, and 5th conv and FC layers	81.34 ± 2.34	75.32 ± 0.49	87.02 ± 1.31
2nd, 3rd, 4th, and 5th conv and FC layers	74.90 ± 0.67	73.39 ± 0.68	74.15 ± 1.08

Table 5-5: Balanced Accuracy, accuracy of low group, and accuracy of high group across five folds.

	Fold	*1*	*2*	*3*	*4*	*5*	*Mean ± STD*
Training	*Balanced Accuracy*	*83.78*	*84.04*	*79.45*	*81.38*	*78.09*	*81.34 ± 2.34*
	Accuracy of low group	*94.8*	*95.35*	*93.88*	*93.92*	*93.2*	*94.22 ± 0.75*
	Accuracy of high group	*72.72*	*72.72*	*65.01*	*68.83*	*62.96*	*68.44 ± 3.96*
Validation	*Balanced Accuracy*	*75.16*	*74.84*	*76.25*	*75.01*	*75.35*	*75.32 ± 0.49*

	Accuracy of low group	*73.76*	*80.76*	*74.24*	*79.96*	*83.46*	*78.43 ± 3.80*
	Accuracy of high group	*76.55*	*68.92*	*78.24*	*70.05*	*67.23*	*72.19 ± 4.37*
	Balanced Accuracy	*88.35*	*88.7*	*86.64*	*86.26*	*85.19*	*87.02 ± 1.31*
Testing	*Accuracy of low group*	*84.7*	*89.16*	*79.16*	*87.5*	*87.5*	*85.60 ± 3.52*
	Accuracy of high group	*91.9*	*88.23*	*94.11*	*85.02*	*82.88*	*88.42 ± 4.16*

To test if the model has learnt to classify subjects based on the working memory or age, we tested its performance on ten bootstrapped subsamples which had age matched individuals from high and low working memory groups. The performance is shown in **Error! Reference source not found.**. On each of the subsamples, the model has achieved better accuracy classifying working memory rather than age. On average, for the classification of memory group the model has achieved mean accuracy of 79.20%, while the accuracy for age classification was mere 58.99%. Moreover, by adding age to the flattened features and training only the fully-connected layer we observed mean balanced accuracy of 81.54% on training, 75.62% on validation, and 87.05% on the holdout set.

Table 5-6: Accuracy of the model for classification of encoded age and working memory on the ten bootstrapped subsamples.

Subsample	*Accuracy of encoded age*	*Accuracy of memory classification*
1	58.88	78.42
2	57.57	80.80
3	59.39	79.94
4	54.84	81.37
5	56.88	77.80

6	61.59	79.12
7	62.06	77.38
8	64.21	77.15
9	57.61	77.66
10	56.92	82.30
Mean	58.99	79.20

5.3.4 Model Interpretation

To understand the final working memory prediction model, regional contribution scores were calculated. T-test after correction for multiple comparisons on the region contributions revealed that 73 regions had significant contribution to the prediction. The full list of 73 regions plotted in Figure 5.2. Among the 73 regions the top five contributors are Right Putamen (p=1.27e-26), Right Parahippocampus (p = 3.29e-25), Left Angular gyrus (p= 1.17e-22), Left Amygdala (p= 1.47e-22), and Left Para hippocampus(p= 3.95e-21), followed by other cortical regions, where left and right hippocampus are ranked 26 and 9 respectively.

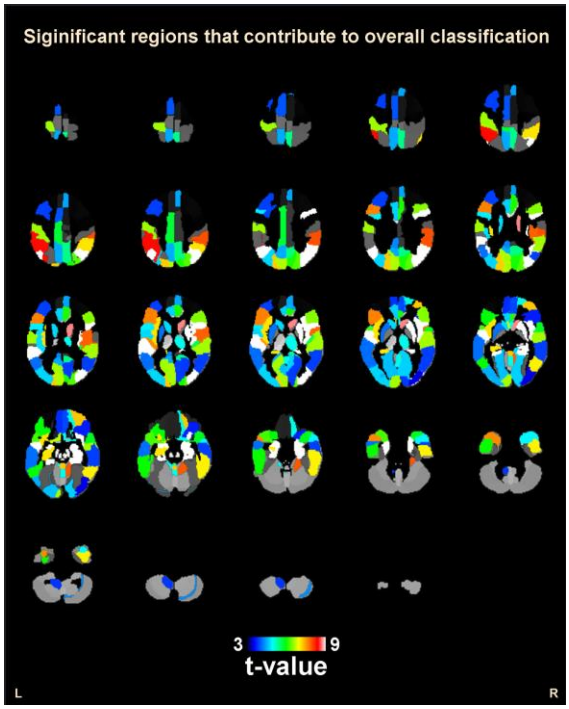

Figure 5.2: Regions that significantly contribute to the overall classification of the working memory group.

Further, to test the influence of either age, sex, or working memory groups on a region's contribution score, ANCOVA was performed. Right Heschl's gyrus (p = 2.89e-57), Right Temporal Superior gyrus (p = 2.71e-54), Left Rolandic Operculum (p = 2.54e-53), Left calcarine fissure and surrounding cortex (V1) (p = 9.17e-53), Right frontal medial orbital gyrus (p = 1.12e-50) are the top five regions of the sixty-two significant regions that showed group differences in contributions. 60 out of the 62 regions showed significantly higher contributions in the high memory group than the low group, and the only two regions contributed more to the low memory group but with less effect sizes**.** Figure 5.3 illustrates the top five regions (Right Heschl (red), Right Temporal Superior (blue), Left Rolandic Operculum (green), Left Calcarine (pink), Right Medial Orbitofrontal (yellow) showing significantly high contributions in high memory group and two

regions, Left Inferior Frontal gyrus Triangular (p = 8.36e-08; cyan), and Right parahippocampal gyrus (p = 7.54e-06; copper) with higher contribution in the low memory group.

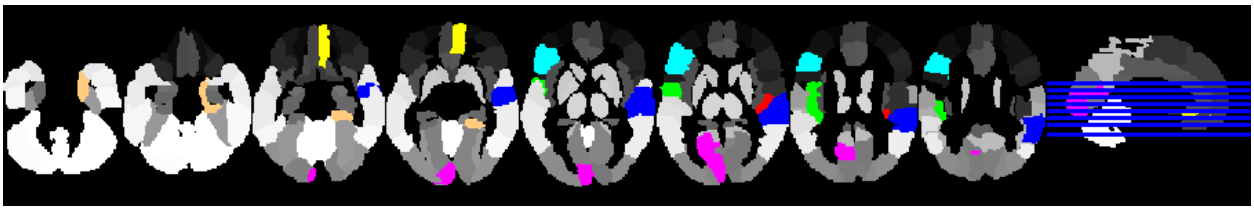

Figure 5.3: Regions that show significantly different contributions in the high versus low working memory groups.

Meanwhile, sex had significant influence on fifty region's contribution scores (supplementary Table 3). Females had higher contributions in all fifty regions**.** Right Putamen (red; p=4.84e-25), Left inferior frontal gyrus, triangular (blue; p=3.89e-17), Left parahippocampal gyrus (green; p = 5.29e-17), Right parahippocampal gyrus (pink; p = 5.5e-17), Left Amygdala (yellow; p = 9.97e-16), Right Hippocampus (cyan; p = 1.01e-14), and Right Amygdala (copper; p = 2.20e-14) are the top seven regions, plotted in Figure 5.4 for illustration purpose. ANCOVA analysis showed only one region, Left Heschl's gyrus, has contribution influenced by age, where increased age is associated with less contribution.

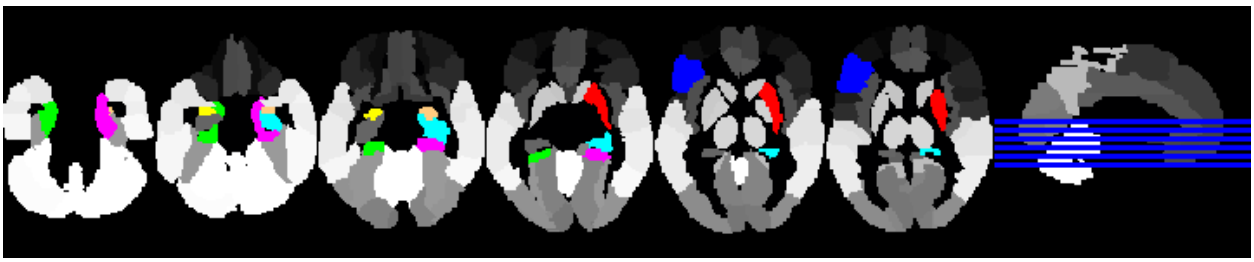

Figure 5.4: Regions whose contribution score is influenced by gender.

5.4 Discussion

The goal of the study was to examine the potential of the convolution neural network (CNN) model trained on structural MRI images to classify working memory capacity, while also enabling us to understand the relevant brain regions that contribute to the memory task. To this end, we devised a simple, yet effective model based on transfer learning technique**.** First, we established a baseline using a regularized SVC which achieved the best performance of mean balanced accuracies of 68.50%, 63.56%, and 64.89% on the training and holdout set, respectively. The addition of age to the baseline model improved its performance by approximately 3% which suggests that the baseline SVC classifier must have not captured the neuronal patterns related to the ageing process. Next, we trained a CNN model to learn the brain age of 39,755 subjects. The convolution layers in the brain age model best present brain structural nonlinear abstract presentations to estimate brain age. Based on assumption that the brain age presentations could be helpful for prediction of memory capacity, we applied transfer learning technique that leverages features learnt on brain age prediction, which is trained on relatively large number of subjects, and trained another CNN model for the working memory classification task which has fewer subjects to learn from.

In particular, using transfer learning, we reused the lower-level features (first several layers of CNN model) learnt on the brain age model and re-trained the high-level features to accurately capture the representations for the working memory classification task. Previous studies have shown that lower layers of CNN model capture local features such as lines, curves, edges etc. (Santosh et al., 2022), we suspect that lower layers of brain age model capture local brain characteristics such as local surface, curvature or volume, which are fundamental and common for any brain function including aging process and working memory. While high level features from

later layers of the CNN model are more task specific, those are different for brain age and memory task. Our study demonstrated the best model for working memory prediction was achieved when the first and second layers of CNN model of brain age were reused, while the rest layers of the model were retrained. Our previous study without transfer learning from brain age model (Pranav Suresh, 2023) reported the best balanced accuracy for prediction of working memory capacity was 73.46%, here with transfer leaning from brain age model, the training accuracy improved to 81.34%, supporting our hypothesis that transfer leaning from brain age model could help in better prediction of working memory. Moreover, our test of the model on the bootstrapped subsamples indicated that the model has indeed learned to classify subjects based on the working memory capacity. In addition, minor improvement of the CNN model with age indicates that most of ageing related neural patterns have already been captured by the model. We speculate that contribution of ageing to the working memory capacity is captured by the lower CNN layers of the pretrained brain age model.

Even though deep learning models have been depicted as black box, many approaches have been proposed to explain the contribution of features including occlusive, gradient based, and Shapely value based methods (Erion et al., 2021; Sundararajan et al., 2017; Zeiler & Fergus, 2014). We have applied gradient based method (Sundararajan et al., 2017) and occlusive method, which provided similar results at large. Here we reported results from occlusive method for simple interpretation. From contribution scores of the best model, T-test results have shown that 73 regions out of 116 are significant for the overall prediction. Among these 73 regions the most significant regions are subcortical regions including the well-known memory related hippocampus and Parahippocampus (Aminoff et al., 2013; Ranganath et al., 2005; Schon et al., 2004), and insula and amygdala. Even though subcortical regions have not been often studied for working memory,

a few studies have emphasized the role of these regions on both the long term memory and working memory (Menon & Uddin, 2010; Schaefer et al., 2006; Yun et al., 2010). In particular, Emch and colleagues reported in a meta-analysis of 42 studies of neural-correlates of verbal working memory that a large network including fronto-parietal areas, right cerebellum, insular and basal ganglia structures are activated [26]. Our results show consistent implications, suggesting broad brain regions including subcortical and cortical regions contribute to working memory, with subcortical regions playing a more important role relatively. While many fMRI studies of working memory highlight the prominent activation of frontal-parietal regions, we speculate that, based on our findings, frontal-parietal regions are most active in working memory process, but their structure variations do not have enough power to differentiate high and low working memory capacity.

The ANCOVA test for group differences with gender and age as covariates has shown 62 regions of the 73 regions had significant discriminating contribution between low and high memory. Of these 62 regions, 60 regions showed higher contribution in the high memory group with much larger effect sizes. The other two regions that had lower contribution in the high memory are Left Frontal Inferior gyri and Right parahippocampal region. The top regions that showed significant group differences are cortical regions, specifically right Heschl's gyrus and right temporal superior gyrus from temporal lobe, left rolandic operculum and right frontal medial orbital gyrus from frontal lobe, and left calcarine fissure and surrounding cortex from occipital lobe. Interestingly, these regions are different from the top regions that contribute to overall prediction. Our results indicate that the high memory group depends on the cortical regions to a much higher degree along with sub-cortical regions, compared to the low memory group. In other words, while subcortical regions are crucial for memory tasks, cortical regions' involvement is also the key to distinguish low and high memory capacity.

To our surprise, all the regions whose contribution differs between sex have significantly higher contribution scores in females, highlighting subcortical and inferior frontal regions with the top five regions as right putamen, left inferior frontal gyrus triangular, left, and right parahippocampal gyrus, and left amygdala. This finding indicates that females involve much more sub-cortical and cortical regions in memory tasks than males which has been found previously. Even though sex differences in brain anatomy and function in context of working memory is well documented (Hill et al., 2014), this wide-range enhanced brain regional participation in females for memory is interesting and warrants further in-depth investigation.

5.5 Conclusion

In sum, we have examined the statistical power of CNN model to discriminate individuals with low vs. high working memory capacity using their structural MRI. To this end, by reusing the low-level features from the brain-age prediction task we were able to achieve higher performance. The final model revealed that 73 regions are significant to the prediction of the working memory capacity. The most significant regions are the subcortical regions including left, right parahippocampal gyri and hippocampus. However, cortical regions play a more significant role in differentiating individuals with high vs. low working memory, individuals with high memory capacity recruit more cortical regions than individuals with low memory capacity. In addition, females have more contributions from fifty regions than males. Clinically, our study supports that normal ageing processing is involved in working memory of older populations, but only to a limited extent through lower level or local brain structures. Working memory capacity in older populations depends on a large integrated brain network of subcortical-cortical regions. Thus, working memory deficit is less likely a specific local brain disfunction.

Our results should be interpreted with the consideration of the following limitations. Our decision on the cut-off for the high memory versus low memory groups was based on sample size and cohort distribution. Future work on more precise memory groups, maybe based on clinical assessments, will be important to confirm our findings. Participants in the UK biobank cohort were recruited from the general population of which some might have various mental health problems. The potential confounding effect of mental condition is not examined in this study. Since we try to leverage as many samples as possible, we do not exclude anyone with known mental disorders. Future works on relationships between brain variations underlying memory capacity and Alzheimer's disease, mood disorder and others in the older population will be vital to enhance the understanding of neurological mechanisms for memory related aging processing.

6 INTEGRATING NEUROIMAGING AND GENETICS VIA CONTRASTIVE LEARNING FOR WORKING MEMORY

6.1 Introduction

Working memory is a fundamental cognitive function, enables individuals to hold and manipulate information over short periods, essential for reasoning, learning, and decision-making. It is influenced by both genetic and neural factors. Understanding its genetic and neural basis can help identify biomarkers for cognitive impairment in neurodegenerative diseases (BADDELEY et al., 1991; Perpetuini et al., 2020) in the old population, as working memory declines in normal aging, Mild Cognitive Impairment and Alzheimer's disease (AD) (A. M. Kirova et al., 2015). Furthermore, working memory is also one of earliest key symptoms in AD (Germano & Kinsella, 2005; Huntley & Howard, 2010), making it a good phenotypical outcome to study for genetic mutations associated with AD.

Previous research has established various links between genetic variants and brain structure/function that underpin working memory performance. As reviewed in (Knowles et al., 2014) one of the most studied genes is COMT (Catechol-O-Methyltransferase), which encodes an enzyme that degrades dopamine in the prefrontal cortex, a region critical for working memory (Meyer-Lindenberg et al., 2005). Yet its genetic variants may code normal working memory variation in the population. Specifically interested in the working memory decline in the old population, we leverage the knowledge of protein-protein interaction networks in AD (V. M. Perreau et al., 2010), and conduct a focused study on genetics involved in pathogenesis of AD with brain structure serving WM function. Among many genes, for instance, ADAM10 (a member of the A Disintegrin And Metalloproteinase (ADAM) family) is known to be involved in the cleavage

of amyloid precursor protein, a key process of AD pathogenesis, and also helps normal synaptic functions and hippocampal neurogenesis (Huang et al., 2018; Yuan et al., 2017).

Neuroimaging studies have identified specific brain regions whose function or structural variations are crucial for WM. Functional MRI (fMRI) studies consistently show that the prefrontal cortex, particularly the dorsolateral prefrontal cortex (DLPFC), is heavily involved in WM tasks (Owen et al., 2005; Rottschy et al., 2012). Recent studies have highlighted the role of the cerebellum in WM, especially the left cerebellum being implicated in verbal WM tasks (Ben-Yehudah et al., 2007; Hayter et al., 2007; Stoodley & Schmahmann, 2010). A transdiagnostic study has revealed consistent patterns of dysfunction in the prefrontal and parietal cortices, as well as cerebellum, across various psychiatric and neurological diagnoses (Robbins, 1996). In parallel, structural MRI (sMRI) studies echo the findings of fMRI, where DLPFC surface area independently contributes to WM performance (Evangelista et al., 2021), and grey matter volumes in the inferior frontal and cerebellum are associated with WM across age groups (Duan et al., 2021).

The integration of genetic and imaging data provides deeper insights into how genetic variants influence brain, thereby affecting WM. Heck et al. performed genome-wide gene set enrichment analyses in multiple data sets, young and aged, and identified the voltage-gated cation channel activity gene set was linked to WM-related tasks and parietal cortex and the cerebellum (Heck et al., 2014). Our group linked a set of single nucleotide polymorphisms (SNP) to gray matter alterations in the frontal region underlying WM deficits in adults and adolescents with attention-deficit/hyperactivity disorder. The SNPs highlighted MEF2C, CADM2, and CADPS2, relevant for modulating neuronal substrates underlying high-level cognition (Duan et al., 2023).

Both traditional data fusion approaches, such as Canonical Correlation Analysis (CCA) (Sapkota et al., 2024; Thompson et al., 2013) and parallel independent component analyses (Pearlson et al., 2015), and deep learning based approaches (Kim et al., 2020) have been implemented for integrating neuroimaging data and genetics. Yet due to heterogeneous characteristics of imaging and genetics, it is a still changeling task to effectively integrate datasets. Contrastive learning techniques have recently emerged as powerful tools for multi-modal data integration. These methods learn shared representations from different data types by maximizing their agreement, making them particularly suitable for tasks involving genetic and imaging data. A recent study by Taleb et al. (2022) introduced ContIG, a self-supervised multimodal contrastive learning framework for medical imaging with genetics. ContIG effectively learns joint representations by contrasting positive pairs (genetic and imaging data from the same subject) against negative pairs (data from different subjects), and subsequently enhances the performance of prediction tasks (Taleb et al., 2022).

In this study, we leverage the strength of both CCA and contrastive learning for integration, along with transfer learning Convolutional Neural Network (CNN) and MLP for latent feature extraction and build a three-stage imaging guided SNP representation model for classification of WM capacity. The contribution of this project includes: 1) a transfer learning component from brain aging to WM for neuroimaging feature extraction, 2) a multi-modal contrastive learning approach that integrates genetic and imaging data to capture their complex relationships, 3) a sCCA interpretation for the learned representations to identify significant imaging and genetic components with shared variance. The findings could provide new insights into the biological pathways for both risk genetics and brain structure involved in WM, identify potential biomarkers for cognitive decline and impairment.

6.2 Materials and Methods

In this section we first introduce our cohort and data. Then we detail the proposed novel model, followed by baseline models for comparison. Finally, we explain the post analyses for model and results interpretation.

6.2.1 Cohort

UK Biobank (Sudlow et al., 2015), a large-scale open access biomedical database, contains de-identified data of a million UK participants and over 40,000 participants with brain MRI and genetic data. Informed consent was obtained from all participants, and the study follows UKB Ethics and Governance Framework, approved by the North-West Multi-center Research Ethics Committee. We focused on T1-weighted MRI and SNP (Single Nucleotide Polymorphism) data in this study.

26,534 subjects participated in the WM assessment and the scores ranged from 2 to 12 with distribution as shown in Figure 6.1. We selected a subpopulation of 5469 participants divided into two groups i) participants with memory scores ranging from 2 to 5 and ii) participants with scores in the range of 9 to 12. The segregation was based on the Miller's Law of clinical psychology which states that individuals, on average, can hold about 7 ± 2 items at a time in their WM (Miller, 1956). And we adjusted based on the distribution of our dataset to 7 ± 1 as the average capacity. Thus, group I is termed as low WM capacity and group II is high WM capacity.**Error! Reference source not found.** Among them, 4995 had both MRI and genetic data for our analyses , with 3192 in low WM group (age: 55.95±7.58, 1317 male), and 1803 in high WM group (age: 42.35±7.08, 1034 male).

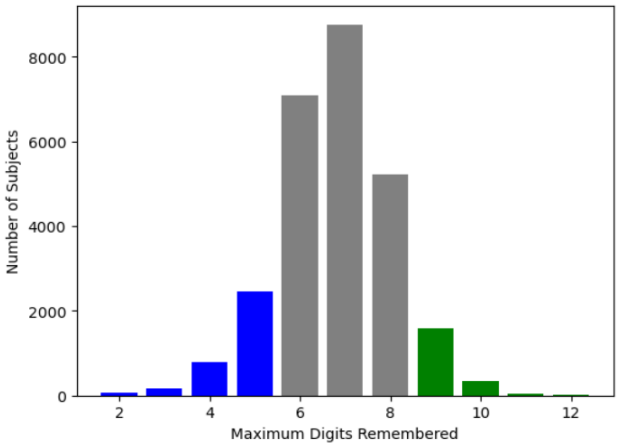

Figure 6.1: Distribution of working memory scores of 26,534 participants.

T1-weighted MRI images were segmented into six types of tissues (gray matter, white matter, etc.) using SPM 12. Gray matter images were normalized into Montreal Neurological Institute space, modulated, and smoothed with a 6×6×6mm3 Gaussian kernel. Each image has a voxels matrix of 128×141×128. Further quality control was conducted to retain individual images with a correlation larger than 0.9 with the averaged gray matter image.

6.2.2 Single Nucleotide Polymorphisms (SNP) Preprocessing

A subset of SNPs were selected from the genomic data, after imputation using Michigan imputation server(Wightman et al., 2021), which are expression quantitative trait loci (eQTL) for brain tissue published by PsychENCODE (Wang et al., 2018), i.e., regulating gene expression in brain. Further, to increase the likelihood of identifying the biologically relevant genes we selected SNPs that are also part of the Protein-Protein Interaction (PPI) interaction network of amyloid precursor protein and Abeta of Alzheimer's disease, yielding 1060 SNPs (Victoria M. Perreau et al., 2010).

6.2.3 Contrastive Genetic-Neuroimaging Integration (CGNI)

We propose a three-stage imaging genetic integration framework as shown in Figure 6.2. The input includes whole brain gray matter images and 1060 SNPs. The output is twofold: one is the classification of WM group, and the other is associated with latent representations of imaging and genetic data. Stage 1 is to extract imaging latent representations using transfer learning. Stage 2 is to extract genetic representations guided by the imaging representations via contrastive learning. Finally, Stage 3 combines these representations to perform WM classification. The details of each stage are provided in the following sections.

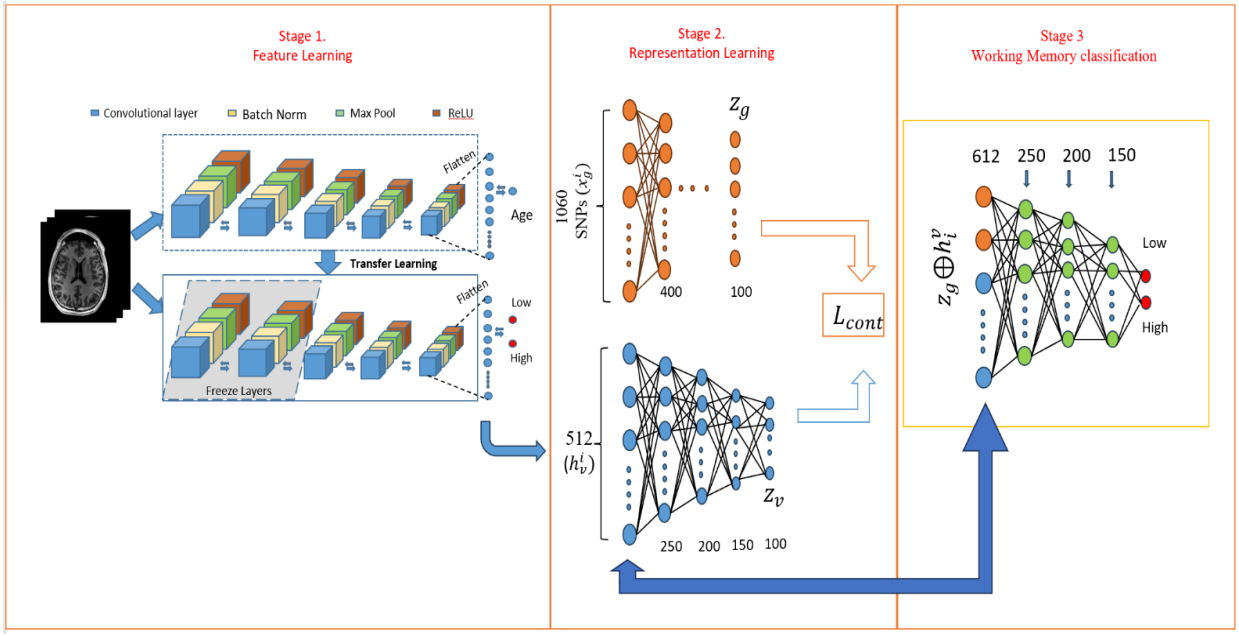

Figure 6.2: Schematic illustration for the steps of our proposed method.

6.2.3.1 Imaging Representation Learning Using Transfer Learning

Stage 1 shows the model to extract imaging representation. First, we pre-trained a 3D CNN model for brain age prediction task following the work of (Han et al., 2021), using a large sample size of 39,755. The 3D CNN architecture is composed of five convolutional blocks and each block has a 3D convolutional layer, a batch normalization layer, followed by a max pool layer, and a

ReLU. The convolutional layers used 32, 64, 128, 256, 256 channels, respectively, with stride of one and no padding was used. The output images from the final convolutional block are flattened and passed to the fully-connected layer which takes 1024 inputs and outputs the predicted brain age. The fully-connected layer has a dropout rate of 0.2.

Using transfer learning combined with heuristic self-transfer-training (Pranav Suresh, 2023) method, the best trained brain age model was used to initialize the classification model for the prediction of the WM. We denote the flattened outputs of the final convolutional block of the 3D CNN model as $h_v^i = f_v(x_v^i)$, where x_v^i is the imaging modality of the participant i ∈ {1, … ,4995}.

6.2.3.2 Imaging Guided SNP Representation Learning via Contrastive Learning

Each individual sample, X^i, where i ∈ {1, … ,4995}, has an imaging modality, x_v^i, a genetic modality, x_g^i, and a label y^i ∈ {low = 0, high = 1}. We train our contrastive model in batches of size b, where b >1. Our model, as shown in stage 2 of **Error! Reference source not found.**, is comprised of two encoders, one for each modality.

The encoders transform each modality into respective representations using the contrastive loss functions described in the following section. For imaging encoder, denoted as e_v, we use the output from the 3D CNN of the baseline model (see section D.i), h_v^i, as the input. The imaging encoder input layer takes 512 inputs and has three hidden layers. The size of each hidden layer is 250, 200, and 150 neurons, respectively. The output layer is of size 100, denoted as $z_v^i = e_v(h_v^i) \in \mathbb{R}^{100}$.Similarly, the genetic encoder, denoted as e_g, is a fully-connected neural network with 1060 SNPs as input and has five hidden layers of size 400, 600, 400, 300, and 150 neurons, respectively. The output layer is of size 100, denoted as $z_g^i = e_g(x_g^i) \in \mathbb{R}^{100}$.

For every **ith** pair of imaging representation and genetic data, (h_v^i, x_g^i), (z_v^i, z_g^i) are representations from the encoders (e_v, e_g), in a batch of **b** samples. We constrain our batch selection such that $|\{y^i = 0\}| > 0$, and $|\{y^i = 1\}| > 0$, to ensure at least one sample from each label. We then define our loss function using following loss terms where $\boldsymbol{\tau}$ is a temperature parameter that scales the embeddings to control the range of the dot product, and $P(i) \equiv \{p \in \{1 \dots \boldsymbol{b}\} \setminus i : y_p = y_i\}$

$$\mathrm{L(v,g)} = -\sum_{\mathrm{i=1}}^{\mathrm{I}} \log \frac{\exp\left(\frac{\mathrm{z_v^i} \,.\, \mathrm{z_g^i}}{\tau}\right)}{\sum_{\mathrm{j=1,j\neq i}}^{\mathrm{I}} \exp\left(\frac{\mathrm{z_v^i}.\,\mathrm{z_g^j}}{\tau}\right)} \tag{6.1}$$

$$\mathrm{L}(g,v) = -\sum_{i=1}^{I} \log \frac{\exp\left(\frac{z_g^i . z_v^i}{\tau}\right)}{\sum_{j=1,j\neq i}^{I} ex\,\mathrm{p}\left(\frac{z_g^i . z_v^j}{\tau}\right)} \tag{6.2}$$

$$\mathrm{L(v,v)} = \sum_{\mathrm{i=1}}^{\mathrm{I}} \frac{-1}{|\mathrm{P(i)}|} \sum_{\mathrm{p\in P(i)}} \log \frac{\exp\left(\frac{\mathrm{z_v^i}.\,\mathrm{z_v^p}}{\tau}\right)}{\sum_{\mathrm{j=1,j\neq i}}^{\mathrm{I}} \exp\left(\frac{\mathrm{z_v^i}.\,\mathrm{z_v^j}}{\tau}\right)} \tag{6.3}$$

$$\mathrm{L(g,g)} = \sum_{\mathrm{i=1}}^{\mathrm{I}} \frac{-1}{|\mathrm{P(i)}|} \sum_{\mathrm{p\in P(i)}} \log \frac{\exp\left(\frac{\mathrm{z_g^i}.\,\mathrm{z_g^p}}{\tau}\right)}{\sum_{\mathrm{j=1,j\neq i}}^{\mathrm{I}} \exp\left(\frac{\mathrm{z_g^i}.\,\mathrm{z_g^j}}{\tau}\right)} \tag{6.4}$$

In Eq. (6.1)—image-to-genetics, for every imaging modality (h_v^i) in a batch, we consider its corresponding genetic pair (x_g^i) as the positive sample with all other genetic samples $(x_g^j;\ j \neq$

i) as negatives to be contrasted against. Similarly, in Eq. (6.2)—genetics-to-imaging, imaging h_v^i is the positive of the genetic sample x_g^i and contrasted against all other images in the batch ($h_v^j;\ j \neq i$). In Eq. (3)—imaging-to-imaging, and Eq. (4)—genetic-to-genetic loss terms, by taking advantage of the labels, we use intra-modal contrasting to align the representations of the samples of same class to be close to each other, while the samples from the other class are pushed apart. Finally, we combine the four loss terms and define the contrastive batch loss function as:

$$L_{cont}(v,g) = \lambda L(v,g) + \sigma L(g,v) + \gamma L(v,v) + \theta L(g,g) \tag{6.5}$$

where $\lambda, \sigma, \gamma, \theta \in [0,1]$ are weighting hyperparameters. By incorporating these inter- and intra-modal contrastive losses, our model ensures that each modality independently learns meaningful and discriminative representations. These representations are then combined for the final classification task, enhancing the overall performance of the model. In addition, we trained the model with different combinations of these loss terms and compare the quality of the representations by fine-tuning to the classification task shown in Stage 3.

6.2.4 Classification of Working Memory

In stage 3, we combined genetic representations obtained from the contrastive training (z_g^i) with the imaging representations from the 3D CNN model (h_v^i), resulting in an input dimension of 612 (100 from genetic encoder and 512 from the imaging CNN) and trained a fully-connected neural network. The neural network has three hidden layers of size 250, 200, and 150, respectively. The output layer has two neurons for classification of WM.**Error! Reference source not found.**

6.2.5 Baseline Models

We compare the performance of our model with the following four baseline models. For the first two models, we trained two supervised models for each modality separately. Next, we combined the latent representations from the individual modalities and trained iii) a linear classifier using Support Vector Machine (SVM), and iv) a fully-connected neural network classifier.

Imaging CNN: For classification of WM using only the imaging modality we used the same model described in the stage 1 of the CGNI framework.

Genetic Classification Models: The genetic data was processed using a fully connected neural network (NN) designed to capture the complex relationships within the 1060 SNPs. The architecture of the NN is as follows: the input layer of the network takes an input of 1060 SNP features. The hidden layers are of size 800, 600, and 400 neurons respectively. The final layer is a 2-neuron output layer to classify the WM scores. To prevent overfitting and ensure sparsity, L1 regularization was applied to the hidden layers. The activation function used for the hidden layers is the ReLU. We denote the output of the last hidden layer (size of 400 neurons) as $h_g^i = f_g(x_g^i) \in \mathbb{R}^{400}$, where x_g^i is the genetic modality of the participant i $\in \{1, \ldots, 4995\}$.

Imaging Genetic Integration Models (linear and non-linear): Finally, we combined the output embeddings of the two modalities, $h_v^i \oplus h_g^i$, and trained a Support Vector Machine (SVM) for linear classification and a fully-connected NN. The input layer of this NN has 912 neurons. The input layer is followed by two hidden layers of size 500 and 200 neurons. The output layer has 2 nodes corresponding to high memory or low memory. ReLU activation was used after each layer to incorporate non-linearity into the model. While training, L1 regularization was applied to all the layers to prevent overfitting.

6.2.6 Post Analyses for results interpretation

In our post analyses, first, we utilized Sparse Canonical Correlation Analysis (SCCA) to identify the relationships between the imaging and genetic latent representations, and top contributing features. Next, from the identified genetic features, we further performed gene enrichment analysis to reveal their biological significance.

6.2.6.1 Sparse CCA Analysis for Understanding Imaging-Genetics Relationships

To understand the relationships between the imaging and genetic representations of the contrastive training, we performed SCCA on the encoder outputs z_v^i, z_g^i. We utilized the iterative penalized SCCA method proposed by Mai et. al. (Mai & Zhang, 2019) due to its ability to handle high-dimensional and enforce sparsity to reduce overfitting. We considered the number of components as one of the hyperparameter along with the sparsity penalization for each modality and selected the sCCA model via GridSearchCV and 5-fold cross validation. We used the implementation provided by Chapman et. al. (Chapman & Wang, 2021).

For the correlated components from the imaging and genetic modalities, to identify the top contributing important features, we used feature occlusion sensitivity method. We denote the ith sample with kth feature occluded as x_{mk}^i, where *m* is the modality. The feature occluded imaging encoder$z_{vk}^i = e_v\left(f_v\left(x_{vk}^i\right)\right)$ and$z_{gk}^i = e_g\left(x_{gk}^i\right)$ as the genetic encoder output. For imaging modality, we partitioned the brain into 116 brain regions based on(Edmund et al., 2020) For genetic modality, we considered the individual SNPs as features and computed their contribution. Given for each correlated component identified from sCCA, only fewer latent representation nodes are involved. We computed the contribution of each feature to the largest weighted (highest absolute canonical weight) representation node. The contribution value is computed as the mean

difference of the actual encoder output z_m^i), and encoder output with feature occludedz_{mk}^i) as shown in Eq. (6.6).

$$contribution_k = \frac{\sum_{i=0}^{N} z_m^i - z_{mk}^i}{N} \; \forall \; k \in features \tag{6.6}$$

The top contributing features to each component are the brain regions and SNPs whose contribution scores are greater than 2.5 and 3 standard deviations away, respectively, from the mean contribution scores.

6.2.6.2 Gene Set Enrichment Analysis

To further understand the biological significance of the set of SNPs that are identified to have significant contribution to the sCCA components, we have performed a gene enrichment analysis using the gProfiler online software (Raudvere et al., 2019). First, we matched the SNPs to the Ensemble ID of the genes (these were part of the eQTL dataset obtained from psychEncode) and used the g:Convert function to get the gene names, then used g:GOSt function to perform the enrichment test (Raudvere et al., 2019).

6.2.7 Experimental Setup

Across all experiments, we used the same splits of data for training, validation, and test set. We ensured there was no cross-contamination of samples between the splits. We split the data into two sets, 90% for training and 10% for test set. Using the training set we performed five-fold cross validation for each set of hyperparameters. For fully-connected networks, we vary the number of hidden layers and the size of each layer, learning rate. We used the Adam optimizer for optimizing the neural networks. For the CNN models we used a batch size of 25 images on A100 GPU. For

the contrastive model we used a batch size of 50 and for the WM classification model the batch size is 75. For classification tasks we used balanced accuracy as our metric.

6.3 Results

6.3.1 Baseline Model Results

As a benchmark comparison for the contrastive training model, we have reported the performance of several baselines. In Table 6-1, we report the mean balanced accuracy across five-folds of the imaging-genetic baseline model along with other models trained on individual modalities.

Table 6-1: Comparison of balanced accuracies of models

WM Classification	Training	Validation	Holdout
Imaging CNN	81.34 ± 2.34	75.32 ± 0.49	87.02 ± 1.31
Sparse Genetic NN	59.80 ± 0.42	59.35 ± 0.45	59.28 ± 0.57
Imaging-Genetic SVM	95.5 ± 2.59	65.08 ± 1.56	65.23 ± 2.38
Imaging-Genetic NN	87.47 ± 0.45	87.08 ± 0.80	87.02 ± 0.67

To pre-train the CNN model for brain age prediction task, we achieved the best results (MAE of 2.82 ± 0.04 on training, 2.88 ± 0.05 on validation, 2.47 ± 0.2 on test set). By transferring the first two layers of the brain age model, we achieved high mean balanced accuracy (87.02) on the holdout set. For genetic modality, With the addition of L1 sparsity explicitly and L2 sparsity via the weight decay parameter of the Adam optimizer the model achieved balanced accuracies around 59% Finally, the multi-modal imaging-genetic model exhibited the highest performance with balanced accuracies above 87% across all splits, indicating robust generalization.

6.3.2 Comparison of Combinations of Contrastive Loss Terms

We systematically tested various combinations of loss terms in (5) and recorded the balanced accuracies on the training, validation, and test sets. The results are summarized in the **Error! Reference source not found.**.

Table 6-2: Balanced accuracies achieved for different loss term combinations

Loss Term	*Train*	*Validation*	*Holdout*
Imaging-to-genetics (L1)	89.96 ± 0.80	88.55 ± 1.10	88.31 ± 0.31
Genetics-to-imaging (L2)	89.81 ± 0.95	87.97 ± 0.91	87.51 ± 0.20
Imaging-to-imaging (L3)	88.99 ± 0.74	87.45 ± 1.60	86.80 ± 0.34
Genetics-to-genetics (L4)	90.03 ± 0.87	88.04 ± 0.76	88.1 ± 0.41
L1 + L2	88.98 ± 1.13	88.03 ± 1.26	87.76 ± 0.94
L1 + L3	90.09 ± 1.1	88.14 ± 0.98	88.19 ± 0.67
L1 + L4	89.75 ± 1.21	89.33 ± 0.11	88.01 ± 0.08
L2 + L3	90.45 ± 0.37	87.89 ± 0.87	89.66 ± 0.31
L2 + L4	90.49 ±0.84	88.27 ± 1.31	88.07 ± 0.83
L3 + L4	88.95 ± 1.71	87.96 ± 0.86	87.74 ± 0.43
L1 + L2 + L3	89.60 ± 0.98	88.22 ± 1.03	88.18 ± 0.34
L2 + L3 + L4	90.00 ± 1.09	88.14 ± 1.01	87.79 ± 0.33
L1 + L2 + L4	91.37 ± 0.30	90.39 ± 0.11	88.91 ± 0.66
L1+ L2+ L3+ L4	89.81 ± 0.73	88.38 ± 0.99	88.61 ± 0.56

All individual loss terms have shown improvement over the baseline accuracies. The combination of loss terms (1), (2), and (4) yielded the highest balanced accuracies on the training (91.37 ± 0.30%), validation (90.39 ± 0.11%), and test sets (88.91 ± 0.66%). The values of the loss term weighting hyperparameters $(\lambda, \sigma, \theta)$ for each of the loss term were 0.7, 0.3, and 0.4,

respectively. Individual loss terms (1) and (4) also performed well, particularly in the holdout sets (88.31 ± 0.31% and 88.10 ± 0.41%, respectively).

6.3.3 Post Analysis Results

The SCCA analysis performed on the representations of the contrastive model with loss terms (1), (2), and (4) using the GridSearchCV resulted in selection of five components. In , we reported the correlation coefficients for these five component pairs across the training, validation, and holdout sets. The correlations for each component pair are relatively consistent between the training and validation sets, indicating the stability of the CCA model. The top contributing brain regions and SNPs are listed in Table 6-4 and Table 6-5 and plotted in Figure 6.3: Significant brain regions identified across five SCCA components. Brain regions in red indicate increased effect and blue regions indicate decreased effect.

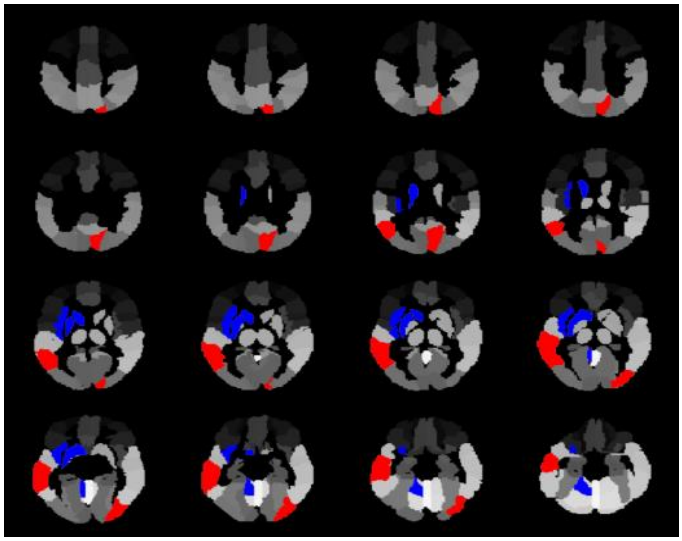

Figure 6.3: Significant brain regions identified across five SCCA components

Table 6-3: CCA correlation of components

Component	*Training*	*Validation*	*Holdout*
1	0.68	0.67	0.57

2	0.67	0.65	0.54
3	0.66	0.65	0.55
4	0.65	0.65	0.52
5	0.63	0.63	0.57

Across five SCCA components **Error! Reference source not found.**we identified seven brain regions and **Error! Reference source not found.Error! Reference source not found.** the 28 genes corresponding to the identified SNPs. Most of the selected regions and SNPs are similar among all the components.

Table 6-4: Genes with significant contribution scores for each component

Component	Genes
1	ADAM10, LRRK2, RAB6A, GSK3B, BTBD1, RBM11, BIN1, FIS1, RNH1, STAU1, CD9
2	ADAM10, LRRK2, RAB6A, ATP9A, BTBD1, MAPT, CALHM1, RPL28, FIS1, STAU1, GSE1, CD9
3	ADAM10, LRRK2, RAB6A, BTBD1, MAPT, RPL28, RCAN1, FYN, KLHL35, STAU1, CD9
4	MFF, RAB6A, BTBD1, BIN1, CALHM1, FIS1, SLC40A1, CENPV, RNH1, STAU1
5	LRRK2, ATP9A, BTBD1, CALHM1, FIS1, CCNA1, SLC40A1, RNH1, STAU1

Table 6-5: Brain regions with significant contribution scores for each component

Component	Brain Regions

1	Left Cerebellum, Left Insula, Left Putamen, Left Caudate
2	Right Occipital Inferior, Left Caudate, Right Cuneus
3	Left Cerebellum, Left Insula, Left Caudate
4	Left Temporal Middle, Right Cuneus, Left Caudate
5	Right Occipital Inferior, Right Cuneus, Left Caudate

6.3.4 Gene Enrichment Pathway Analysis

The gene enrichment test in three GO categories revealed enrichment in dendrite (p = 9.69e-6), synapse (p= 5.08e-5), and exocytic vesicle (p = 3.87e-4) in cellular components; regulation of mitochondrial fission, and developmental process in biological pathways, and protein binding in molecular function. The results of the analysis can be found here (https://biit.cs.ut.ee/gplink/l/H8Pp77ilQy).

6.4 Discussion

This study aimed to integrate genetic and imaging data using a novel contrastive learning framework to identify significant associations between genetic variants and brain regions associated with cognitive function of WM. Our comprehensive analysis, which included transfer learning contrastive learning, SCCA, and gene enrichment tests, yielded several important findings.

The performance of various models on WM classification tasks demonstrated that integrating imaging and genetic data outperformed models using only one data type. The Imaging-genetic neural network achieved the highest balanced accuracy (87.02 ± 0.67) on the holdout set, indicating the potential of multi-modal approaches in classification of WM. The study of different combinations of the loss terms further showed that including terms (L1, L2, L4) resulted in the

best performance, highlighting the importance of capturing relationships between both modalities. The inclusion of (4) in the loss function (i.e., the loss term L(g,g)) showed substantial improvement in validation accuracy (89.33 ± 0.11%) compared to other combinations, indicating its importance for generalization. This combination effectively leverages the complementary information from both imaging and genetic data, resulting in superior performance in WM classification tasks.

Our post analysis performed to identify the associations between brain regions and genes indicate that a decrease in the Grey Matter Volume (GMV) of regions left cerebellum, left insula, left putamen, left Caudate, and increase in the GMV of regions right occipital inferior, right cuneus, and left temporal middle is associated with the increase in the minor allele in the SNPs of all identified genes except gene STAU1. Recent research has shown that the reductions in cerebellar volume accompanying aging and are correlated with cognitive decline (Arleo et al., 2024) which underscores our finding regarding left cerebellum in relation to working memory in older population.

The gene enrichment analysis highlighted several biological processes and cellular components significantly associated with the identified genes. The identified SNPs and associated genes provide insights into the genetic underpinnings of cognitive function. Notably, the regulation of mitochondrial fission and developmental processes were prominent, suggesting that these pathways may play crucial roles in maintaining WM capacity and preventing neurodegeneration. Recent research has identified several genetic variants that significantly impact WM performance. For instance, genes like ADAM10, LRRK2, RAB6A, and BTBD1 have been implicated in various neural processes relevant to WM. ADAM10, involved in amyloid precursor protein processing, has been linked to Alzheimer's disease and cognitive decline (Huang et al., 2018). Variants in LRRK2, associated with synaptic vesicle trafficking, also play a role in neurodegenerative diseases

such as Parkinson's, influencing cognitive functions (Zimprich et al., 2004). The integration of these genetic data with neuroimaging findings helps elucidate the complex interplay between genetic predispositions and brain structure in maintaining WM. While our study provides valuable insights, several limitations should be noted. The sample size, while sufficient for the current analysis, limits the generalizability of the findings. Larger, more diverse cohorts are needed to validate these results. The identified genetic variants and pathways require further functional validation to establish causal relationships with WM capacity.

6.5 Conclusion

In conclusion, our study demonstrates the power of integrating genetic and imaging data using contrastive learning techniques. The identified genetic variants and brain regions, along with their associated biological pathways, provide a foundation for further exploration into the genetic basis of WM. This integrated approach holds promise for advancing our understanding of the complex interactions underlying WM capacity and its decline in neurodegenerative diseases.

7 CONCLUSIONS AND FUTURE DIRECTIONS

7.1 Summary of Key Findings

This dissertation has explored the integration of neuroimaging and genetic data to predict cognitive functions and symptoms in both small and large cohorts. The research focused on the following key areas:

1. **Neuroimaging-Genetic Prediction of Symptom Changes in ADHD**: By integrating structural MRI (sMRI) and genetic data, we identified significant genetic variants and brain regions associated with changes in ADHD symptoms. This study demonstrated the potential of multimodal data integration in understanding the genetic underpinnings of neuropsychiatric disorders.
2. **Training Strategy for Neural Network Models with Limited Samples**: We proposed a novel self-transfer-training (STT) strategy for training convolutional neural networks (CNNs) with limited samples. This approach improved the performance of CNN models in predicting cognitive functions from neuroimaging data, highlighting the importance of effective training strategies in machine learning applications.
3. **CNN Models for Working Memory Classification Using sMRI**: By applying CNNs to sMRI data, we were able to classify working memory capacity with high accuracy. This study demonstrated the utility of deep learning techniques in identifying relevant brain regions and predicting cognitive functions from structural neuroimaging data.
4. **Integration of Neuroimaging and Genetics via Contrastive Learning for Working Memory**: Using contrastive learning, we integrated neuroimaging and genetic data to enhance the prediction of working memory capacity. This approach revealed significant

associations between specific genetic variants and brain imaging phenotypes, providing insights into the genetic basis of cognitive functions.

7.2 Contributions to the Field

The research presented in this dissertation makes several important contributions to the field of imaging genomics:

1. **Advancement in Multimodal Data Integration**: The studies demonstrate the effectiveness of integrating neuroimaging and genetic data to uncover the genetic basis of cognitive functions and neuropsychiatric disorders. This approach provides a more comprehensive understanding of the complex interactions between genes and brain structure.
2. **Development of Novel Machine Learning Strategies**: The self-transfer-training strategy and the application of contrastive learning represent significant advancements in the use of machine learning techniques for neuroimaging genomics. These methods enhance the predictive power and interpretability of models, particularly in the context of limited sample sizes.
3. **Identification of Genetic Influences on Brain Structure and Function**: The findings from the studies contribute to our understanding of how specific genetic variants influence brain morphology and cognitive functions. This knowledge can inform the development of targeted interventions and personalized treatment strategies for neuropsychiatric disorders.

7.3 Limitations of the Study

Despite the significant contributions, this dissertation also has several limitations:

1. **Sample Size**: Some studies were conducted with relatively small sample sizes, which may limit the generalizability of the findings. Larger cohorts are needed to validate the results and improve the robustness of the models.
2. **Complexity of Multimodal Data Integration**: Integrating neuroimaging and genetic data is inherently complex and computationally intensive. The methodologies used in this dissertation, while effective, could benefit from further refinement and optimization to handle even larger and more diverse datasets.
3. **Interpretability of Machine Learning Models**: Although the machine learning models used in this research provided valuable insights, their interpretability remains a challenge. Future work should focus on developing more interpretable models to better understand the underlying biological mechanisms.

7.4 Recommendations for Future Research

Based on the findings and limitations of this dissertation, several recommendations for future research are proposed:

1. **Increase Sample Sizes**: Future studies should aim to include larger and more diverse cohorts to validate the findings and enhance the generalizability of the results. Collaborative efforts and data-sharing initiatives can help achieve this goal.
2. **Refine Multimodal Integration Techniques**: Continued development and refinement of multimodal data integration techniques are needed to handle the increasing complexity and volume of neuroimaging and genetic data. This includes improving computational efficiency and addressing potential confounding factors.
3. **Focus on Interpretability**: Developing more interpretable machine learning models is crucial for translating research findings into clinical practice. Efforts

should be made to design models that not only provide accurate predictions but also offer insights into the underlying biological mechanisms.

4. **Explore Longitudinal Studies**: Longitudinal studies tracking individuals over time can provide valuable information on the dynamics of brain development and the progression of neuropsychiatric disorders. Future research should incorporate longitudinal data to capture these temporal changes.
5. **Investigate Additional Cognitive Functions and Disorders**: Expanding the scope of research to include other cognitive functions and neuropsychiatric disorders can provide a broader understanding of the genetic and neuroimaging correlates of brain function. This can help identify common and distinct mechanisms underlying different conditions.

In conclusion, this dissertation has demonstrated the potential of integrating neuroimaging and genetic data to predict cognitive functions and symptoms in both small and large cohorts. The findings contribute to the growing field of imaging genomics and provide a foundation for future research aimed at understanding the genetic basis of brain function and developing personalized interventions for neuropsychiatric disorders.

REFERENCES

Ackerman, P. L., Beier, M. E., & Boyle, M. O. (2005). Working memory and intelligence: the same or different constructs? *Psychol Bull*, *131*(1), 30-60. https://doi.org/10.1037/0033-2909.131.1.30

Alfaro-Almagro, F., Jenkinson, M., Bangerter, N. K., Andersson, J. L. R., Griffanti, L., Douaud, G., Sotiropoulos, S. N., Jbabdi, S., Hernandez-Fernandez, M., Vallee, E., Vidaurre, D., Webster, M., McCarthy, P., Rorden, C., Daducci, A., Alexander, D. C., Zhang, H., Dragonu, I., Matthews, P. M., . . . Smith, S. M. (2018). Image processing and Quality Control for the first 10,000 brain imaging datasets from UK Biobank. *Neuroimage*, *166*, 400-424. https://doi.org/10.1016/j.neuroimage.2017.10.034

Almeida Montes, L. G., Prado Alcántara, H., Martínez García, R. B., De La Torre, L. B., Avila Acosta, D., & Duarte, M. G. (2013). Brain cortical thickness in ADHD: age, sex, and clinical correlations. *J Atten Disord*, *17*(8), 641-654. https://doi.org/10.1177/1087054711434351

Aminoff, E. M., Kveraga, K., & Bar, M. (2013). The role of the parahippocampal cortex in cognition. *Trends Cogn Sci*, *17*(8), 379-390. https://doi.org/10.1016/j.tics.2013.06.009

Ancona, M., Ceolini, E., Öztireli, C., & Gross, M. (2017). Towards better understanding of gradient-based attribution methods for Deep Neural Networks. arXiv:1711.06104. Retrieved November 01, 2017, from https://ui.adsabs.harvard.edu/abs/2017arXiv171106104A

Ardalan, Z., & Subbian, V. (2022). Transfer Learning Approaches for Neuroimaging Analysis: A Scoping Review [Review]. *Frontiers in Artificial Intelligence*, *5*. https://doi.org/10.3389/frai.2022.780405

Arleo, A., Bareš, M., Bernard, J. A., Bogoian, H. R., Bruchhage, M. M. K., Bryant, P., Carlson, E. S., Chan, C. C. H., Chen, L. K., Chung, C. P., Dotson, V. M., Filip, P., Guell, X., Habas, C., Jacobs, H. I. L., Kakei, S., Lee, T. M. C., Leggio, M., Misiura, M., . . . Manto, M. (2024). Consensus Paper: Cerebellum and Ageing. *Cerebellum*, *23*(2), 802-832. https://doi.org/10.1007/s12311-023-01577-7

Ashburner, J., & Friston, K. J. (2000). Voxel-Based Morphometry—The Methods. *Neuroimage*, *11*(6), 805-821. https://doi.org/https://doi.org/10.1006/nimg.2000.0582

Association, A. s. (2015). 2015 Alzheimer's disease facts and figures. *Alzheimer's & Dementia*, *11*(3), 332-384. https://doi.org/https://doi.org/10.1016/j.jalz.2015.02.003

Baddeley, A. D. (2000). Short-term and working memory. *The Oxford handbook of memory*, *4*, 77-92.

BADDELEY, A. D., BRESSI, S., DELLA SALA, S., LOGIE, R., & SPINNLER, H. (1991). THE DECLINE OF WORKING MEMORY IN ALZHEIMER'S DISEASE: A

LONGITUDINAL STUDY. *Brain*, *114*(6), 2521-2542. https://doi.org/10.1093/brain/114.6.2521

Baddeley, A. D., & Hitch, G. (1974). Working memory. In *Psychology of learning and motivation* (Vol. 8, pp. 47-89). Elsevier.

Barlati, S., Deste, G., De Peri, L., Ariu, C., & Vita, A. (2013). Cognitive remediation in schizophrenia: current status and future perspectives. *Schizophr Res Treatment*, *2013*, 156084. https://doi.org/10.1155/2013/156084

Barlow, J. S. (1983). Electroencephalography: Basic Principles, Clinical Applications and Related Fields. *JAMA*, *250*(22), 3108-3108. https://doi.org/10.1001/jama.1983.03340220076048

Basser, P. J., Mattiello, J., & LeBihan, D. (1994). MR diffusion tensor spectroscopy and imaging. *Biophys J*, *66*(1), 259-267. https://doi.org/10.1016/s0006-3495(94)80775-1

Batty, M. J., Liddle, E. B., Pitiot, A., Toro, R., Groom, M. J., Scerif, G., Liotti, M., Liddle, P. F., Paus, T., & Hollis, C. (2010). Cortical gray matter in attention-deficit/hyperactivity disorder: a structural magnetic resonance imaging study. *J Am Acad Child Adolesc Psychiatry*, *49*(3), 229-238. https://doi.org/10.1016/j.jaac.2009.11.008

Beckmann, C. F., & Smith, S. M. (2004). Probabilistic independent component analysis for functional magnetic resonance imaging. *IEEE Trans Med Imaging*, *23*(2), 137-152. https://doi.org/10.1109/tmi.2003.822821

Belin, D., Belin-Rauscent, A., Everitt, B. J., & Dalley, J. W. (2016). In search of predictive endophenotypes in addiction: insights from preclinical research. *Genes Brain Behav*, *15*(1), 74-88. https://doi.org/10.1111/gbb.12265

Ben-Yehudah, G., Guediche, S., & Fiez, J. A. (2007). Cerebellar contributions to verbal working memory: beyond cognitive theory. *Cerebellum*, *6*(3), 193-201. https://doi.org/10.1080/14734220701286195

Biederman, J., & Faraone, S. V. (2005). Attention-deficit hyperactivity disorder. *Lancet*, *366*(9481), 237-248. https://doi.org/10.1016/s0140-6736(05)66915-2

Biederman, J., Faraone, S. V., Mick, E., Spencer, T., Wilens, T., Kiely, K., Guite, J., Ablon, J. S., Reed, E., & Warburton, R. (1995). High risk for attention deficit hyperactivity disorder among children of parents with childhood onset of the disorder: a pilot study. *Am J Psychiatry*, *152*(3), 431-435. https://doi.org/10.1176/ajp.152.3.431

Bird, A. (2007). Perceptions of epigenetics. *Nature*, *447*(7143), 396-398. https://doi.org/10.1038/nature05913

Bleckley, M. K., Durso, F. T., Crutchfield, J. M., Engle, R. W., & Khanna, M. M. (2003). Individual differences in working memory capacity predict visual attention allocation. *Psychonomic bulletin & review*, *10*, 884-889.

Bodalal, Z., Trebeschi, S., Nguyen-Kim, T. D. L., Schats, W., & Beets-Tan, R. (2019). Radiogenomics: bridging imaging and genomics. *Abdominal Radiology*, *44*(6), 1960-1984. https://doi.org/10.1007/s00261-019-02028-w

Bopp, K. L., & Verhaeghen, P. (2005). Aging and verbal memory span: a meta-analysis. *J Gerontol B Psychol Sci Soc Sci*, *60*(5), P223-233. https://doi.org/10.1093/geronb/60.5.p223

Brandman, T., Malach, R., & Simony, E. (2021). The surprising role of the default mode network in naturalistic perception. *Communications Biology*, *4*(1), 79. https://doi.org/10.1038/s42003-020-01602-z

Brans, R. G., Kahn, R. S., Schnack, H. G., van Baal, G. C., Posthuma, D., van Haren, N. E., Lepage, C., Lerch, J. P., Collins, D. L., Evans, A. C., Boomsma, D. I., & Hulshoff Pol, H. E. (2010). Brain plasticity and intellectual ability are influenced by shared genes. *J Neurosci*, *30*(16), 5519-5524. https://doi.org/10.1523/jneurosci.5841-09.2010

Brans, R. G. H., Kahn, R. S., Schnack, H. G., van Baal, G. C. M., Posthuma, D., van Haren, N. E. M., Lepage, C., Lerch, J. P., Collins, D. L., Evans, A. C., Boomsma, D. I., & Hulshoff Pol, H. E. (2010). Brain Plasticity and Intellectual Ability Are Influenced by Shared Genes. *The Journal of Neuroscience*, *30*(16), 5519-5524. https://doi.org/10.1523/jneurosci.5841-09.2010

Buch, A. M., & Liston, C. (2021). Dissecting diagnostic heterogeneity in depression by integrating neuroimaging and genetics. *Neuropsychopharmacology*, *46*(1), 156-175. https://doi.org/10.1038/s41386-020-00789-3

Calhoun, V. D., & Adalı, T. (2012). Multisubject independent component analysis of fMRI: a decade of intrinsic networks, default mode, and neurodiagnostic discovery. *IEEE Rev Biomed Eng*, *5*, 60-73. https://doi.org/10.1109/rbme.2012.2211076

Caspi, A., Sugden, K., Moffitt, T. E., Taylor, A., Craig, I. W., Harrington, H., McClay, J., Mill, J., Martin, J., Braithwaite, A., & Poulton, R. (2003). Influence of life stress on depression: moderation by a polymorphism in the 5-HTT gene. *Science*, *301*(5631), 386-389. https://doi.org/10.1126/science.1083968

Caye, A., Swanson, J., Thapar, A., Sibley, M., Arseneault, L., Hechtman, L., Arnold, L. E., Niclasen, J., Moffitt, T., & Rohde, L. A. (2016). Life Span Studies of ADHD-Conceptual Challenges and Predictors of Persistence and Outcome. *Curr Psychiatry Rep*, *18*(12), 111. https://doi.org/10.1007/s11920-016-0750-x

Chapman, J., & Wang, H.-T. (2021). CCA-Zoo: A collection of Regularized, Deep Learning based, Kernel, and Probabilistic CCA methods in a scikit-learn style framework. *Journal of Open Source Software*, *6*(68), 3823. https://doi.org/10.21105/joss.03823

Chatterjee, I., Kumar, V., Sharma, S., Dhingra, D., Rana, B., Agarwal, M., & Kumar, N. (2019). Identification of brain regions associated with working memory deficit in schizophrenia. *F1000Res*, *8*, 124. https://doi.org/10.12688/f1000research.17731.1

Choi, S. W., Mak, T. S.-H., & O'Reilly, P. F. (2020). Tutorial: a guide to performing polygenic risk score analyses. *Nature Protocols*, *15*(9), 2759-2772. https://doi.org/10.1038/s41596-020-0353-1

Cowan, N. (2001). The magical number 4 in short-term memory: a reconsideration of mental storage capacity. *Behav Brain Sci*, *24*(1), 87-114; discussion 114-185. https://doi.org/10.1017/s0140525x01003922

Cowan, N. (2014). Working Memory Underpins Cognitive Development, Learning, and Education. *Educ Psychol Rev*, *26*(2), 197-223. https://doi.org/10.1007/s10648-013-9246-y

Cupertino, R. B., Soheili-Nezhad, S., Grevet, E. H., Bandeira, C. E., Picon, F. A., Tavares, M. E. A., Naaijen, J., van Rooij, D., Akkermans, S., Vitola, E. S., Zwiers, M. P., Rovaris, D. L., Hoekstra, P. J., Breda, V., Oosterlaan, J., Hartman, C. A., Beckmann, C. F., Buitelaar, J. K., Franke, B., . . . Sprooten, E. (2020). Reduced fronto-striatal volume in attention-deficit/hyperactivity disorder in two cohorts across the lifespan. *Neuroimage Clin*, *28*, 102403. https://doi.org/10.1016/j.nicl.2020.102403

D'Esposito, M., & Postle, B. (2015). The Cognitive Neuroscience of Working Memory,(66), 115–142. In.

Damatac, C. G., Chauvin, R. J. M., Zwiers, M. P., van Rooij, D., Akkermans, S. E. A., Naaijen, J., Hoekstra, P. J., Hartman, C. A., Oosterlaan, J., Franke, B., Buitelaar, J. K., Beckmann, C. F., & Sprooten, E. (2022). White Matter Microstructure in Attention-Deficit/Hyperactivity Disorder: A Systematic Tractography Study in 654 Individuals. *Biol Psychiatry Cogn Neurosci Neuroimaging*, *7*(10), 979-988. https://doi.org/10.1016/j.bpsc.2020.07.015

Demontis, D., Walters, R. K., Martin, J., Mattheisen, M., Als, T. D., Agerbo, E., Baldursson, G., Belliveau, R., Bybjerg-Grauholm, J., Bækvad-Hansen, M., Cerrato, F., Chambert, K., Churchhouse, C., Dumont, A., Eriksson, N., Gandal, M., Goldstein, J. I., Grasby, K. L., Grove, J., . . . Neale, B. M. (2019). Discovery of the first genome-wide significant risk loci for attention deficit/hyperactivity disorder. *Nat Genet*, *51*(1), 63-75. https://doi.org/10.1038/s41588-018-0269-7

Deng, J., Dong, W., Socher, R., Li, L. J., Kai, L., & Li, F.-F. (2009, 20-25 June 2009). ImageNet: A large-scale hierarchical image database. 2009 IEEE Conference on Computer Vision and Pattern Recognition,

Dennis, N. A., & Cabeza, R. (2011). Neuroimaging of healthy cognitive aging. In *The handbook of aging and cognition* (pp. 10-63). Psychology Press.

Dick, D. M. (2011). Gene-environment interaction in psychological traits and disorders. *Annu Rev Clin Psychol*, *7*, 383-409. https://doi.org/10.1146/annurev-clinpsy-032210-104518

Duan, K., Chen, J., Calhoun, V. D., Jiang, W., Rootes-Murdy, K., Schoenmacker, G., Silva, R. F., Franke, B., Buitelaar, J. K., Hoogman, M., Oosterlaan, J., Hoekstra, P. J., Heslenfeld,

D., Hartman, C. A., Sprooten, E., Arias-Vasquez, A., Turner, J. A., & Liu, J. (2023). Genomic patterns linked to gray matter alterations underlying working memory deficits in adults and adolescents with attention-deficit/hyperactivity disorder. *Transl Psychiatry*, *13*(1), 50. https://doi.org/10.1038/s41398-023-02349-x

Duan, K., Chen, J., Calhoun, V. D., Lin, D., Jiang, W., Franke, B., Buitelaar, J. K., Hoogman, M., Arias-Vasquez, A., Turner, J. A., & Liu, J. (2018). Neural correlates of cognitive function and symptoms in attention-deficit/hyperactivity disorder in adults. *Neuroimage Clin*, *19*, 374-383. https://doi.org/10.1016/j.nicl.2018.04.035

Duan, K., Jiang, W., Rootes-Murdy, K., Schoenmacker, G. H., Arias-Vasquez, A., Buitelaar, J. K., Hoogman, M., Oosterlaan, J., Hoekstra, P. J., Heslenfeld, D. J., Hartman, C. A., Calhoun, V. D., Turner, J. A., & Liu, J. (2021). Gray matter networks associated with attention and working memory deficit in ADHD across adolescence and adulthood. *Translational Psychiatry*, *11*(1), 184. https://doi.org/10.1038/s41398-021-01301-1

Edmund, T. R., Chu-Chung, H., Ching-Po, L., Jianfeng, F., & Marc, J. (2020). Automated anatomical labelling atlas 3. *Neuroimage*, *206*, 116189. https://doi.org/https://doi.org/10.1016/j.neuroimage.2019.116189

Efron, B. (1979). Bootstrap Methods: Another Look at the Jackknife. *The Annals of Statistics*, *7*(1), 1-26, 26. https://doi.org/10.1214/aos/1176344552

Ein Shoka, A. A., Dessouky, M. M., El-Sayed, A., & Hemdan, E. E. (2023). EEG seizure detection: concepts, techniques, challenges, and future trends. *Multimed Tools Appl*, 1-31. https://doi.org/10.1007/s11042-023-15052-2

Elliott, L. T., Sharp, K., Alfaro-Almagro, F., Shi, S., Miller, K. L., Douaud, G., Marchini, J., & Smith, S. M. (2018). Genome-wide association studies of brain imaging phenotypes in UK Biobank. *Nature*, *562*(7726), 210-216. https://doi.org/10.1038/s41586-018-0571-7

Ellison-Wright, I., Ellison-Wright, Z., & Bullmore, E. (2008). Structural brain change in Attention Deficit Hyperactivity Disorder identified by meta-analysis. *BMC Psychiatry*, *8*, 51. https://doi.org/10.1186/1471-244x-8-51

Emch, M., von Bastian, C. C., & Koch, K. (2019). Neural Correlates of Verbal Working Memory: An fMRI Meta-Analysis [Systematic Review]. *Frontiers in Human Neuroscience*, *13*. https://doi.org/10.3389/fnhum.2019.00180

Erion, G., Janizek, J. D., Sturmfels, P., Lundberg, S. M., & Lee, S.-I. (2021). Improving performance of deep learning models with axiomatic attribution priors and expected gradients. *Nature Machine Intelligence*, *3*(7), 620-631. https://doi.org/10.1038/s42256-021-00343-w

Evangelista, N. D., O'Shea, A., Kraft, J. N., Hausman, H. K., Boutzoukas, E. M., Nissim, N. R., Albizu, A., Hardcastle, C., Van Etten, E. J., Bharadwaj, P. K., Smith, S. G., Song, H., Hishaw, G. A., DeKosky, S., Wu, S., Porges, E., Alexander, G. E., Marsiske, M., Cohen, R., & Woods, A. J. (2021). Independent Contributions of Dorsolateral Prefrontal

Structure and Function to Working Memory in Healthy Older Adults. *Cereb Cortex, 31*(3), 1732-1743. https://doi.org/10.1093/cercor/bhaa322

Fischl, B., Salat, D. H., Busa, E., Albert, M., Dieterich, M., Haselgrove, C., van der Kouwe, A., Killiany, R., Kennedy, D., Klaveness, S., Montillo, A., Makris, N., Rosen, B., & Dale, A. M. (2002). Whole Brain Segmentation: Automated Labeling of Neuroanatomical Structures in the Human Brain. *Neuron, 33*(3), 341-355. https://doi.org/https://doi.org/10.1016/S0896-6273(02)00569-X

Forbes, N., Carrick, L., McIntosh, A., & Lawrie, S. (2009). Working memory in schizophrenia: a meta-analysis. *Psychological medicine*, *39*(6), 889-905.

Fournet, N., Roulin, J. L., Vallet, F., Beaudoin, M., Agrigoroaei, S., Paignon, A., Dantzer, C., & Desrichard, O. (2012). Evaluating short-term and working memory in older adults: French normative data. *Aging Ment Health*, *16*(7), 922-930. https://doi.org/10.1080/13607863.2012.674487

Francx, W., Oldehinkel, M., Oosterlaan, J., Heslenfeld, D., Hartman, C. A., Hoekstra, P. J., Franke, B., Beckmann, C. F., Buitelaar, J. K., & Mennes, M. (2015). The executive control network and symptomatic improvement in attention-deficit/hyperactivity disorder. *Cortex, 73*, 62-72. https://doi.org/https://doi.org/10.1016/j.cortex.2015.08.012

Friston, K. J., Holmes, A. P., Worsley, K. J., Poline, J.-P., Frith, C. D., & Frackowiak, R. S. J. (1994). Statistical parametric maps in functional imaging: A general linear approach. *Human Brain Mapping*, *2*(4), 189-210. https://doi.org/https://doi.org/10.1002/hbm.460020402

Ge, T., Feng, J., Hibar, D. P., Thompson, P. M., & Nichols, T. E. (2012). Increasing power for voxel-wise genome-wide association studies: the random field theory, least square kernel machines and fast permutation procedures. *Neuroimage, 63*(2), 858-873. https://doi.org/10.1016/j.neuroimage.2012.07.012

Germano, C., & Kinsella, G. J. (2005). Working memory and learning in early Alzheimer's disease. *Neuropsychology review*, *15*, 1-10.

Glahn, D. C., Thompson, P. M., & Blangero, J. (2007). Neuroimaging endophenotypes: strategies for finding genes influencing brain structure and function. *Hum Brain Mapp, 28*(6), 488-501. https://doi.org/10.1002/hbm.20401

Gogtay, N., Giedd, J. N., Lusk, L., Hayashi, K. M., Greenstein, D., Vaituzis, A. C., Nugent, T. F., 3rd, Herman, D. H., Clasen, L. S., Toga, A. W., Rapoport, J. L., & Thompson, P. M. (2004). Dynamic mapping of human cortical development during childhood through early adulthood. *Proc Natl Acad Sci U S A, 101*(21), 8174-8179. https://doi.org/10.1073/pnas.0402680101

Goldman, N., Glei, D. A., Lin, Y. H., & Weinstein, M. (2010). The serotonin transporter polymorphism (5-HTTLPR): allelic variation and links with depressive symptoms. *Depress Anxiety, 27*(3), 260-269. https://doi.org/10.1002/da.20660

Gorbach, T., Pudas, S., Lundquist, A., Orädd, G., Josefsson, M., Salami, A., de Luna, X., & Nyberg, L. (2017). Longitudinal association between hippocampus atrophy and episodic-memory decline. *Neurobiol Aging*, *51*, 167-176. https://doi.org/10.1016/j.neurobiolaging.2016.12.002

Griffiths, E. A., & Gore, S. D. (2008). DNA methyltransferase and histone deacetylase inhibitors in the treatment of myelodysplastic syndromes. *Semin Hematol*, *45*(1), 23-30. https://doi.org/10.1053/j.seminhematol.2007.11.007

Grünberg, K., Jimenez-del-Toro, O., Jakab, A., Langs, G., Salas, T., Winterstein, M., Weber, A., & Krenn, M. (2017). Annotating Medical Image Data. In (pp. 45-67). https://doi.org/10.1007/978-3-319-49644-3_4

Han, P., Weikang, G., Christian, F. B., Andrea, V., & Stephen, M. S. (2021). Accurate brain age prediction with lightweight deep neural networks. *Medical Image Analysis*, *68*, 101871. https://doi.org/https://doi.org/10.1016/j.media.2020.101871

Hawkins, D. M., Basak, S. C., & Mills, D. (2003). Assessing model fit by cross-validation. *J Chem Inf Comput Sci*, *43*(2), 579-586. https://doi.org/10.1021/ci025626i

Hayter, A. L., Langdon, D. W., & Ramnani, N. (2007). Cerebellar contributions to working memory. *Neuroimage*, *36*(3), 943-954. https://doi.org/https://doi.org/10.1016/j.neuroimage.2007.03.011

Health, N. I. o. (2019). What are single nucleotide polymorphisms (SNPs). *Genetics Home Reference-NIH. US National Library ofMedicine. URL: https://ghr. nlm. nih. gov/primer/genomicresearch/snp*.

Heck, A., Fastenrath, M., Ackermann, S., Auschra, B., Bickel, H., Coynel, D., Gschwind, L., Jessen, F., Kaduszkiewicz, H., Maier, W., Milnik, A., Pentzek, M., Riedel-Heller, S. G., Ripke, S., Spalek, K., Sullivan, P., Vogler, C., Wagner, M., Weyerer, S., . . . Papassotiropoulos, A. (2014). Converging genetic and functional brain imaging evidence links neuronal excitability to working memory, psychiatric disease, and brain activity. *Neuron*, *81*(5), 1203-1213. https://doi.org/10.1016/j.neuron.2014.01.010

Henseler, I., & Gruber, O. (2007). Arbeitsgedächtnisstörungen bei psychiatrischen Erkrankungen. *Der Nervenarzt*, *78*(9), 991-996. https://doi.org/10.1007/s00115-007-2256-6

Hill, A. C., Laird, A. R., & Robinson, J. L. (2014). Gender differences in working memory networks: A BrainMap meta-analysis. *Biological Psychology*, *102*, 18-29. https://doi.org/https://doi.org/10.1016/j.biopsycho.2014.06.008

Holland, J., & Sayal, K. (2019). Relative age and ADHD symptoms, diagnosis and medication: a systematic review. *Eur Child Adolesc Psychiatry*, *28*(11), 1417-1429. https://doi.org/10.1007/s00787-018-1229-6

Honea, R., Crow, T. J., Passingham, D., & Mackay, C. E. (2005). Regional Deficits in Brain Volume in Schizophrenia: A Meta-Analysis of Voxel-Based Morphometry Studies. *American Journal of Psychiatry*, *162*(12), 2233-2245. https://doi.org/10.1176/appi.ajp.162.12.2233

Horgusluoglu-Moloch, E., Risacher, S. L., Crane, P. K., Hibar, D., Thompson, P. M., Saykin, A. J., Nho, K., Weiner, M. W., Aisen, P., Petersen, R., Jack, C. R., Jagust, W., Trojanowki, J. Q., Toga, A. W., Beckett, L., Green, R. C., Morris, J., Shaw, L. M., Kaye, J., . . . Alzheimer's Disease Neuroimaging, I. (2019). Genome-wide association analysis of hippocampal volume identifies enrichment of neurogenesis-related pathways. *Scientific Reports*, *9*(1), 14498. https://doi.org/10.1038/s41598-019-50507-3

Huang, W. H., Chen, W., Jiang, L. Y., Yang, Y. X., Yao, L. F., & Li, K. S. (2018). Influence of ADAM10 Polymorphisms on Plasma Level of Soluble Receptor for Advanced Glycation End Products and The Association With Alzheimer's Disease Risk. *Front Genet*, *9*, 540. https://doi.org/10.3389/fgene.2018.00540

Huntley, J., & Howard, R. (2010). Working memory in early Alzheimer's disease: a neuropsychological review. *International Journal of Geriatric Psychiatry: A journal of the psychiatry of late life and allied sciences*, *25*(2), 121-132.

Irving I. Gottesman, Ph.D., Hon. F.R.C.Psych. , and, & Todd D. Gould, M.D. (2003). The Endophenotype Concept in Psychiatry: Etymology and Strategic Intentions. *American Journal of Psychiatry*, *160*(4), 636-645. https://doi.org/10.1176/appi.ajp.160.4.636

Jack, C. R., Jr., Petersen, R. C., Xu, Y., O'Brien, P. C., Smith, G. E., Ivnik, R. J., Tangalos, E. G., & Kokmen, E. (1998). Rate of medial temporal lobe atrophy in typical aging and Alzheimer's disease. *Neurology*, *51*(4), 993-999. https://doi.org/10.1212/wnl.51.4.993

Jang, H., Kwon, H., Yang, J.-J., Hong, J., Kim, Y., Kim, K., Lee, J., Jang, Y., Kim, S. T., Lee, K., Lee, J., Na, D., Seo, S., & Lee, J.-M. (2017). Correlations between Gray Matter and White Matter Degeneration in Pure Alzheimer's Disease, Pure Subcortical Vascular Dementia, and Mixed Dementia. *Scientific Reports*, *7*. https://doi.org/10.1038/s41598-017-10074-x

Jansen, P. R., Nagel, M., Watanabe, K., Wei, Y., Savage, J. E., de Leeuw, C. A., van den Heuvel, M. P., van der Sluis, S., & Posthuma, D. (2020). Genome-wide meta-analysis of brain volume identifies genomic loci and genes shared with intelligence. *Nat Commun*, *11*(1), 5606. https://doi.org/10.1038/s41467-020-19378-5

Jiang, W., Duan, K., Rootes-Murdy, K., Hoekstra, P. J., Hartman, C. A., Oosterlaan, J., Heslenfeld, D., Franke, B., Buitelaar, J., Arias-Vasquez, A., Liu, J., & Turner, J. A. (2020). Structural brain alterations and their association with cognitive function and symptoms in Attention-deficit/Hyperactivity Disorder families. *NeuroImage: Clinical*, *27*, 102273. https://doi.org/https://doi.org/10.1016/j.nicl.2020.102273

Johnson, S. B., Blum, R. W., & Giedd, J. N. (2009). Adolescent maturity and the brain: the promise and pitfalls of neuroscience research in adolescent health policy. *J Adolesc Health*, *45*(3), 216-221. https://doi.org/10.1016/j.jadohealth.2009.05.016

Kane, M. J., Bleckley, M. K., Conway, A. R., & Engle, R. W. (2001). A controlled-attention view of working-memory capacity. *Journal of experimental psychology: General*, *130*(2), 169.

Khadka, S., Pearlson, G. D., Calhoun, V. D., Liu, J., Gelernter, J., Bessette, K. L., & Stevens, M. C. (2016). Multivariate Imaging Genetics Study of MRI Gray Matter Volume and SNPs Reveals Biological Pathways Correlated with Brain Structural Differences in Attention Deficit Hyperactivity Disorder. *Frontiers in Psychiatry*, *7*. https://doi.org/10.3389/fpsyt.2016.00128

Kharbanda, M., Pilz, D. T., Tomkins, S., Chandler, K., Saggar, A., Fryer, A., McKay, V., Louro, P., Smith, J. C., Burn, J., Kini, U., De Burca, A., FitzPatrick, D. R., & Kinning, E. (2017). Clinical features associated with CTNNB1 de novo loss of function mutations in ten individuals. *Eur J Med Genet*, *60*(2), 130-135. https://doi.org/10.1016/j.ejmg.2016.11.008

Kim, M., Won, J. H., Hong, J., Kwon, J., Park, H., & Shen, L. (2020). DEEP NETWORK-BASED FEATURE SELECTION FOR IMAGING GENETICS: APPLICATION TO IDENTIFYING BIOMARKERS FOR PARKINSON'S DISEASE. *Proc IEEE Int Symp Biomed Imaging*, *2020*. https://doi.org/10.1109/isbi45749.2020.9098471

Kirchner, K., Garvert, L., Wittfeld, K., Ameling, S., Bülow, R., Meyer Zu Schwabedissen, H., Nauck, M., Völzke, H., Grabe, H. J., & Van der Auwera, S. (2023). Deciphering the Effect of Different Genetic Variants on Hippocampal Subfield Volumes in the General Population. *Int J Mol Sci*, *24*(2). https://doi.org/10.3390/ijms24021120

Kirova, A.-M., Bays, R. B., & Lagalwar, S. (2015). Working Memory and Executive Function Decline across Normal Aging, Mild Cognitive Impairment, and Alzheimer's Disease. *BioMed Research International*, *2015*, 748212. https://doi.org/10.1155/2015/748212

Kirova, A. M., Bays, R. B., & Lagalwar, S. (2015). Working memory and executive function decline across normal aging, mild cognitive impairment, and Alzheimer's disease. *Biomed Res Int*, *2015*, 748212. https://doi.org/10.1155/2015/748212

Knowles, E. E., Mathias, S. R., McKay, D. R., Sprooten, E., Blangero, J., Almasy, L., & Glahn, D. C. (2014). Genome-Wide Analyses of Working-Memory Ability: A Review. *Curr Behav Neurosci Rep*, *1*(4), 224-233. https://doi.org/10.1007/s40473-014-0028-8

Kular, L., & Kular, S. (2018). Epigenetics applied to psychiatry: Clinical opportunities and future challenges. *Psychiatry and Clinical Neurosciences*, *72*(4), 195-211. https://doi.org/https://doi.org/10.1111/pcn.12634

Kustubayeva, A., Eliassen, J., Matthews, G., & Nelson, E. (2023). FMRI study of implicit emotional face processing in patients with MDD with melancholic subtype. *Frontiers in Human Neuroscience, 17*. https://doi.org/10.3389/fnhum.2023.1029789

Larsson, J. O., Larsson, H., & Lichtenstein, P. (2004). Genetic and environmental contributions to stability and change of ADHD symptoms between 8 and 13 years of age: a longitudinal twin study. *J Am Acad Child Adolesc Psychiatry*, *43*(10), 1267-1275. https://doi.org/10.1097/01.chi.0000135622.05219.bf

Lee, J. J., Wedow, R., Okbay, A., Kong, E., Maghzian, O., Zacher, M., Nguyen-Viet, T. A., Bowers, P., Sidorenko, J., Karlsson Linnér, R., Fontana, M. A., Kundu, T., Lee, C., Li, H., Li, R., Royer, R., Timshel, P. N., Walters, R. K., Willoughby, E. A., . . . Cesarini, D. (2018). Gene discovery and polygenic prediction from a genome-wide association study of educational attainment in 1.1 million individuals. *Nat Genet*, *50*(8), 1112-1121. https://doi.org/10.1038/s41588-018-0147-3

Leonenko, G., Di Florio, A., Allardyce, J., Forty, L., Knott, S., Jones, L., Gordon-Smith, K., Owen, M. J., Jones, I., Walters, J., Craddock, N., O'Donovan, M. C., & Escott-Price, V. (2018). A data-driven investigation of relationships between bipolar psychotic symptoms and schizophrenia genome-wide significant genetic loci. *Am J Med Genet B Neuropsychiatr Genet*, *177*(4), 468-475. https://doi.org/10.1002/ajmg.b.32635

Li, S., Zhao, Y., Varma, R., Salpekar, O., Noordhuis, P., Li, T., Paszke, A., Smith, J., Vaughan, B., Damania, P., & Chintala, S. (2020). PyTorch distributed: experiences on accelerating data parallel training. *Proc. VLDB Endow.*, *13*(12), 3005–3018. https://doi.org/10.14778/3415478.3415530

Lippert, C., Sabatini, R., Maher, M. C., Kang, E. Y., Lee, S., Arikan, O., Harley, A., Bernal, A., Garst, P., Lavrenko, V., Yocum, K., Wong, T., Zhu, M., Yang, W.-Y., Chang, C., Lu, T., Lee, C. W. H., Hicks, B., Ramakrishnan, S., . . . Venter, J. C. (2017). Identification of individuals by trait prediction using whole-genome sequencing data. *Proceedings of the National Academy of Sciences*, *114*(38), 10166-10171. https://doi.org/doi:10.1073/pnas.1711125114

Litjens, G., Kooi, T., Bejnordi, B. E., Setio, A. A. A., Ciompi, F., Ghafoorian, M., van der Laak, J., van Ginneken, B., & Sánchez, C. I. (2017). A survey on deep learning in medical image analysis. *Med Image Anal*, *42*, 60-88. https://doi.org/10.1016/j.media.2017.07.005

Liu, J., Duan, K., Jiang, W., Rootes-Murdy, K., Schoenmacker, G., Buitelaar, J. K., Hoogman, M., Oosterlaan, J., Hoekstra, P. J., Heslenfeld, D. J., Hartman, C. A., Calhoun, V. D., Arias-Vasquez, A., & Turner, J. A. (2020). Gray matter networks associated with cognitive deficit in ADHD across adolescence and adulthood. *medRxiv*, 2020.2004.2022.20059808. https://doi.org/10.1101/2020.04.22.20059808

Liu, Z., Wu, K., Wu, B., Tang, X., Yuan, H., Pang, H., Huang, Y., Zhu, X., Luo, H., & Qi, Y. (2021). Imaging genomics for accurate diagnosis and treatment of tumors: A cutting edge overview. *Biomedicine & Pharmacotherapy*, *135*, 111173. https://doi.org/https://doi.org/10.1016/j.biopha.2020.111173

Loane, C., & Politis, M. (2011). Positron emission tomography neuroimaging in Parkinson's disease. *Am J Transl Res*, *3*(4), 323-341.

Logothetis, N. K. (2008). What we can do and what we cannot do with fMRI. *Nature*, *453*(7197), 869-878. https://doi.org/10.1038/nature06976

Loos, R. J. F., & Yeo, G. S. H. (2014). The bigger picture of FTO—the first GWAS-identified obesity gene. *Nature Reviews Endocrinology*, *10*(1), 51-61. https://doi.org/10.1038/nrendo.2013.227

Lopez-Larson, M. P., King, J. B., Terry, J., McGlade, E. C., & Yurgelun-Todd, D. (2012). Reduced insular volume in attention deficit hyperactivity disorder. *Psychiatry Res*, *204*(1), 32-39. https://doi.org/10.1016/j.pscychresns.2012.09.009

Luo, Y., Schulz, K. P., Alvarez, T. L., Halperin, J. M., & Li, X. (2018). Distinct topological properties of cue-evoked attention processing network in persisters and remitters of childhood ADHD. *Cortex*, *109*, 234-244. https://doi.org/10.1016/j.cortex.2018.09.013

Macoveanu, J., Freeman, K. O., Kjaerstad, H. L., Knudsen, G. M., Kessing, L. V., & Miskowiak, K. W. (2021). Structural brain abnormalities associated with cognitive impairments in bipolar disorder. *Acta Psychiatr Scand*, *144*(4), 379-391. https://doi.org/10.1111/acps.13349

Mai, Q., & Zhang, X. (2019). An iterative penalized least squares approach to sparse canonical correlation analysis. *Biometrics*, *75*(3), 734-744. https://doi.org/10.1111/biom.13043

Manolio, T. A., Collins, F. S., Cox, N. J., Goldstein, D. B., Hindorff, L. A., Hunter, D. J., McCarthy, M. I., Ramos, E. M., Cardon, L. R., Chakravarti, A., Cho, J. H., Guttmacher, A. E., Kong, A., Kruglyak, L., Mardis, E., Rotimi, C. N., Slatkin, M., Valle, D., Whittemore, A. S., . . . Visscher, P. M. (2009). Finding the missing heritability of complex diseases. *Nature*, *461*(7265), 747-753. https://doi.org/10.1038/nature08494

Meda, S. A., Jagannathan, K., Gelernter, J., Calhoun, V. D., Liu, J., Stevens, M. C., & Pearlson, G. D. (2010). A pilot multivariate parallel ICA study to investigate differential linkage between neural networks and genetic profiles in schizophrenia. *Neuroimage*, *53*(3), 1007-1015. https://doi.org/10.1016/j.neuroimage.2009.11.052

Mega, J. L., Close, S. L., Wiviott, S. D., Shen, L., Hockett, R. D., Brandt, J. T., Walker, J. R., Antman, E. M., Macias, W., Braunwald, E., & Sabatine, M. S. (2009). Cytochrome P-450 Polymorphisms and Response to Clopidogrel. *New England Journal of Medicine*, *360*(4), 354-362. https://doi.org/doi:10.1056/NEJMoa0809171

Meinshausen, N., & Bühlmann, P. (2010). Stability Selection. *Journal of the Royal Statistical Society Series B: Statistical Methodology*, *72*(4), 417-473. https://doi.org/10.1111/j.1467-9868.2010.00740.x

Meng, X., Navoly, G., Giannakopoulou, O., Levey, D. F., Koller, D., Pathak, G. A., Koen, N., Lin, K., Adams, M. J., Rentería, M. E., Feng, Y., Gaziano, J. M., Stein, D. J., Zar, H. J.,

Campbell, M. L., van Heel, D. A., Trivedi, B., Finer, S., McQuillin, A., . . . BioBank Japan, P. (2024). Multi-ancestry genome-wide association study of major depression aids locus discovery, fine mapping, gene prioritization and causal inference. *Nature Genetics*, *56*(2), 222-233. https://doi.org/10.1038/s41588-023-01596-4

Menon, V., & Uddin, L. Q. (2010). Saliency, switching, attention and control: a network model of insula function. *Brain structure and function*, *214*, 655-667.

Meyer-Lindenberg, A., Kohn, P. D., Kolachana, B., Kippenhan, S., McInerney-Leo, A., Nussbaum, R., Weinberger, D. R., & Berman, K. F. (2005). Midbrain dopamine and prefrontal function in humans: interaction and modulation by COMT genotype. *Nat Neurosci*, *8*(5), 594-596. https://doi.org/10.1038/nn1438

Miller, G. A. (1956). The magical number seven, plus or minus two: Some limits on our capacity for processing information. *Psychological Review*, *63*, 81-97. https://doi.org/10.1037/h0043158

Miyake, A., & Shah, P. (1999). *Models of working memory*. Citeseer.

Mullins, N., Forstner, A. J., O'Connell, K. S., Coombes, B., Coleman, J. R. I., Qiao, Z., Als, T. D., Bigdeli, T. B., Børte, S., Bryois, J., Charney, A. W., Drange, O. K., Gandal, M. J., Hagenaars, S. P., Ikeda, M., Kamitaki, N., Kim, M., Krebs, K., Panagiotaropoulou, G., . . . Psychiatry, H. A.-I. (2021). Genome-wide association study of more than 40,000 bipolar disorder cases provides new insights into the underlying biology. *Nature Genetics*, *53*(6), 817-829. https://doi.org/10.1038/s41588-021-00857-4

Nemoto, K. (2017). [Understanding Voxel-Based Morphometry]. *Brain Nerve*, *69*(5), 505-511. https://doi.org/10.11477/mf.1416200776

Nikolin, S., Tan, Y. Y., Martin, D., Moffa, A., Loo, C. K., & Boonstra, T. W. (2021). Behavioural and neurophysiological differences in working memory function of depressed patients and healthy controls. *J Affect Disord*, *295*, 559-568. https://doi.org/10.1016/j.jad.2021.08.083

Nissim, N. R., O'Shea, A. M., Bryant, V., Porges, E. C., Cohen, R., & Woods, A. J. (2016). Frontal Structural Neural Correlates of Working Memory Performance in Older Adults. *Front Aging Neurosci*, *8*, 328. https://doi.org/10.3389/fnagi.2016.00328

Nyberg, L., Salami, A., Andersson, M., Eriksson, J., Kalpouzos, G., Kauppi, K., Lind, J., Pudas, S., Persson, J., & Nilsson, L.-G. (2010). Longitudinal evidence for diminished frontal cortex function in aging. *Proceedings of the National Academy of Sciences*, *107*(52), 22682-22686. https://doi.org/doi:10.1073/pnas.1012651108

Oberauer, K. (2019). Working Memory and Attention – A Conceptual Analysis and Review. *Journal of Cognition*. https://doi.org/10.5334/joc.58

Ojala, M., & Garriga, G. C. (2009, 6-9 Dec. 2009). Permutation Tests for Studying Classifier Performance. 2009 Ninth IEEE International Conference on Data Mining,

Owen, A. M., McMillan, K. M., Laird, A. R., & Bullmore, E. (2005). N-back working memory paradigm: a meta-analysis of normative functional neuroimaging studies. *Hum Brain Mapp*, *25*(1), 46-59. https://doi.org/10.1002/hbm.20131

Park, S., & Gooding, D. C. (2014). WORKING MEMORY IMPAIRMENT AS AN ENDOPHENOTYPIC MARKER OF A SCHIZOPHRENIA DIATHESIS. *Schizophr Res Cogn*, *1*(3), 127-136. https://doi.org/10.1016/j.scog.2014.09.005

Park, S. T., & Kim, J. (2016). Trends in Next-Generation Sequencing and a New Era for Whole Genome Sequencing. *Int Neurourol J*, *20*(Suppl 2), S76-83. https://doi.org/10.5213/inj.1632742.371

Pascual-Leone, J., & Smith, J. (1969). The encoding and decoding of symbols by children: A new experimental paradigm and a neo-Piagetian model. *Journal of Experimental Child Psychology*, *8*(2), 328-355. https://doi.org/https://doi.org/10.1016/0022-0965(69)90107-6

Pearlson, G. D., Liu, J., & Calhoun, V. D. (2015). An introductory review of parallel independent component analysis (p-ICA) and a guide to applying p-ICA to genetic data and imaging phenotypes to identify disease-associated biological pathways and systems in common complex disorders. *Front Genet*, *6*, 276. https://doi.org/10.3389/fgene.2015.00276

Perpetuini, D., Chiarelli, A. M., Filippini, C., Cardone, D., Croce, P., Rotunno, L., Anzoletti, N., Zito, M., Zappasodi, F., & Merla, A. (2020). Working Memory Decline in Alzheimer's Disease Is Detected by Complexity Analysis of Multimodal EEG-fNIRS. *Entropy (Basel)*, *22*(12). https://doi.org/10.3390/e22121380

Perreau, V. M., Orchard, S., Adlard, P. A., Bellingham, S. A., Cappai, R., Ciccotosto, G. D., Cowie, T. F., Crouch, P. J., Duce, J. A., Evin, G., Faux, N. G., Hill, A. F., Hung, Y. H., James, S. A., Li, Q.-X., Mok, S. S., Tew, D. J., White, A. R., Bush, A. I., . . . Masters, C. L. (2010). A domain level interaction network of amyloid precursor protein and Abeta of Alzheimer's disease. *Proteomics*, *10*(12), 2377-2395. https://doi.org/10.1002/pmic.200900773

Perreau, V. M., Orchard, S., Adlard, P. A., Bellingham, S. A., Cappai, R., Ciccotosto, G. D., Cowie, T. F., Crouch, P. J., Duce, J. A., Evin, G., Faux, N. G., Hill, A. F., Hung, Y. H., James, S. A., Li, Q. X., Mok, S. S., Tew, D. J., White, A. R., Bush, A. I., . . . Masters, C. L. (2010). A domain level interaction network of amyloid precursor protein and Abeta of Alzheimer's disease. *Proteomics*, *10*(12), 2377-2395. https://doi.org/10.1002/pmic.200900773

Petersen, R. C., Aisen, P. S., Beckett, L. A., Donohue, M. C., Gamst, A. C., Harvey, D. J., Jack, C. R., Jr., Jagust, W. J., Shaw, L. M., Toga, A. W., Trojanowski, J. Q., & Weiner, M. W. (2010). Alzheimer's Disease Neuroimaging Initiative (ADNI): clinical characterization. *Neurology*, *74*(3), 201-209. https://doi.org/10.1212/WNL.0b013e3181cb3e25

Pettersson, E., Lichtenstein, P., Larsson, H., Song, J., Agrawal, A., Børglum, A. D., Bulik, C. M., Daly, M. J., Davis, L. K., Demontis, D., Edenberg, H. J., Grove, J., Gelernter, J., Neale,

B. M., Pardiñas, A. F., Stahl, E., Walters, J. T. R., Walters, R., Sullivan, P. F., . . . Polderman, T. J. C. (2019). Genetic influences on eight psychiatric disorders based on family data of 4 408 646 full and half-siblings, and genetic data of 333 748 cases and controls. *Psychol Med*, *49*(7), 1166-1173. https://doi.org/10.1017/s0033291718002039

Pezawas, L., Meyer-Lindenberg, A., Drabant, E. M., Verchinski, B. A., Munoz, K. E., Kolachana, B. S., Egan, M. F., Mattay, V. S., Hariri, A. R., & Weinberger, D. R. (2005). 5-HTTLPR polymorphism impacts human cingulate-amygdala interactions: a genetic susceptibility mechanism for depression. *Nature neuroscience*, *8*(6), 828-834. https://doi.org/10.1038/nn1463

Pilmeyer, J., Huijbers, W., Lamerichs, R., Jansen, J. F. A., Breeuwer, M., & Zinger, S. (2022). Functional MRI in major depressive disorder: A review of findings, limitations, and future prospects. *J Neuroimaging*, *32*(4), 582-595. https://doi.org/10.1111/jon.13011

Pliatsikas, C., Veríssimo, J., Babcock, L., Pullman, M. Y., Glei, D. A., Weinstein, M., Goldman, N., & Ullman, M. T. (2019). Working memory in older adults declines with age, but is modulated by sex and education. *Q J Exp Psychol (Hove)*, *72*(6), 1308-1327. https://doi.org/10.1177/1747021818791994

Pontil, M. (2002). Leave-one-out error and stability of learning algorithms with applications. *International Journal of Systems Science*.

Posner, M. I., & Petersen, S. E. (1990). The attention system of the human brain. *Annu Rev Neurosci*, *13*, 25-42. https://doi.org/10.1146/annurev.ne.13.030190.000325

Pranav Suresh, B. R., Bishal Thapaliya, Britny Farahdel, Behnam kazemivash, Jiayu Chen, Kuaikuai Duan, Vince D. Calhoun, Jingyu Liu. (2023). *Effective Training Strategy for NN Models of Working Memory Classification With Limited Samples* ISBI,

Provençal, N., & Binder, E. B. (2015). The effects of early life stress on the epigenome: From the womb to adulthood and even before. *Exp Neurol*, *268*, 10-20. https://doi.org/10.1016/j.expneurol.2014.09.001

Rabiee, A., Vasaghi-Gharamaleki, B., Samadi, S. A., Amiri-Shavaki, Y., & Alaghband-Rad, J. (2020). Working Memory Deficits and its Relationship to Autism Spectrum Disorders. *Iran J Med Sci*, *45*(2), 100-109. https://doi.org/10.30476/ijms.2019.45315

Ranganath, C., Cohen, M. X., & Brozinsky, C. J. (2005). Working Memory Maintenance Contributes to Long-term Memory Formation: Neural and Behavioral Evidence. *Journal of Cognitive Neuroscience*, *17*(7), 994-1010. https://doi.org/10.1162/0898929054475118

Raudvere, U., Kolberg, L., Kuzmin, I., Arak, T., Adler, P., Peterson, H., & Vilo, J. (2019). g:Profiler: a web server for functional enrichment analysis and conversions of gene lists (2019 update). *Nucleic Acids Research*, *47*(W1), W191-W198. https://doi.org/10.1093/nar/gkz369

Ray, B., Duan, K., Chen, J., Fu, Z., Suresh, P., Johnson, S., Calhoun, V. D., & Liu, J. (2021, 1-5 Nov. 2021). Multimodal Brain Age Prediction with Feature Selection and Comparison. 2021 43rd Annual International Conference of the IEEE Engineering in Medicine & Biology Society (EMBC),

Raz, N., & Rodrigue, K. M. (2006). Differential aging of the brain: patterns, cognitive correlates and modifiers. *Neuroscience & Biobehavioral Reviews*, *30*(6), 730-748.

Raz, N., Rodrigue, K. M., Kennedy, K. M., & Acker, J. D. (2007). Vascular health and longitudinal changes in brain and cognition in middle-aged and older adults. *Neuropsychology*, *21*(2), 149-157. https://doi.org/10.1037/0894-4105.21.2.149

Raza, N., Naseer, A., Tamoor, M., & Zafar, K. (2023). Alzheimer Disease Classification through Transfer Learning Approach. *Diagnostics (Basel)*, *13*(4). https://doi.org/10.3390/diagnostics13040801

Ripke, S., Neale, B. M., Corvin, A., Walters, J. T. R., Farh, K.-H., Holmans, P. A., Lee, P., Bulik-Sullivan, B., Collier, D. A., Huang, H., Pers, T. H., Agartz, I., Agerbo, E., Albus, M., Alexander, M., Amin, F., Bacanu, S. A., Begemann, M., Belliveau Jr, R. A., . . . Psychosis Endophenotypes International, C. (2014). Biological insights from 108 schizophrenia-associated genetic loci. *Nature*, *511*(7510), 421-427. https://doi.org/10.1038/nature13595

Ripke, S., O'Dushlaine, C., Chambert, K., Moran, J. L., Kähler, A. K., Akterin, S., Bergen, S. E., Collins, A. L., Crowley, J. J., Fromer, M., Kim, Y., Lee, S. H., Magnusson, P. K. E., Sanchez, N., Stahl, E. A., Williams, S., Wray, N. R., Xia, K., Bettella, F., . . . Publications, C. (2013). Genome-wide association analysis identifies 13 new risk loci for schizophrenia. *Nature Genetics*, *45*(10), 1150-1159. https://doi.org/10.1038/ng.2742

Robbins, T. W. (1996). Dissociating executive functions of the prefrontal cortex. *Philos Trans R Soc Lond B Biol Sci*, *351*(1346), 1463-1470; discussion 1470-1461. https://doi.org/10.1098/rstb.1996.0131

Rolls, E. T., Huang, C.-C., Lin, C.-P., Feng, J., & Joliot, M. (2020). Automated anatomical labelling atlas 3. *Neuroimage*, *206*, 116189. https://doi.org/https://doi.org/10.1016/j.neuroimage.2019.116189

Rottschy, C., Langner, R., Dogan, I., Reetz, K., Laird, A. R., Schulz, J. B., Fox, P. T., & Eickhoff, S. B. (2012). Modelling neural correlates of working memory: A coordinate-based meta-analysis. *Neuroimage*, *60*(1), 830-846. https://doi.org/https://doi.org/10.1016/j.neuroimage.2011.11.050

Salami, A., Rieckmann, A., Karalija, N., Avelar-Pereira, B., Andersson, M., Wåhlin, A., Papenberg, G., Garrett, D. D., Riklund, K., Lövdén, M., Lindenberger, U., Bäckman, L., & Nyberg, L. (2018). Neurocognitive Profiles of Older Adults with Working-Memory Dysfunction. *Cerebral cortex*, *28*(7), 2525-2539. https://doi.org/10.1093/cercor/bhy062

Salman, M. S., Du, Y., Lin, D., Fu, Z., Fedorov, A., Damaraju, E., Sui, J., Chen, J., Mayer, A. R., Posse, S., Mathalon, D. H., Ford, J. M., Van Erp, T., & Calhoun, V. D. (2019). Group ICA for identifying biomarkers in schizophrenia: 'Adaptive' networks via spatially constrained ICA show more sensitivity to group differences than spatio-temporal regression. *Neuroimage Clin*, *22*, 101747. https://doi.org/10.1016/j.nicl.2019.101747

Santosh, K. C., Das, N., & Ghosh, S. (2022). Chapter 2 - Deep learning: a review. In K. C. Santosh, N. Das, & S. Ghosh (Eds.), *Deep Learning Models for Medical Imaging* (pp. 29-63). Academic Press. https://doi.org/https://doi.org/10.1016/B978-0-12-823504-1.00012-X

Sapkota, R., Thapaliya, B., Suresh, P., Ray, B., Calhoun, V. D., & Liu, J. (2024, 14-19 April 2024). Multimodal Imaging Feature Extraction with Reference Canonical Correlation Analysis Underlying Intelligence. ICASSP 2024 - 2024 IEEE International Conference on Acoustics, Speech and Signal Processing (ICASSP),

Saragosa-Harris, N. M., Chaku, N., MacSweeney, N., Guazzelli Williamson, V., Scheuplein, M., Feola, B., Cardenas-Iniguez, C., Demir-Lira, E., McNeilly, E. A., Huffman, L. G., Whitmore, L., Michalska, K. J., Damme, K. S., Rakesh, D., & Mills, K. L. (2022). A practical guide for researchers and reviewers using the ABCD Study and other large longitudinal datasets. *Dev Cogn Neurosci*, *55*, 101115. https://doi.org/10.1016/j.dcn.2022.101115

Sasser, T. R., Kalvin, C. B., & Bierman, K. L. (2016). Developmental trajectories of clinically significant attention-deficit/hyperactivity disorder (ADHD) symptoms from grade 3 through 12 in a high-risk sample: Predictors and outcomes. *J Abnorm Psychol*, *125*(2), 207-219. https://doi.org/10.1037/abn0000112

Schaefer, A., Braver, T. S., Reynolds, J. R., Burgess, G. C., Yarkoni, T., & Gray, J. R. (2006). Individual differences in amygdala activity predict response speed during working memory. *Journal of Neuroscience*, *26*(40), 10120-10128.

Schoenmacker, G., Claassen, T., Heskes, T., Franke, B., Buitelaar, J., & Arias-Vásquez, A. (2019). M17 - NOVEL QUANTITATIVE METHOD FOR GENETIC ASSOCIATION TESTING. *European Neuropsychopharmacology*, *29*, S963-S964. https://doi.org/https://doi.org/10.1016/j.euroneuro.2017.08.324

Schon, K., Hasselmo, M. E., LoPresti, M. L., Tricarico, M. D., & Stern, C. E. (2004). Persistence of parahippocampal representation in the absence of stimulus input enhances long-term encoding: a functional magnetic resonance imaging study of subsequent memory after a delayed match-to-sample task. *Journal of Neuroscience*, *24*(49), 11088-11097.

Shen, L., & Thompson, P. M. (2020). Brain Imaging Genomics: Integrated Analysis and Machine Learning. *Proc IEEE Inst Electr Electron Eng*, *108*(1), 125-162. https://doi.org/10.1109/jproc.2019.2947272

Simonyan, K., & Zisserman, A. (2014). Very deep convolutional networks for large-scale image recognition. *arXiv preprint arXiv:1409.1556*.

Singh, S. B., Tiwari, A., Katta, M. R., Kafle, R., Ayubcha, C., Patel, K. H., Bhattarai, Y., Werner, T. J., Alavi, A., & Revheim, M.-E. (2024). The utility of PET imaging in depression. *Frontiers in Psychiatry*, *15*. https://doi.org/10.3389/fpsyt.2024.1322118

Smith, N. M., Ford, J. N., Haghdel, A., Glodzik, L., Li, Y., D'Angelo, D., RoyChoudhury, A., Wang, X., Blennow, K., de Leon, M. J., & Ivanidze, J. (2022/04/25). Frontiers | Statistical Parametric Mapping in Amyloid Positron Emission Tomography. *Frontiers in Aging Neuroscience*, *14*. https://doi.org/10.3389/fnagi.2022.849932

Sobczak-Edmans, M., Ng, T. H. B., Chan, Y. C., Chew, E., Chuang, K. H., & Chen, S. H. A. (2016). Temporal dynamics of visual working memory. *Neuroimage*, *124*, 1021-1030. https://doi.org/https://doi.org/10.1016/j.neuroimage.2015.09.038

Song, P., Wang, Y., Yuan, X., Wang, S., & Song, X. (2022). Exploring Brain Structural and Functional Biomarkers in Schizophrenia via Brain-Network-Constrained Multi-View SCCA. *Front Neurosci*, *16*, 879703. https://doi.org/10.3389/fnins.2022.879703

Stein, J. L., Hua, X., Lee, S., Ho, A. J., Leow, A. D., Toga, A. W., Saykin, A. J., Shen, L., Foroud, T., Pankratz, N., Huentelman, M. J., Craig, D. W., Gerber, J. D., Allen, A. N., Corneveaux, J. J., Dechairo, B. M., Potkin, S. G., Weiner, M. W., & Thompson, P. (2010). Voxelwise genome-wide association study (vGWAS). *Neuroimage*, *53*(3), 1160-1174. https://doi.org/10.1016/j.neuroimage.2010.02.032

Stein, J. L., Hua, X., Lee, S., Ho, A. J., Leow, A. D., Toga, A. W., Saykin, A. J., Shen, L., Foroud, T., Pankratz, N., Huentelman, M. J., Craig, D. W., Gerber, J. D., Allen, A. N., Corneveaux, J. J., DeChairo, B. M., Potkin, S. G., Weiner, M. W., & Thompson, P. M. (2010/11/11). Voxelwise genome-wide association study (vGWAS). *Neuroimage*, *53*(3). https://doi.org/10.1016/j.neuroimage.2010.02.032

Stein, J. L., Medland, S. E., Vasquez, A. A., Hibar, D. P., Senstad, R. E., Winkler, A. M., Toro, R., Appel, K., Bartecek, R., Bergmann, Ø., Bernard, M., Brown, A. A., Cannon, D. M., Chakravarty, M. M., Christoforou, A., Domin, M., Grimm, O., Hollinshead, M., Holmes, A. J., . . . for the Enhancing Neuro Imaging Genetics through Meta-Analysis, C. (2012). Identification of common variants associated with human hippocampal and intracranial volumes. *Nature Genetics*, *44*(5), 552-561. https://doi.org/10.1038/ng.2250

Stoodley, C. J., & Schmahmann, J. D. (2010). Evidence for topographic organization in the cerebellum of motor control versus cognitive and affective processing. *Cortex*, *46*(7), 831-844. https://doi.org/10.1016/j.cortex.2009.11.008

Sudlow, C., Gallacher, J., Allen, N., Beral, V., Burton, P., Danesh, J., Downey, P., Elliott, P., Green, J., Landray, M., Liu, B., Matthews, P., Ong, G., Pell, J., Silman, A., Young, A., Sprosen, T., Peakman, T., & Collins, R. (2015). UK biobank: an open access resource for identifying the causes of a wide range of complex diseases of middle and old age. *PLoS Med*, *12*(3), e1001779. https://doi.org/10.1371/journal.pmed.1001779

Sudre, G., Sharp, W., Kundzicz, P., Bouyssi-Kobar, M., Norman, L., Choudhury, S., & Shaw, P. (2021). Predicting the course of ADHD symptoms through the integration of childhood

genomic, neural, and cognitive features. *Mol Psychiatry*, *26*(8), 4046-4054. https://doi.org/10.1038/s41380-020-00941-x

Sui, J., Adali, T., Yu, Q., Chen, J., & Calhoun, V. D. (2012). A review of multivariate methods for multimodal fusion of brain imaging data. *J Neurosci Methods*, *204*(1), 68-81. https://doi.org/10.1016/j.jneumeth.2011.10.031

Sundararajan, M., Taly, A., & Yan, Q. (2017). Axiomatic Attribution for Deep Networks. *arXiv pre-print server*. https://doi.org/None
arxiv:1703.01365

Suresh, P., Ray, B., Duan, K., Chen, J., Schoenmacker, G., Franke, B., Buitelaar, J. K., Sprooten, E., Arias-Vasquez, A., Turner, J. A., & Liu, J. (2021, 1-5 Nov. 2021). Evaluating the Neuroimaging-Genetic Prediction of Symptom Changes in Individuals with ADHD. 2021 43rd Annual International Conference of the IEEE Engineering in Medicine & Biology Society (EMBC),

Takeuchi, H., & Kawashima, R. (2017). [Voxel-Based Morphometry and Cognitive Function]. *Brain Nerve*, *69*(5), 547-556. https://doi.org/10.11477/mf.1416200781

Taleb, A., Kirchler, M., Monti, R., & Lippert, C. (2022, 18-24 June 2022). ContIG: Self-supervised Multimodal Contrastive Learning for Medical Imaging with Genetics. 2022 IEEE/CVF Conference on Computer Vision and Pattern Recognition (CVPR),

Tam, V., Patel, N., Turcotte, M., Bossé, Y., Paré, G., & Meyre, D. (2019). Benefits and limitations of genome-wide association studies. *Nat Rev Genet*, *20*(8), 467-484. https://doi.org/10.1038/s41576-019-0127-1

Tammen, S. A., Friso, S., & Choi, S. W. (2013). Epigenetics: the link between nature and nurture. *Mol Aspects Med*, *34*(4), 753-764. https://doi.org/10.1016/j.mam.2012.07.018

Tcheandjieu, C., Zhu, X., Hilliard, A. T., Clarke, S. L., Napolioni, V., Ma, S., Lee, K. M., Fang, H., Chen, F., Lu, Y., Tsao, N. L., Raghavan, S., Koyama, S., Gorman, B. R., Vujkovic, M., Klarin, D., Levin, M. G., Sinnott-Armstrong, N., Wojcik, G. L., . . . Million Veteran, P. (2022). Large-scale genome-wide association study of coronary artery disease in genetically diverse populations. *Nature Medicine*, *28*(8), 1679-1692. https://doi.org/10.1038/s41591-022-01891-3

Thompson, P. M., Ge, T., Glahn, D. C., Jahanshad, N., & Nichols, T. E. (2013). Genetics of the connectome. *Neuroimage*, *80*, 475-488. https://doi.org/10.1016/j.neuroimage.2013.05.013

Tomaszewski Farias, S., Cahn-Weiner, D. A., Harvey, D. J., Reed, B. R., Mungas, D., Kramer, J. H., & Chui, H. (2009). Longitudinal changes in memory and executive functioning are associated with longitudinal change in instrumental activities of daily living in older adults. *The Clinical Neuropsychologist*, *23*(3), 446-461.

Tordjman, S., Somogyi, E., Coulon, N., Kermarrec, S., Cohen, D., Bronsard, G., Bonnot, O., Weismann-Arcache, C., Botbol, M., Lauth, B., Ginchat, V., Roubertoux, P., Barburoth, M., Kovess, V., Geoffray, M. M., & Xavier, J. (2014). Gene × Environment interactions in autism spectrum disorders: role of epigenetic mechanisms. *Front Psychiatry*, *5*, 53. https://doi.org/10.3389/fpsyt.2014.00053

Turetsky, B. I., Calkins, M. E., Light, G. A., Olincy, A., Radant, A. D., & Swerdlow, N. R. (2007). Neurophysiological endophenotypes of schizophrenia: the viability of selected candidate measures. *Schizophr Bull*, *33*(1), 69-94. https://doi.org/10.1093/schbul/sbl060

Unsworth, N., & Spillers, G. J. (2010). Working memory capacity: Attention control, secondary memory, or both? A direct test of the dual-component model. *Journal of Memory and Language*, *62*, 392-406. https://doi.org/10.1016/j.jml.2010.02.001

Vatansever, D., Manktelow, A. E., Sahakian, B. J., Menon, D. K., & Stamatakis, E. A. (2017). Angular default mode network connectivity across working memory load. *Human Brain Mapping*, *38*(1), 41-52. https://doi.org/https://doi.org/10.1002/hbm.23341

Verlouw, J. A. M., Clemens, E., de Vries, J. H., Zolk, O., Verkerk, A. J. M. H., am Zehnhoff-Dinnesen, A., Medina-Gomez, C., Lanvers-Kaminsky, C., Rivadeneira, F., Langer, T., van Meurs, J. B. J., van den Heuvel-Eibrink, M. M., Uitterlinden, A. G., & Broer, L. (2021). A comparison of genotyping arrays. *European Journal of Human Genetics*, *29*(11), 1611-1624. https://doi.org/10.1038/s41431-021-00917-7

Virolainen, S. J., VonHandorf, A., Viel, K. C. M. F., Weirauch, M. T., Kottyan, L. C., Virolainen, S. J., VonHandorf, A., Viel, K. C. M. F., Weirauch, M. T., & Kottyan, L. C. (2022-12-30). Gene–environment interactions and their impact on human health. *Genes & Immunity 2022 24:1*, *24*(1). https://doi.org/10.1038/s41435-022-00192-6

Visscher, P. M., Brown, M. A., McCarthy, M. I., & Yang, J. (2012). Five years of GWAS discovery. *Am J Hum Genet*, *90*(1), 7-24. https://doi.org/10.1016/j.ajhg.2011.11.029

von Rhein, D., Mennes, M., van Ewijk, H., Groenman, A. P., Zwiers, M. P., Oosterlaan, J., Heslenfeld, D., Franke, B., Hoekstra, P. J., Faraone, S. V., Hartman, C., & Buitelaar, J. (2015). The NeuroIMAGE study: a prospective phenotypic, cognitive, genetic and MRI study in children with attention-deficit/hyperactivity disorder. Design and descriptives. *Eur Child Adolesc Psychiatry*, *24*(3), 265-281. https://doi.org/10.1007/s00787-014-0573-4

von Stumm, S., Kandaswamy, R., & Maxwell, J. (2023). Gene-environment interplay in early life cognitive development. *Intelligence*, *98*, 101748. https://doi.org/https://doi.org/10.1016/j.intell.2023.101748

Wang, D., Liu, S., Warrell, J., Won, H., Shi, X., Navarro, F. C. P., Clarke, D., Gu, M., Emani, P., Yang, Y. T., Xu, M., Gandal, M. J., Lou, S., Zhang, J., Park, J. J., Yan, C., Rhie, S. K., Manakongtreecheep, K., Zhou, H., . . . Abyzov, A. (2018). Comprehensive functional genomic resource and integrative model for the human brain. *Science*, *362*(6420), eaat8464. https://doi.org/doi:10.1126/science.aat8464

Weiss, K., Khoshgoftaar, T. M., & Wang, D. (2016). A survey of transfer learning. *Journal of Big Data*, *3*(1), 9. https://doi.org/10.1186/s40537-016-0043-6

Wenzel, S. E., Balzar, S., Ampleford, E., Hawkins, G. A., Busse, W. W., Calhoun, W. J., Castro, M., Chung, K. F., Erzurum, S., Gaston, B., Israel, E., Teague, W. G., Curran-Everett, D., Meyers, D. A., & Bleecker, E. R. (2007). IL4R alpha mutations are associated with asthma exacerbations and mast cell/IgE expression. *Am J Respir Crit Care Med*, *175*(6), 570-576. https://doi.org/10.1164/rccm.200607-909OC

Wightman, D. P., Jansen, I. E., Savage, J. E., Shadrin, A. A., Bahrami, S., Holland, D., Rongve, A., Børte, S., Winsvold, B. S., Drange, O. K., Martinsen, A. E., Skogholt, A. H., Willer, C., Bråthen, G., Bosnes, I., Nielsen, J. B., Fritsche, L. G., Thomas, L. F., Pedersen, L. M., . . . Posthuma, D. (2021). A genome-wide association study with 1,126,563 individuals identifies new risk loci for Alzheimer's disease. *Nat Genet*, *53*(9), 1276-1282. https://doi.org/10.1038/s41588-021-00921-z

Witten, D. M., & Tibshirani, R. J. (2009). Extensions of sparse canonical correlation analysis with applications to genomic data. *Stat Appl Genet Mol Biol*, *8*(1), Article28. https://doi.org/10.2202/1544-6115.1470

Worsley, K. J., Evans, A. C., Marrett, S., & Neelin, P. (1992). A three-dimensional statistical analysis for CBF activation studies in human brain. *J Cereb Blood Flow Metab*, *12*(6), 900-918. https://doi.org/10.1038/jcbfm.1992.127

Wray, N. R., Ripke, S., Mattheisen, M., Trzaskowski, M., Byrne, E. M., Abdellaoui, A., Adams, M. J., Agerbo, E., Air, T. M., Andlauer, T. M. F., Bacanu, S.-A., Bækvad-Hansen, M., Beekman, A. F. T., Bigdeli, T. B., Binder, E. B., Blackwood, D. R. H., Bryois, J., Buttenschøn, H. N., Bybjerg-Grauholm, J., . . . the Major Depressive Disorder Working Group of the Psychiatric Genomics, C. (2018). Genome-wide association analyses identify 44 risk variants and refine the genetic architecture of major depression. *Nature Genetics*, *50*(5), 668-681. https://doi.org/10.1038/s41588-018-0090-3

Wu, H., Melicher, T., Bauer, I. E., Sanches, M., & Soares, J. C. (2020). Chapter 3 - Brain Structural Abnormalities of Major Depressive Disorder. In R. S. McIntyre (Ed.), *Major Depressive Disorder* (pp. 39-49). Elsevier. https://doi.org/https://doi.org/10.1016/B978-0-323-58131-8.00003-3

Xia, S., Li, X., Kimball, A. E., Kelly, M. S., Lesser, I., & Branch, C. (2012). Thalamic shape and connectivity abnormalities in children with attention-deficit/hyperactivity disorder. *Psychiatry Res*, *204*(2-3), 161-167. https://doi.org/10.1016/j.pscychresns.2012.04.011

Xiao, Y., Hu, Y., & Huang, K. (2023). Atrophy of hippocampal subfields relates to memory decline during the pathological progression of Alzheimer's disease. *Frontiers in Aging Neuroscience*, *15*. https://doi.org/10.3389/fnagi.2023.1287122

Xu, Y., Liu, Y., Ridgway, N. D., & McMaster, C. R. (2001). Novel members of the human oxysterol-binding protein family bind phospholipids and regulate vesicle transport. *J Biol Chem*, *276*(21), 18407-18414. https://doi.org/10.1074/jbc.M101204200

Yuan, X. Z., Sun, S., Tan, C. C., Yu, J. T., & Tan, L. (2017). The Role of ADAM10 in Alzheimer's Disease. *J Alzheimers Dis*, *58*(2), 303-322. https://doi.org/10.3233/jad-170061

Yun, R. J., Krystal, J. H., & Mathalon, D. H. (2010). Working memory overload: fronto-limbic interactions and effects on subsequent working memory function. *Brain imaging and behavior*, *4*, 96-108.

Zeiler, M. D., & Fergus, R. (2014). Visualizing and Understanding Convolutional Networks. In D. Fleet, T. Pajdla, B. Schiele, & T. Tuytelaars, *Computer Vision – ECCV 2014* Cham.

Zimprich, A., Biskup, S., Leitner, P., Lichtner, P., Farrer, M., Lincoln, S., Kachergus, J., Hulihan, M., Uitti, R. J., Calne, D. B., Stoessl, A. J., Pfeiffer, R. F., Patenge, N., Carbajal, I. C., Vieregge, P., Asmus, F., Müller-Myhsok, B., Dickson, D. W., Meitinger, T., . . . Gasser, T. (2004). Mutations in LRRK2 cause autosomal-dominant parkinsonism with pleomorphic pathology. *Neuron*, *44*(4), 601-607. https://doi.org/10.1016/j.neuron.2004.11.005

Zwir, I., Arnedo, J., Del-Val, C., Pulkki-Råback, L., Konte, B., Yang, S. S., Romero-Zaliz, R., Hintsanen, M., Cloninger, K. M., Garcia, D., Svrakic, D. M., Rozsa, S., Martinez, M., Lyytikäinen, L. P., Giegling, I., Kähönen, M., Hernandez-Cuervo, H., Seppälä, I., Raitoharju, E., . . . Cloninger, C. R. (2020). Uncovering the complex genetics of human character. *Mol Psychiatry*, *25*(10), 2295-2312. https://doi.org/10.1038/s41380-018-0263-6